

An algebraic framework for finding and analyzing self-affine tiles and fractals

Inauguraldissertation

zur

Erlangung des akademischen Grades eines
Doktors der naturwissenschaften (Dr. rer. nat.)

der

Mathematisch-Naturwissenschaftlichen Fakultät

der

Universität Greifswald

vorgelegt von

Dmitry Mekhontsev

geboren am 06.03.1977

in Ust-Kamenogorsk, UdSSR

Greifswald, den 25.09.2018

Dekan: Prof. Dr. Werner Weitschies

1. Gutachter: Prof. Dr. Christoph Bandt

2. Gutachter: PD Dr. Dirk Frettlöh

Tag der Promotion: 22.01.2019

Contents

A	Introduction	5
1.	History and overview	5
2.	First examples: new rep-tiles	8
3.	Basic concepts	13
B	The main concepts and procedures	17
4.	Graph-directed IFS	17
5.	Bounding balls	22
6.	Neighbor graphs	26
C	Algebraic iterated function systems	37
7.	Lifting algebraic IFS to rational ones	37
8.	Projection of IFS	45
9.	Examples of rational forms	54
D	Invariants of GIFS attractors	63
10.	Hausdorff measure and dimension	64
11.	Moments	67
E	Notes on the IFStile program	71
12.	The language of IFStile	71
13.	Using the IFStile package	75
14.	The creator module	80
	Bibliography	83

Publications related to this thesis

- (1) C. Bandt, D. Mekhontsev and A. Tetenov, A single fractal pinwheel tile, *Proc. Amer. Math. Soc.*, 146:1271–1285, 2018.
- (2) C. Bandt and D. Mekhontsev, Elementary fractal geometry. New relatives of the Sierpinski gasket, *Chaos: An Interdisciplinary Journal of Nonlinear Science.*, 28(6):063104, 2018.
- (3) M. Samuel, D. Mekhontsev and A. Tetenov, On dendrites generated by symmetric polygonal systems: The case of regular polygons. In *Internat. Conf. on Advances in Math. Sciences 2017*, Trends in Mathematics (Book 1), 17-25, Springer, 2019.

A Introduction

1. History and overview

The present thesis subsumes many years of work. From 1999 to 2010, the author developed the program IFS Builder together with Alexey Kravchenko. It was designed to study iterated function systems (IFS) in two and three dimensions. It could draw self-similar and self-affine attractors generated by IFS, construct new fractals by modifying old ones, and study their geometrical properties by visual inspection. From 2009 to 2015, I developed another package Fractracer, which focused on IFS with nonlinear maps and included better algorithms for polygonization and three-dimensional representation. Here we are concerned with the latest package IFStile which was presented 2016 in the web and is presently available as version 1.8.1.4 for free download at ifstile.com [Mek18].

Self-affine tilings and fractals have found a lot of attention in recent years. Mathematical papers on various types of self-affine tiles come from different fields, like discrete geometry, algebraic number theory, dynamical systems, and theoretical computer science. A strong motivation came from physics with the discovery of quasicrystals by Shechtman et al. in 1984 which won the 2011 Nobel prize in chemistry. The best-known model of quasicrystals, the quasiperiodic tilings designed by Penrose, precluded the discovery of the materials by more than 10 years. See [GS87, Sen95, Rad99] for an introduction and [BG13, BG17] for a recent rigorous approach to aperiodic tilings, and the tiling encyclopedia [Fre18] for a large collection of geometrically defined examples.

IFStile can be helpful for research in all these fields. The package considers self-affine tilings as a particular perfect case of self-affine fractals, and thus is particularly relevant for fractal geometry. Many experts study tilings and fractals for their own sake. Their beauty has attracted a large non-mathematical audience. Among others, several artists have been using IFStile.

The new package offers improved graphic procedures of its predecessors. However, it has a much greater functionality. It can construct and search large families of self-similar tiles and fractals, and analyze them automatically in different ways. A lot of new examples with extraordinary properties were found by computer search. A few examples are shown in Section 2 before we go into technical details. Many others can be found at ifstile.com, and in the papers [BMT18, BM18] in the appendix.

Various novel algorithms had to be developed for the IFStile package. Procedures had to be optimized in order to mathematically construct up to several thousand

fractals per second and at the same time analyze their properties. The purpose of this thesis is to give a first rigorous account of various mathematical concepts and methods underlying these algorithms.

Basic notions are given in Section 3. The main subject of this thesis is the class of graph-directed iterated function systems (GIFS) of affine maps in Euclidean space \mathbb{R}^d which fulfill the open set condition. This class together with some basic tools is introduced in Section 4. A central theme is the automatic check of open set condition and finite type property described in Chapter B. The method of bounding balls, which seems new for GIFS, is used for controlling the size of fractals and their pieces. An algorithm for the calculation of all neighbor maps seems also new in the general case of GIFS, similarity mappings with different factors, and affine mappings. When there are only finitely many proper neighbor maps, we say that the GIFS has finite type.

Calculations with IFStile are rigorous and very fast due to the use of integer arithmetics. Numerical approximation is also possible. It is applied only when the data input consists of real numbers. The majority of interesting tiles and fractals in the literature, however, is given by algebraic numbers. Certain self-similar tiles must be given by Perron numbers, as shown by Kenyon and Solomyak [KS10], see also [Ken96, Kwa16, Thu89]. If the mappings contain only algebraic numbers, they can be lifted to maps with rational coefficients in a higher-dimensional space, and all computations can be performed very fast with exact integer arithmetics. Then they can be projected down again to appropriate eigenspaces of operators. The corresponding techniques of linear algebra, which differ a bit from the cut-and-project method often used for quasiperiodic tilings [BG13, BG17], are presented in Chapter C.

In particular it will be explained that finite type tilings and fractals do organize in families. Each family is characterized by an algebraic expansion map, a compatible symmetry group of matrices with algebraic entries, and a graph structure for the IFS. Once this family is defined, the IFStile package can search for all instances of the family, varying the symmetry maps and integer translation vectors, and checking the finite type condition.

The neighbor graph is a starting point to determine many properties and invariants which code the geometric appearance of the fractals. Among others, such properties are required to automatically detect isomorphic GIFS during a search. We determine Hausdorff dimension of both sets and their various boundary sets, and also relative Hausdorff measures in the respective dimension as well as some of their moments. Combinatorial invariants are derived from the neighbor graph of the IFS. All this will be discussed in Chapter D.

The last chapter contains a brief manual of the IFStile package and the description of some of its features. Great effort was done to save the user of IFStile from calculations with lots of coordinates and coefficients of mappings. The program comes with a special language, introduced after the basic definitions in Section 12. It provides a convenient notation of the GIFS and their generated families by both the user and the computer. The program is able to fill gaps in the initial data

and find the right fractals by random search. The creator module, described in the last section, allows to construct fractals by only prescribing dimension and graph structure, without providing any detail information.

The appendix contains three papers which are based on the use of IFStile. The fractal pinwheel is a simple self-similar tile with fractal boundaries and irrational rotations involved. The new Sierpinski relatives are unusual fractals which were found with IFStile by taking the well-known Sierpinski triangle as initial dataset. For the study of fractal trees related to polygons, the use of program was also crucial. Many other applications seem to be possible.

This thesis is only a first step towards a more careful computer-assisted mathematical analysis of tilings and fractals. Time constraints did not allow for a discussion of all mathematical features implemented in IFStile. There are many open problems, and a lot of mathematical experiments have to be performed. I strongly hope that the description of the program and the verification of its mathematical correctness will motivate researchers to use IFStile as a standard tool.

I thank my advisor Prof. Christoph Bandt for inviting me for one-month visits at Greifswald university in spring 2017, spring 2018, and autumn 2018, for accepting me as a PhD student, and for many discussions and suggestions concerning this thesis. I gratefully acknowledge the financial support of Deutsche Forschungsgemeinschaft, project Ba 1332/11-1.

2. First examples: new rep-tiles

A closed set A with non-empty interior in plane or space is called a rep- m tile [Gar63, Gol64, Ban91, GS87] if there are sets A_1, A_2, \dots, A_m congruent to A , such that different sets A_i, A_j have no common interior points, and a similarity mapping g with

$$(1) \quad g(A) = A_1 \cup A_2 \dots \cup A_m .$$

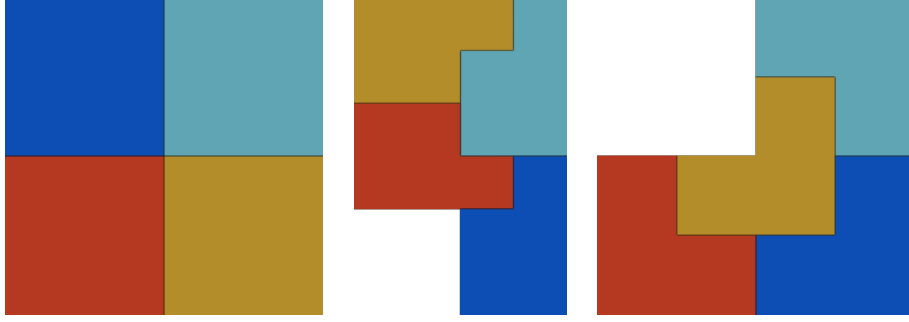


FIGURE 1. rep-4 tiles on the plane.

For the plane, plenty of rep- m tiles are known for every m . Figure 1 shows three examples for $m = 4$ and $g(x) = 2x$. The congruence maps h_i which transform A to A_i have the form $h_i(x) = q_i(x) + t_i$ where t_i is a vector with integer coordinates and q_i is a symmetry map of the unit square (with vertices $(\pm 1, \pm 1)$ and centre zero). It is custom to take $A = A_1$ so that h_1 is the identity map.

In three-dimensional space, there are few rep- m tiles for $m < 8$ [MS11, Ban10]. Even for $m = 8$, not too many examples are known. Some are shown in Figure 2. The regular tetrahedron or octahedron is not a rep- m tile.

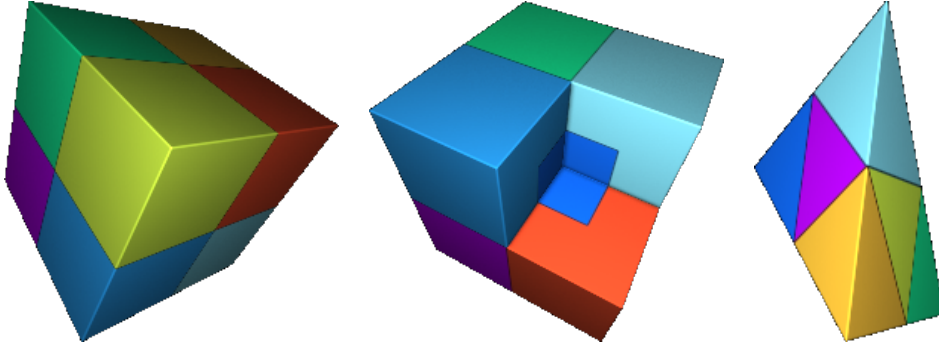


FIGURE 2. Cube, Notched cube [HR00] and Hill tetrahedron [Hil95].

Again, the similarity map is $g(x) = 2x$, and the congruence maps have the form $h_i(x) = q_i(x) + t_i$ where t_i denotes an integer translation and q_i a symmetry map of the unit cube with center 0. If this family of maps is given to the IFStile program, and a search is started, many thousand examples are found within minutes. Most

of them have a fairly intricate structure but some are also polyhedra and can be understood by eyesight. Figure 3 shows three examples which seem to be new.

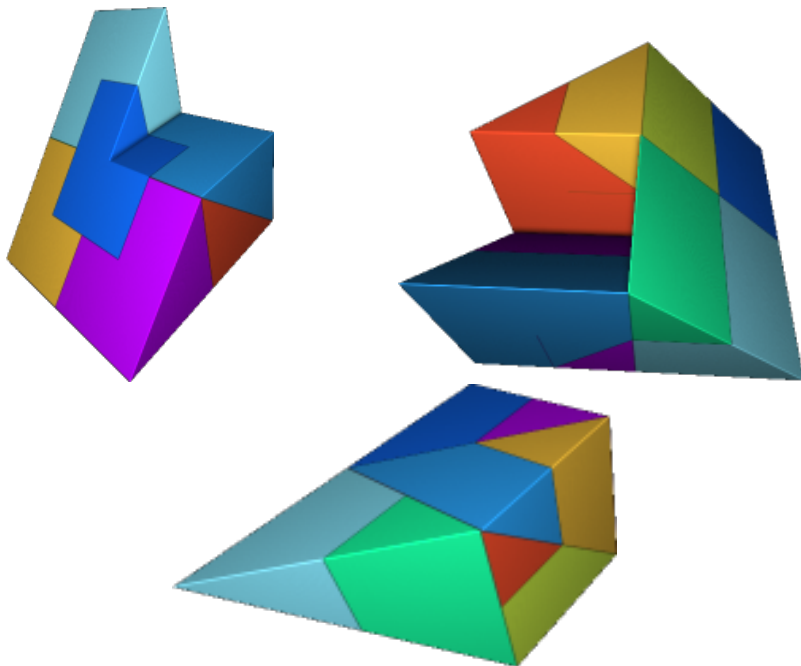


FIGURE 3. Some new polyhedral tiles with connected interior.



FIGURE 4. New polyhedral rep-8 tile with a hole.

A few years ago, it was not so clear whether rep- m tiles can have holes. In [FS10] an example with $m = 24$ was given, in [CT16] a more sophisticated and interesting

example with very large m . Figure 4 shows one of several polyhedral rep-8 tiles with a hole which was found by the program.

Since three-dimensional fractal structure is difficult to visualize in a single static picture, we shall mainly confine ourselves to two-dimensional figures in this thesis. Even for the simple family of Figure 1, the program finds lots of interesting fractal modifications. In Figure 5 we see a tile which is homeomorphic to a disc, so its boundary is topologically a circle. However, the length of the boundary, defined as one-dimensional Hausdorff measure, is infinite. This can be proved by the methods described in Chapter D. Boundary dimension and measure belong to the standard properties which are determined by the IFStile program for each example.

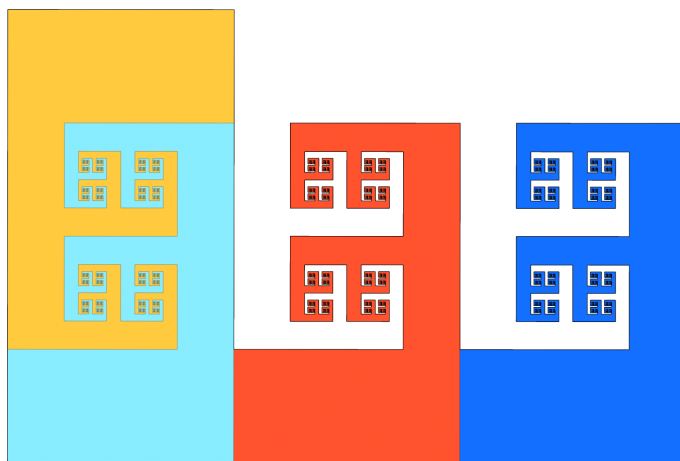


FIGURE 5. Reptile with infinite border of dimension 1.

The following tile is not a topological disc but still has a fairly simple structure. Its interior consists of two components. The closures of these interior components have an interval in common.

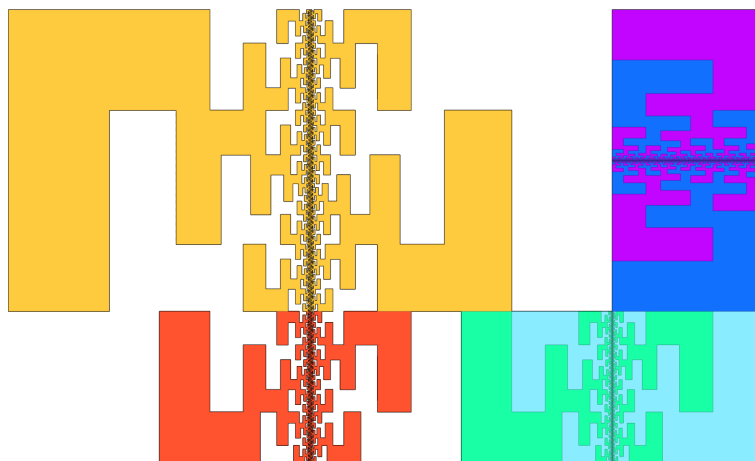


FIGURE 6. Tile with incomparable factors $1/3$ and $2/3$.

This tile is not a rep-tile since the pieces are not congruent, only similar to each other. Self-similar and self-affine tiles are defined in the next section. The factors $1/3$ and $2/3$ are not rationally related on logarithmic scale, and it seems difficult to find such tilings, except for trivial cases like a square or triangle.

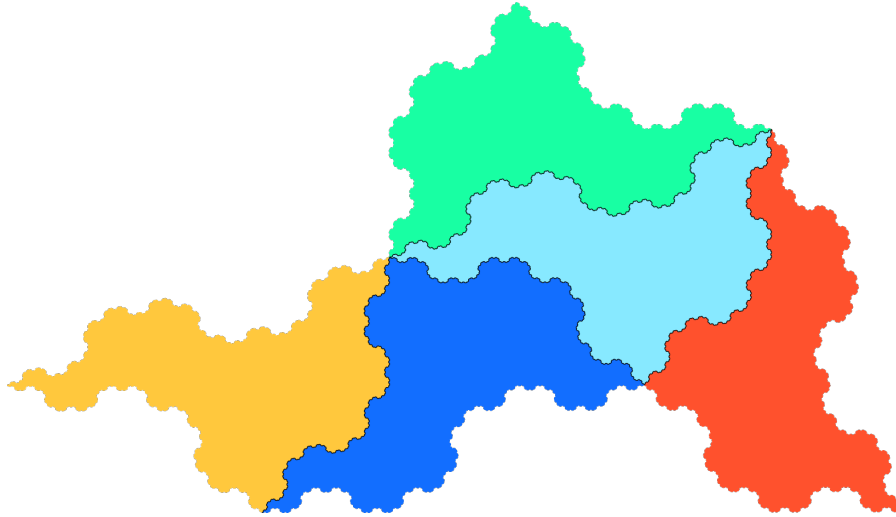


FIGURE 7. Fractal pinwheel.

The fractal pinwheel tile from Figure 7 with statistical circular symmetry [Fre08] was found using a computer search [BMT18] [Ven12]. It is an analogue of the well-known Pinwheel tile [Rad94] with a fractal boundary.

We finish this section with a self-similar topological disc with five pieces of two different sizes which I termed “bird”. Here we have two sizes of pieces. The similarity ratio between the whole and the pieces is $r_1 = 1/3$ and $r_2 = 1/\sqrt{3}$. Since $\log r_1 / \log r_2 = 2$, the factors are rationally related on logarithmic scale. It is known that in such cases the factors must be algebraic numbers [Ken96, KS10, Kwa16], and the framework developed in Chapter C will cover such examples while Figure 6 goes beyond this class.

There is a great variety of other tiles found by IFStile. Some of them are shown as a gallery on the web page ifstile.com. This thesis is devoted to the theory which underlies the program.

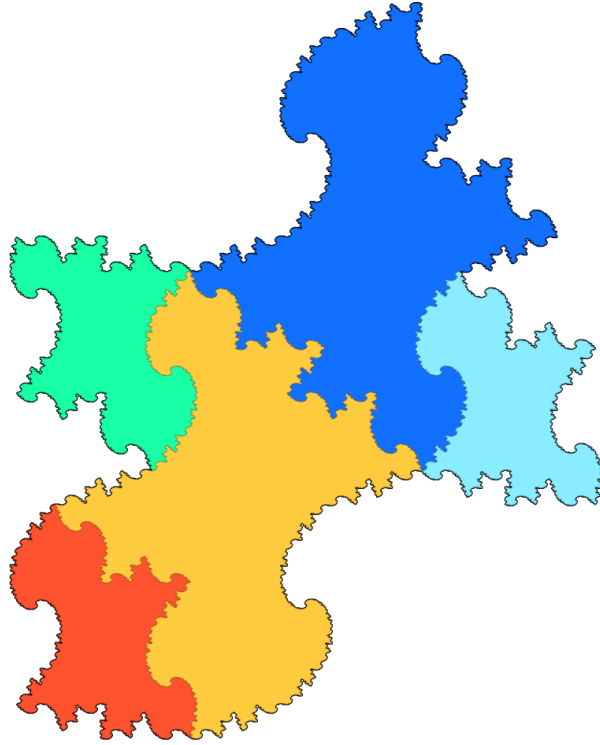


FIGURE 8. “Bird” tile with factors $1/3$ and $1/\sqrt{3}$.

3. Basic concepts

3.1. Metric geometry. We recall some definitions which apply to an arbitrary metric space X . In our case, X will be the Euclidean space \mathbb{R}^d , or sometimes \mathbb{C}^d . Let $\|x - y\|$ denote the Euclidean distance between two points x, y . For any $S \subset X$ and $x \in X$, the distance between S and x is written as

$$\|x - S\| = \inf_{y \in S} \|x - y\| .$$

For $\epsilon > 0$ the open ϵ -neighborhood of S is

$$U(S, \epsilon) = \{x \in \mathbb{R}^d : \|x - S\| < \epsilon\} .$$

For $S = \{x\}$, this is the open ball with center x and radius ϵ . For the closed ball with center x and radius r we write $B(x, r)$. Closure and interior of a set S are denoted by \overline{S} and $\text{int } S$, respectively. The diameter of a set S is

$$\text{diam}(S) = \sup_{x, y \in S} \|x - y\| .$$

For subsets $S, T \subset X$ the Hausdorff distance between S and T is

$$d_H(S, T) = \max\left\{\sup_{s \in S} \inf_{t \in T} \|s - t\|, \sup_{t \in T} \inf_{s \in S} \|s - t\|\right\} .$$

3.2. Matrices and affine maps. When $x \in \mathbb{R}^d$ is considered as a vector V , it will be a column vector, and $V(i)$ denotes the i th coordinate for $1 \leq i \leq d$. The elements of a matrix A are written $A(i, j)$. Let \mathcal{M}_d denote the set of square matrices with d rows and columns. The identity matrix from \mathcal{M}_d is called I_d .

For $A \in \mathcal{M}_d$ the spectrum is denoted by $\text{sp}(A)$, the spectral radius is denoted by $\rho(A)$. An affine map on \mathbb{R}^d has the form

$$f(x) = Ax + b \quad \text{with} \quad A \in \mathcal{M}_d \quad \text{and} \quad b \in \mathbb{R}^d .$$

For any affine map f we define

$$\|f\| = \sup_{x, y \in X} \frac{\|f(x) - f(y)\|}{\|x - y\|} = \sup_{x \in X \setminus \{0\}} \frac{\|Ax\|}{\|x\|} = \|A\| = \sqrt{\rho(A^T A)}$$

We call f a **contraction** if $\|A\| < 1$. If f is invertible we write f^{-1} for the inverse of f . The determinant of an affine map $f(x) = Ax + b$ is the determinant of the matrix A . Define

$$r(f) = |\det(f)|^{1/d} .$$

For any affine maps f_1 and f_2 we have the following property.

$$r(f_1 f_2) = r(f_1) r(f_2)$$

The map f is called a similarity map with factor $r = r(f) > 0$ if

$$\|f(x) - f(y)\| = r \cdot \|x - y\| \quad \text{for all } x, y \in \mathbb{R}^d .$$

This means that $A = rB$ where B is an orthogonal matrix.

3.3. Iterated function systems. A finite set F of affine maps is called an iterated function system or IFS:

$$(2) \quad F = \{f_1, \dots, f_m\} \quad \text{with} \quad f_k(x) = a_k x + b_k, \quad a_k \in \mathcal{M}_d, \quad b_k \in \mathbb{R}^d$$

An IFS is called **contractive** if there is an integer $N > 0$ that every composition of the maps from F of length N is contractive: $\|f_{k_1} f_{k_2} \dots f_{k_N}\| < 1$.

A compact and non-empty set $C \subset \mathbb{R}^d$ is called **attractor** if it is a solution of the following equation:

$$(3) \quad C = f_1(C) \cup f_2(C) \cup \dots \cup f_m(C).$$

PROPOSITION 1 (Hutchinson's theorem [Hut81], cf. [Bar93, Fal14]). *Any contractive IFS has unique attractor.*

The attractor C will also be called a self-affine set, or self-similar set when all f_k are similarity maps. This was the case for the rep-tiles in the section above. Equation (1) is a special case of equation (3), with $C = A$ and $f_k(x) = g^{-1}h_k(x)$, where h_k is the congruence map transforming A into A_k .

3.4. Tilings and open set condition. An important property of an IFS F is the open set condition, briefly OSC: there exists a non-empty open set $U \subset \mathbb{R}^d$ such that

$$(4) \quad f(U) \subset U \quad \text{and} \quad f(U) \cap f'(U) = \emptyset \quad \text{for} \quad f, f' \in F, f \neq f'.$$

When the OSC is fulfilled, then the attractor C of F has a nice structure. In particular, when C has non-empty interior and OSC holds then C is a tile. That means that

$$\mathbb{R}^d = C_1 \cup C_2 \cup C_3 \cup \dots$$

where each $C_j = h_j(C)$ is a copy of C by some affine map h_j , and the intersection $C_j \cap C_k$ of any two different copies has empty interior. The rep-tiles of the preceding section are examples of tiles. Since for a rep- m tile with an expanding similarity map g , all f_k are similarity maps with the same contraction factor, the C_j are all congruent to C . However, in this thesis we shall consider much more general tilings. We can always imagine that tilings can be obtained by magnifying the structure of C in the vicinity of an interior point of C .

3.5. The Levy curve. We conclude this chapter with a well-known example shown in Figure 9. It is in fact a rep-2 tile but this fact was not so obvious even for the great probabilist Paul Levy who discovered it. In (3) we have $m = 2$, and the mappings are $f_1 = g^{-1}h_1$, $f_2 = h_2g^{-1}$ where

$$g(x) = \begin{pmatrix} 1 & -1 \\ 1 & 1 \end{pmatrix} \cdot x, \quad h_1(x) = x + \begin{pmatrix} 0 \\ 1 \end{pmatrix}, \quad h_2(x) = \begin{pmatrix} 0 & -1 \\ 1 & 0 \end{pmatrix} \cdot x + \begin{pmatrix} -1 \\ 0 \end{pmatrix}.$$

This representation of f_k by expanding integer matrix and congruence mappings h_k is used for many examples analyzed by the IFStile package. The Levy curve fulfills the OSC and is a tile, but its structure is very complicated. Only after 2000, the dimension of its boundary was calculated as 1.97... With IFStile, structure and boundary of such examples can now be determined within milliseconds.

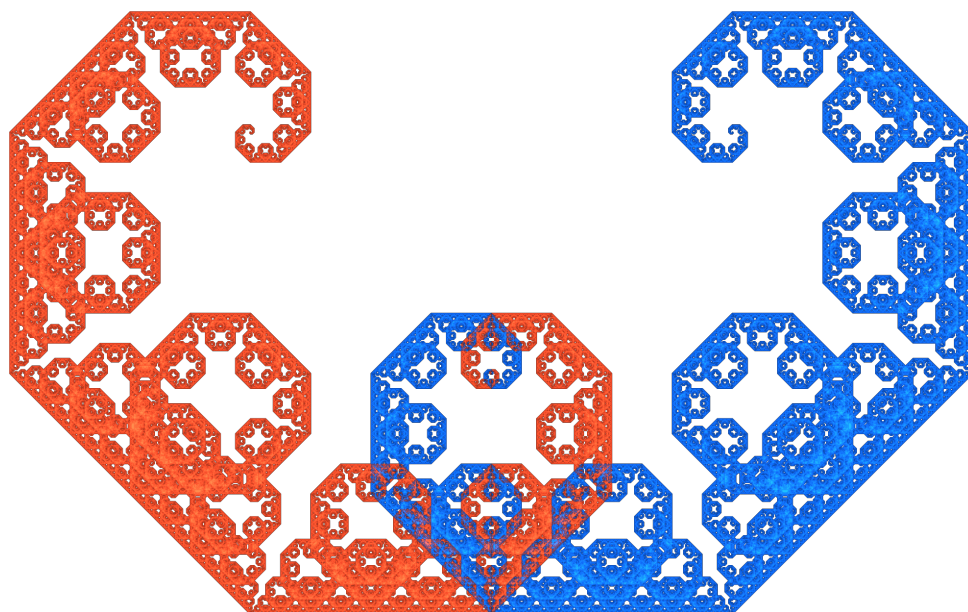


FIGURE 9. Levy curve: a rep-2 tile with complicated boundary.

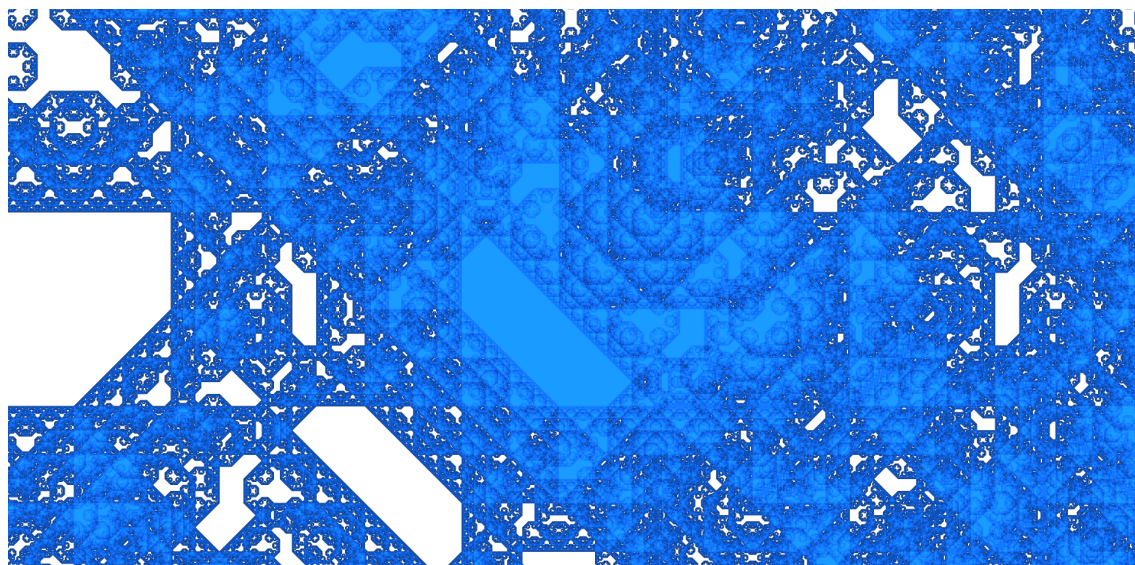


FIGURE 10. Zoomed Levy curve with interior components.

B The main concepts and procedures

4. Graph-directed IFS

4.1. A GIFS dragon. In Figure 11 you see an interesting "dragon" with sets C_1 and C_2 that consist of smaller copies of each other.

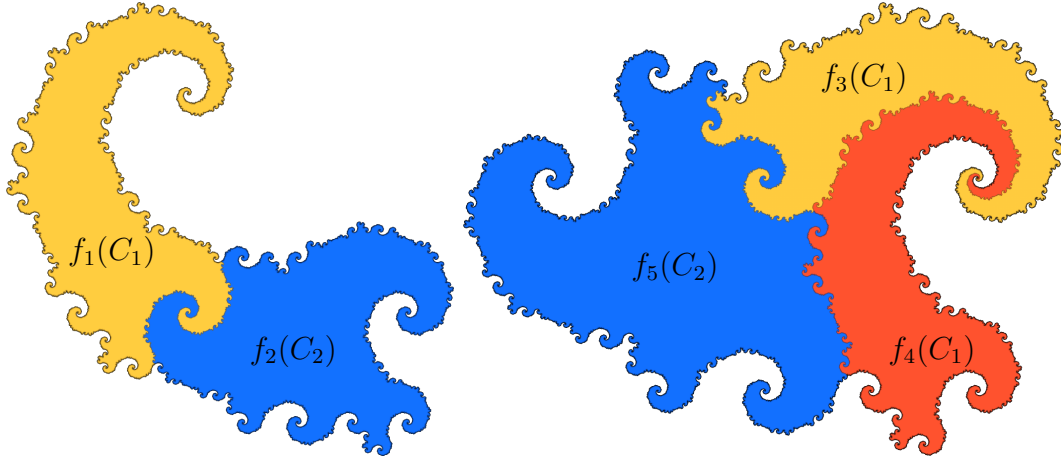


FIGURE 11. GIFS dragon C_1 and C_2 .

This can be expressed by the following equations:

$$\begin{aligned}
 C_1 &= f_1(C_1) \cup f_2(C_2) \\
 C_2 &= f_3(C_1) \cup f_4(C_1) \cup f_5(C_2) \\
 f_1(x) &= g^{-1}(x) \\
 g &= \begin{pmatrix} 1 & -1 \\ 1 & 1 \end{pmatrix} & f_2(x) &= g^{-2}s(x + [1, -1]) \\
 s &= \begin{pmatrix} 0 & -1 \\ 1 & 0 \end{pmatrix} & f_3(x) &= g^{-1}(x + [1, 0]) \\
 & & f_4(x) &= g^{-1}s^3(x + [0, 1]) \\
 & & f_5(x) &= g^{-1}s^2(x + [0, 2])
 \end{aligned}$$

It turns out that this GIFS has the same integer-valued expansion matrix and the same symmetry group as Twindragon, Heighway dragon, the and Levy Curve in Figure 9.

Another way to describe the sets C_1 and C_2 is the graph from Figure 12 below.

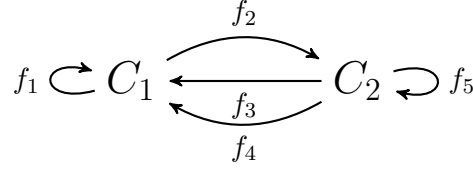


FIGURE 12. Graph of the dragons.

4.2. Definition. The graph from Figure 12 has the following features:

- (1) All edges have a direction (**directed graph**).
- (2) All edges are labeled by affine maps on \mathbb{R}^d (**labeled graph**).
- (3) Two vertices can be connected by multiple edges (**multigraph**).
- (4) Every vertex have at least one outgoing edge.
- (5) An edge can connect a vertex to itself.

A graph with vertices $\{1, \dots, n\}$ that fulfills the above properties is called a graph-directed IFS or **GIFS**. The case of an ordinary IFS corresponds to a graph with one vertex.

We use **adjacency lists** of outgoing edges to represent a GIFS: for every vertex $i = 1, \dots, n$ we define a non-empty set Q_i as a list of pairs (f, j) where each pair corresponds to exactly one directed edge $i \xrightarrow{f} j$ from the vertex i to the vertex j labeled by the affine map f .

We denote by $\phi(G)$ the set of all affine maps that are used to label edges in a GIFS G :

$$(5) \quad \phi(G) = \{f \mid (f, j) \in Q_i \text{ for some } i, j \in \{1, \dots, n\}\}$$

A vector of compact and non-empty sets (C_1, C_2, \dots, C_n) where $C_i \subset \mathbb{R}^d$ is an **attractor** of G if the sets fulfill the following equations:

$$(6) \quad C_i = \bigcup_{(f,j) \in Q_i} f(C_j) \quad i = 1 \dots n$$

THEOREM 2 (Mauldin and Williams [MW88]). *Let G be a GIFS. If $\|f\| < 1$ for all $f \in \phi(G)$ then there is a unique attractor.*

Like for an ordinary IFS (4), a GIFS fulfills **open set condition** if there exist non-empty open sets U_1, \dots, U_n , $U_i \subset \mathbb{R}^d$ such that

$$(7) \quad \bigcup_{(f,j) \in Q_i} f(U_j) \subset U_i \quad i = 1 \dots n$$

and the union in (7) is disjoint. Although we usually do not require the OSC, all examples in the paper fulfill it.

Define the following set of maps:

$$(8) \quad \phi^*(G) = \{f_1 f_2 \dots f_m \mid \text{there is a path } i_1 \xrightarrow{f_1} i_2 \xrightarrow{f_2} i_3 \dots i_m \xrightarrow{f_m} i_{m+1} \text{ in } G\}$$

We assume that $\phi^*(G)$ contains the identity map that corresponds to the path of length zero. For ordinary IFS $\phi^*(G)$ is a semigroup generated by the maps from

$\phi(G)$. Usually, $\phi^*(G)$ is used to describe the small subcopies of attractors C_i which appear as “parts of parts” on level 2,3,... Since we generally study maps with different contraction ratios, we shall not speak about levels, but about uniform subdivisions. This will be explained below.

Let T be some rectangular matrix. We denote by TG and GT the GIFS which are obtained from G by replacing all maps $f \in \phi(G)$ by compositions Tf and fT respectively (if they are defined). If all maps from $\phi(G)$ are invertible and every vertex has at least one incoming edge, then we can define G^{-1} as a GIFS that is obtained by reversing the direction of every edge in G and replacing all label maps $f \in \phi(G)$ by f^{-1} .

DEFINITION 3. *Two GIFS G and G' are **isomorphic** if there is an invertible matrix T such that $TG = G'T$.*

If (C_1, \dots, C_n) is the attractor of G then (TC_1, \dots, TC_n) is the attractor of TGT^{-1} .

4.3. Uniform subdivisions. Considering (6) as a system of equations, we can substitute the definition of any C_j in any place where it occurs on the right side. This corresponds to the replacement of some edge $(f, j) \in Q_i$ starting at vertex i by the edges $\{(fg, k) \mid (g, k) \in Q_j\}$. We call this operation an **elementary edge subdivision**. It produces a new GIFS with the same vertices, but with other outgoing edges Q'_i for the vertex i . We can do such substitutions several times in any order, and, by construction, all new GIFS have the same attractor as the original one.

For every vertex i of G we now define an infinite sequence of special edge subdivisions that we call **uniform**:

$$Q_i^0, Q_i^1, Q_i^2, \dots$$

Every Q_i^r is a set of pairs (f, j) where $f \in \phi^*(G)$ and $j = 1, \dots, n$ is a vertex. Define $Q_i^0 = \{(i, I_d)\}$ and $Q_i^1 = Q_i$ and denote

$$\|Q_i^r\| = \max_{(f,k) \in Q_i^r} \|f\|$$

Then Q_i^{r+1} is obtained from the previous Q_i^r by replacing “the biggest edges”: every $(f, j) \in Q_i^r$ with $\|f\| = \|Q_i^r\|$ will be replaced by pairs $(f \cdot f_1, j_1), (f \cdot f_2, j_2), \dots$ where $(f_s, j_s) \in Q_j$.

PROPOSITION 4. *We can replace Q_i in the definition of the attractor (23) with Q_i^r for any $r \geq 1$.*

PROOF. The replacement of the biggest edges is a series of elementary edge subdivisions that preserve the attractors. \square

DEFINITION 5. *A GIFS is called **contractive** if there is an integer $N > 0$ such that $\|Q_i^N\| < 1$ for any vertex i . In other words, there are only finitely many maps f in $\phi^*(G)$ with $\|f\| \geq 1$.*

A contractive GIFS always has a unique attractor. This follows from Proposition 4 and Theorem 2. In this case

$$(9) \quad \lim_{r \rightarrow \infty} \|Q_i^r\| = 0$$

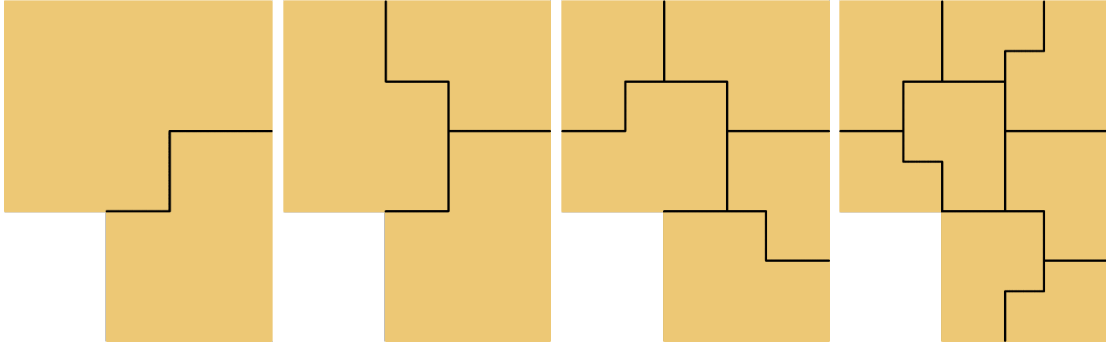


FIGURE 13. Uniform subdivisions of the Ammann hexagon (Section 7.4).

Although some non-contractive GIFS have a unique attractor, in this work we are only interested in attractors of contractive GIFS. In practice it is useful to have a constructive way to verify that a GIFS is **not** contractive.

PROPOSITION 6. *If there is a vertex i , $1 \leq i \leq n$ and an integer $N > 0$ such that $(f, i) \in Q_i^N$ and $|\det(f)| \geq 1$ then the GIFS is not contractive.*

PROOF. $(f, i) \in Q_i^N$ means that there is a loop in the graph defined by Q_1^N, \dots, Q_n^N , and this loop is labeled by f with $|\det(f)| \geq 1$. If we continue to subdivide Q_i , we will get an increasing sequence $N = N_1 < N_2 < \dots$ with $(f^k, i) \in Q_i^{N_k}$ and $|\det(f^k)| \geq 1$ which contradicts Definition 5. \square

For any contractive GIFS we define the ϵ -subdivision using (9):

$$(10) \quad Q_i(\epsilon) = Q_i^s \quad \text{where} \quad \|Q_i^s\| \leq \epsilon \quad \text{and} \quad \|Q_i^r\| > \epsilon \quad \text{for any} \quad r < s.$$

So for every vertex i

$$(11) \quad \lim_{\epsilon \rightarrow 0} \|Q_i(\epsilon)\| = 0$$

4.4. Strongly connected components. GIFS that we can usually find in mathematical works have relatively simple structure. In particular, there is a directed path between any vertices. Such GIFS are called **strongly connected**. But when we start to work with intersections and boundaries of attractors which can be also described as GIFS, we immediately get huge exotic graphs. As explained in Section 6.8, the GIFS of intersections for the dragons in Figure 11 is not strongly connected. Such features of the boundary GIFS carry a lot of useful topological information about the attractor itself. This is one of the reasons why we consider the most general case of GIFS.

We call a subset of the vertex set V of a graph G a **strongly-connected component** if there is a directed path between any two vertices of the subset. Each vertex that does not have a directed path to itself is also considered as a component. Then the vertex set V is a disjoint union $V = V_1 \cup V_2 \dots \cup V_s$ of strongly connected components [CLRS09]. Vertices from different components do not belong to any directed cycle of edges. We can define a directed acyclic graph (DAG) with vertices $1, 2, \dots, s$, by connecting vertices i and j of the DAG with an edge iff there is a

directed path from some vertex in V_i to some vertex in V_j . We can assume that numeration of the components agrees with topological sorting of the DAG. That is, if there is a path from component V_i to V_j then $i \geq j$. Finally we can label all vertices of G by **component index**:

$$(12) \quad \psi_i = j \Leftrightarrow i \in V_j \quad i = 1, \dots, n$$

By definition, we have the following properties for ψ_1, \dots, ψ_n :

- (1) If there is a directed path from i to j then $\psi_i \geq \psi_j$.
- (2) $\psi_i = \psi_j$ only if i and j belong to the same directed cycle of G .
- (3) $1 = \psi_1 \leq \psi_2 \leq \dots \leq \psi_n$ for some numeration of vertices of G .

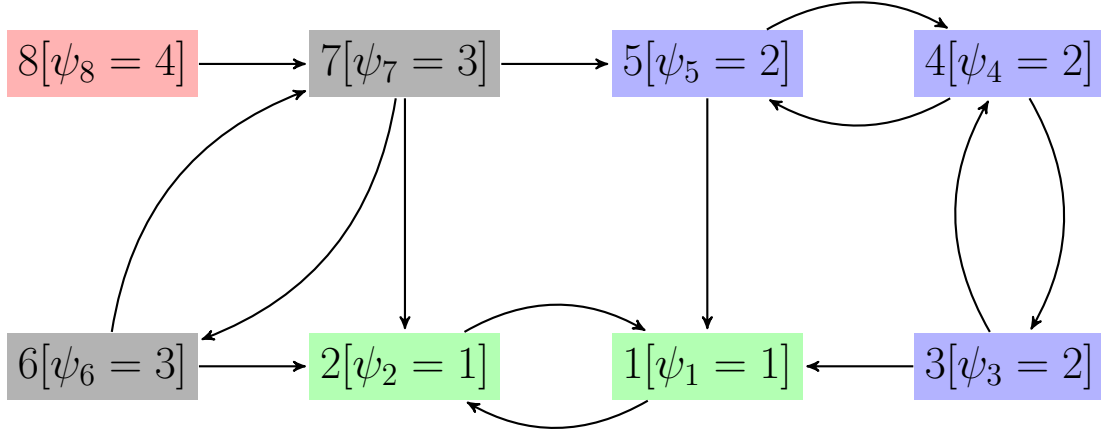


FIGURE 14. Graph with 4 components.

In Figure 14 we can see a graph with the vertices $V = \{1, \dots, 8\}$ and components $V_1 = \{1, 2\}$ (green), $V_2 = \{3, 4, 5\}$ (blue), $V_3 = \{6, 7\}$ (black), $V_4 = \{8\}$ (red). The vertices 1 and 2 have minimal component index $\psi_1 = \psi_2 = 1$ because there are no paths from them to any other component. The vertex 8 forms its own component with maximal index $\psi_8 = 4$.

4.5. Substitution tiles. Many examples in this paper are **substitution tiles**. According to [Fre05], a strongly connected GIFS G can be considered as a tile substitution if all C_i have non-empty interior, the interiors of the components $f(C_j)$ in (6) do not intersect, and there is a linear expanding map Q in \mathbb{R}^d such that Qf is an isometry for any $f \in \phi(G)$. The map Q is called an **inflation factor** [Fre18]. It is easy to see that such GIFS fulfill the OSC (7) if we take interiors of C_i as open sets U_i . Note that not every tile can be considered as a substitution tile, see Figure 6.

5. Bounding balls

5.1. Overview and motivation. The method of bounding balls is an extremely useful tool for analyzing GIFS. We use it for the basic question whether a GIFS is contractive, which can be non-trivial even for ordinary IFS. Bounding balls have to be constructed in such cases to verify that the attractor exists. Furthermore, bounding balls will be used

- (1) for effectively drawing and zooming attractors,
- (2) for the calculation of the neighbor graph in Section 6,
- (3) for computing some attractor invariants like diameters (cf. Chapter D).

Let (C_1, \dots, C_n) be the attractor of G . We call a ball $B_i = B(x_i, r_i)$ bounding ball of C_i if $C_i \subset B_i$. Obviously, bounding balls for a GIFS exist if and only if the attractor exists. Let r_i^* be the minimal radius of a bounding ball of C_i . Given a system (B_1, \dots, B_n) of bounding balls of the attractor, the **defect** of the system is the maximum of the ratios r_i/r_i^* for $i = 1, \dots, n$. The computing time of many algorithms greatly depends on the defect. On the other side, we need too much time to calculate ideal minimal bounding balls. Usually it is a good idea to have balls that have defect strictly greater than one, but less than some constant like $3/2$.

Our algorithm consists of several stages. At the first stage we check the existence of attractors and calculate preliminary bounding balls without estimates for the defect. At the second stage we calculate bounding **boxes** with prescribed precision. Then we switch to enclosing balls for the boxes and further decreasing their radii.

We present the algorithm for an arbitrary GIFS. For the case of ordinary self-similar sets, similar estimates were done by several authors in the 1990s. For GIFS, we have to proceed inductively, using the definition of the component index. We can calculate bounding balls for sets with lower index independently on sets with higher index, so we start from the sets with index 1, then do calculations for sets with index 2 and so on. This allows us to use already defined balls from the previous steps. We denote the current component index by ψ .

5.2. Centers of the balls. At first we calculate some point of every set C_i and use it as the center of a bounding ball B_i . If some vertex j belongs to a directed cycle in G labeled by $f_{i_1}, f_{i_2}, \dots, f_{i_s}$ then the fixed point of the composition $x_j = f_{i_1}f_{i_2}\dots f_{i_s}(x_j)$ must be contained in C_j . By the definition of the component index, every set C_j with $\psi_j = 1$ belongs to some directed cycle. So we can always calculate at least one point for such set. Induction is used to define the centers for vertices with higher component index. If a vertex j with $\psi_j > 1$ does not belong to a directed cycle, there must be a directed path from j to some vertex k with lower component index $\psi_k < \psi_j$, such that $C_j \supseteq f_{i_1}f_{i_2}\dots f_{i_s}(C_k)$. From previous steps we already have a center $x_k \in C_k$, so we can define $x_j = f_{i_1}\dots f_{i_s}(x_k) \in C_j$.

5.3. Radius of the balls and attractor existence. We begin by creating a uniform subdivisions $Q_i(\epsilon)$ (see Definition 10) for all i with $\psi_i = \psi$ and some $0 < \epsilon < 1$.

$$(13) \quad C_i = \bigcup_{(f,j) \in Q_i(\epsilon)} f(C_j) \quad i = 1 \dots n$$

To create the subdivisions we iteratively use Procedure 4.3. If it fails (that means that number of maps in some Q_i^m is greater than some prescribed constant), then we state that the GIFS is not contractive, the attractor does not exist and interrupt the procedure.

At this stage we need only rough estimates for the balls, so we use $\epsilon = 1/2$. Also we use the same radius r for all sets with the same component index: $r_i = r_j = r$ if $\psi_i = \psi_j = \psi$.

For every i with $\psi_i = \psi$ and every $(f, j) \in Q_i(\epsilon)$ we require $f(B_j) \subset B_i$, that is

$$(14) \quad \|f(x_j) - x_i\| + \|f\|r \leq r \quad \text{if } \psi_i = \psi_j$$

$$(15) \quad \|f(x_j) - x_i\| + \|f\|r_j \leq r \quad \text{if } \psi_i > \psi_j$$

So we have

$$(16) \quad r \geq \frac{\|f(x_j) - x_i\|}{1 - \|f\|} \quad \text{if } \psi_i = \psi_j$$

Since r_j is already determined at this step and $\|f\| \leq \epsilon$ we can define

$$(17) \quad r = \max(R_1, R_2)$$

where

$$(18) \quad R_1 = \max\left\{\frac{\|f(x_j) - x_i\|}{1 - \epsilon} : (f, j) \in Q_i(\epsilon), \psi_i = \psi = \psi_j\right\}$$

$$(19) \quad R_2 = \max\{\|f(x_j) - x_i\| + \|f\|r_j : (f, j) \in Q_i(\epsilon), \psi_i = \psi > \psi_j\}$$

5.4. Bounding boxes. Bounding balls that are found in the previous step can be arbitrarily greater than minimal balls. But we can use them to calculate **minimal bounding boxes** with required precision. At this stage we can already verify that an attractor exists.

For any $\epsilon > 0$ define a finite set of images of the centers of the bounding balls

$$h_i(\epsilon) = \bigcup_{(f,j) \in Q_i(\epsilon)} f(x_j)$$

Let

$$R_i(\epsilon) = \max_{(f,j) \in Q_i(\epsilon)} \|f\|r_j.$$

Then $R_i(\epsilon)$ converges to zero when ϵ tends to zero. We define the union of the balls around the points of $h_i(\epsilon)$

$$H_i(\epsilon) = \bigcup_{x \in h_i(\epsilon)} B(x, R_i(\epsilon))$$

PROPOSITION 7. $h_i(\epsilon)$ and $H_i(\epsilon)$ are lower and upper estimates of the attractor set C_i for every $i = 1, \dots, n$. More precisely,

$$h_i(\epsilon) \subset C_i \subset H_i(\epsilon) \quad \text{and} \quad d_H(h_i(\epsilon), H_i(\epsilon)) \leq R_i(\epsilon)$$

Consequently,

$$\lim_{\epsilon \rightarrow 0} d_H(h_i(\epsilon), C_i) = \lim_{\epsilon \rightarrow 0} d_H(H_i(\epsilon), C_i) = 0.$$

□

For every $S \subset \mathbb{R}^d$, the minimal box with sides parallel to the axis that contains S is called $\text{Box}(S)$. We define this box by two vectors $u, v \in \mathbb{R}^d$

$$\text{Box}(S) = \{z \in \mathbb{R}^d \mid u(k) \leq z(k) \leq v(k), \text{ for } k = 1, \dots, d\}$$

with $u(k) = \inf\{z(k) \mid z \in S\}$ and $v(k) = \sup\{z(k) \mid z \in S\}$.

There is a simple inequality between diameters of the minimal bounding box and ball.

PROPOSITION 8. Let R be the radius of the minimal ball that contains $S \subset \mathbb{R}^d$. Then

$$(20) \quad \text{diam}(\text{Box}(S)) \geq 2R \geq \text{diam}(\text{Box}(S))/\sqrt{d}$$

PROOF. The left inequality comes from the fact that the ball with radius $\frac{1}{2} \text{diam} S$ and midpoint in the center of $\text{Box}(S)$ contains S . The right inequality holds since $2R \geq v(k) - u(k)$ for $k = 1, \dots, d$. □

PROPOSITION 9. If $\text{diam}(C_i) > 0$ for some $1 \leq i \leq n$ then for any $\delta > 0$ there is an $\epsilon > 0$ such that

$$(21) \quad 1 \leq \frac{\text{diam}(\text{Box}(H_i(\epsilon)))}{\text{diam}(\text{Box}(h_i(\epsilon)))} \leq 1 + \delta$$

PROOF. From Proposition 7 we have

$$\text{diam}(\text{Box}(H_i(\epsilon))) \geq \text{diam}(\text{Box}(h_i(\epsilon)))$$

$$\text{diam}(\text{Box}(H_i(\epsilon)), \text{diam}(\text{Box}(h_i(\epsilon))) \xrightarrow{\epsilon \rightarrow 0} \text{diam}(\text{Box}(C_i)) > 0$$

□

Since $h_i(\epsilon)$ is a finite set that can be calculated by computer we can use the recursive construction of uniform subdivisions to get $\epsilon(\delta)$.

5.5. Improved balls. Let $B'_i(\epsilon) \supset C_i$ be the enclosed ball around $\text{Box}(H_i(\epsilon))$ with radius

$$r'_i = \text{diam}(\text{Box}(H_i(\epsilon)))/2$$

Then from (20) and (21) we have

$$\frac{2r'_i}{\text{diam}(\text{Box}(C_i))} \leq 1 + \delta$$

$$\frac{2r'_i}{2r_i^* \sqrt{d}} \leq 1 + \delta$$

PROPOSITION 10. *For every δ there is a uniform subdivision $Q_i(\epsilon)$ such that the corresponding bounding balls $B'_i(\epsilon)$ are at most $\sqrt{d}(1+\delta)$ times greater than minimal ones:*

$$r'_i \leq r_i^* \sqrt{d}(1 + \delta)$$

□

To reduce B'_i further without changing centers, we can use procedure similar to the preliminary radius calculation (5.3). On Figure 15 we use uniform subdivision $Q_1(\frac{1}{4})$ of the equilateral Sierpinski triangle (9.1) to decrease the initial black ball to the red one.

Remarks. Attractors with $\text{diam}(C_i) = 0$ must be considered separately, they can be easily detected from the graph structure and fixed points of the maps from $\phi^*(G)$.

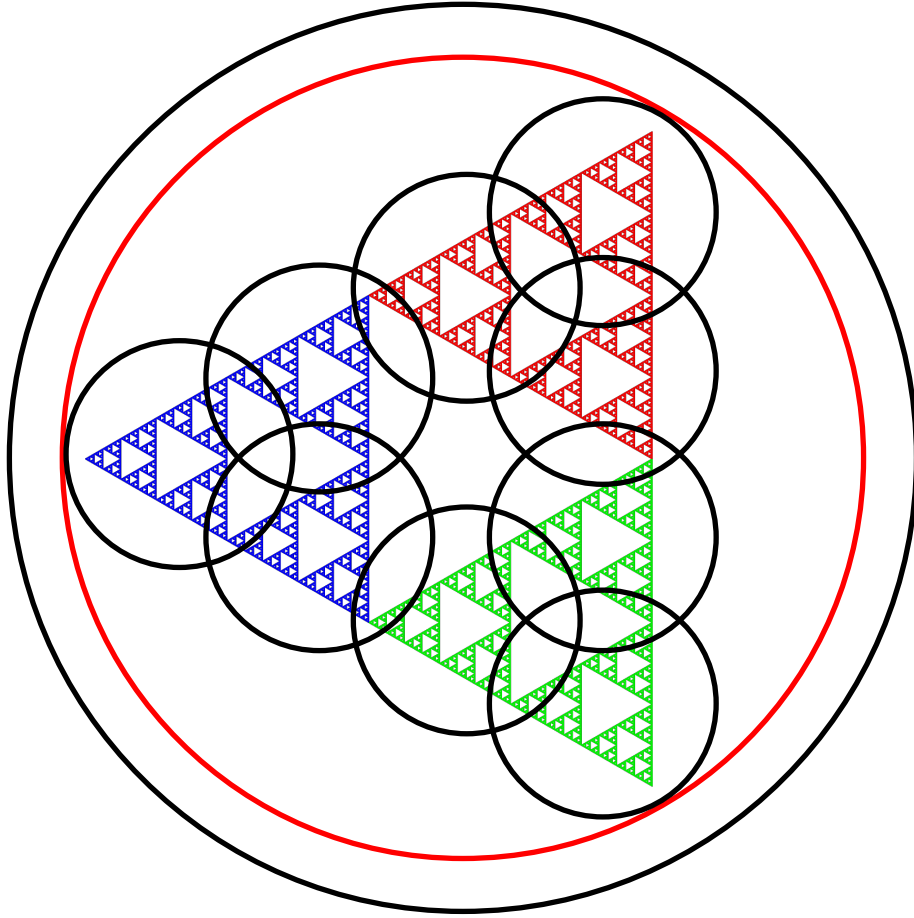


FIGURE 15. Ball refinement.

6. Neighbor graphs

6.1. Motivation. The most important tool that we use for GIFS analysis is the neighbor graph. A concept of neighbors is widely used in the literature [IRI92, SW99, ST03]. If a finite neighbor graph exists, we can determine many properties of the attractor.

- (1) We can check the open set condition.
- (2) We can express the boundary of the tile by a GIFS.
- (3) In the self-similar case we can calculate the Hausdorff dimension of the boundary.
- (4) We can check whether the attractor is connected.
- (5) We can determine various affine invariants, discussed in Chapter D.

The intersection of any two pieces of attractor (C_1, \dots, C_n) of GIFS G can be expressed as $f(C_i) \cap g(C_j)$ for some $f, g \in \phi^*(G)$. It is easy to see, that there are usually infinite number of such intersections. The main trick is a **standardization**: instead of $f(C_i) \cap g(C_j)$ we use "zoom" by f^{-1} and consider $C_i \cap f^{-1}g(C_j)$. Also we use uniform subdivisions (see 4.3). For many GIFS it gives only a **finite** number of intersections through the all levels. A triples $(C_i, C_j, f^{-1}g)$ correspond to the vertices of neighbor graph, and relative maps $f^{-1}g$ between pieces will be called neighbor maps. All intersections inherit the hierarchical structure of the attractor, so we have the opportunity to express every intersection in the same manner as we express attractors of GIFS.

6.2. The neighbors of the GIFS dragon. To demonstrate the neighbor graph concept, we use the GIFS dragon shown in Figure 11 from Section 4. Figure 16 shows a uniform subdivision of the attractor C_2 with smaller pieces. In the picture we can see a periodic pattern and different intersections between pieces. It seems that there are only few types of intersections, and we will not get new types if we further subdivide the attractor. Figure 17 shows all such types.

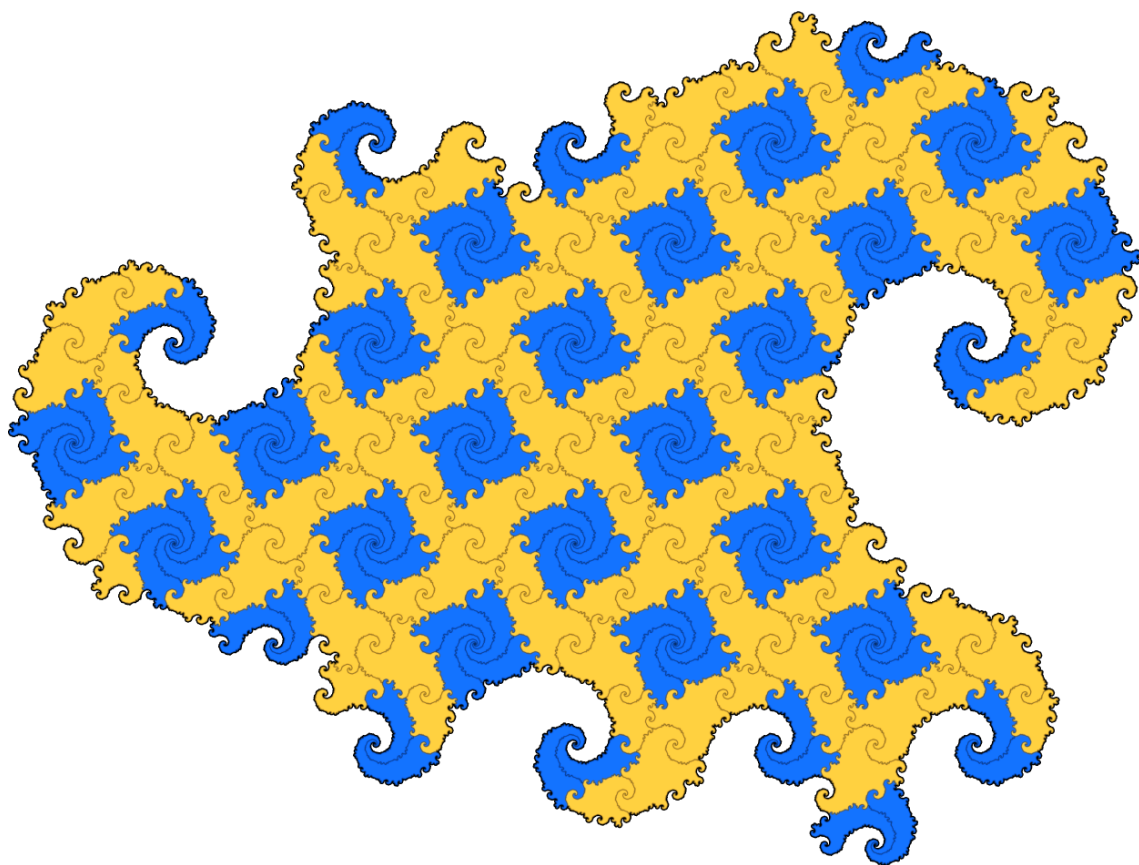


FIGURE 16. Second dragon subdivision.

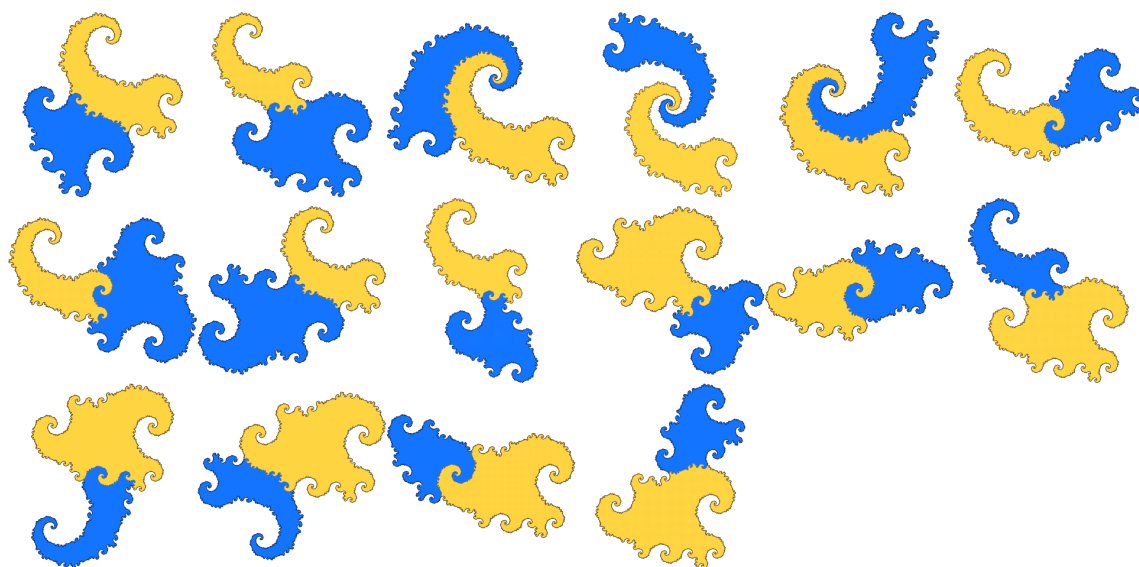


FIGURE 17. Dragon's neighbors

6.3. Construction of the neighbor graph of the GIFS dragon. We can see the hierarchical structure of intersections in Figure 18 where some part of the neighbor graph is shown graphically. The following list describes some steps in the construction of this graph, illustrated by corresponding numbers in the figure.

- (1) We start from the left of the diagram with label 1 - the top left intersection in Figure 17.
- (2) $1 \rightarrow D_1$ We divide the blue piece into three parts - red, blue and yellow.
- (3) $D_1 \rightarrow E_1$ The green piece $f_4(C_1)$ does not intersect the yellow piece. Empty intersections will not be in the neighbor graph.
- (4) $D_1 \rightarrow 2$ The blue piece $f_3(C_1)$ intersects the yellow piece, so we can continue. We don't have this intersection in Figure 17 because sizes of the pieces are very different.
- (5) $2 \rightarrow D_2$ Now we divide the big yellow piece into two parts - yellow and red.
- (6) $D_2 \rightarrow 5$ The red piece equals $f_2(C_2)$ and intersects the blue piece. We continue along f_2 .
- (7) $5 \rightarrow D_3$ We divide the big red piece into 3 parts - blue, red and green.
- (8) $D_3 \rightarrow 1'$ The blue piece is $f_5(C_2)$ and intersects the yellow piece. Now we can see that pieces in the new intersection have exactly the same relative position as in the the first intersection!
- (9) We have intersections labeled by 3 and 7, so we should continue to divide them further. This part of the diagram is not shown.
- (10) After a finite number of steps we will see that there are no elements to divide, and all intersections from Figure 17 are in the diagram.

The complete neighbor graph with 33 vertices is given in Table 1. All edges are labeled by maps f_1, \dots, f_5 . Each line in Table 1 corresponds to one type of intersection. For example, consider the second line: the third column $v_2 = (1, 2, h_2)$ means that $v_2 = C_1 \cap h_2(C_2)$, the last column $(v_2, v_{10}, f_1), (v_2, v_{11}, f_2)$ means that $v_2 = f_1(v_{10}) \cup f_2(v_{11})$.

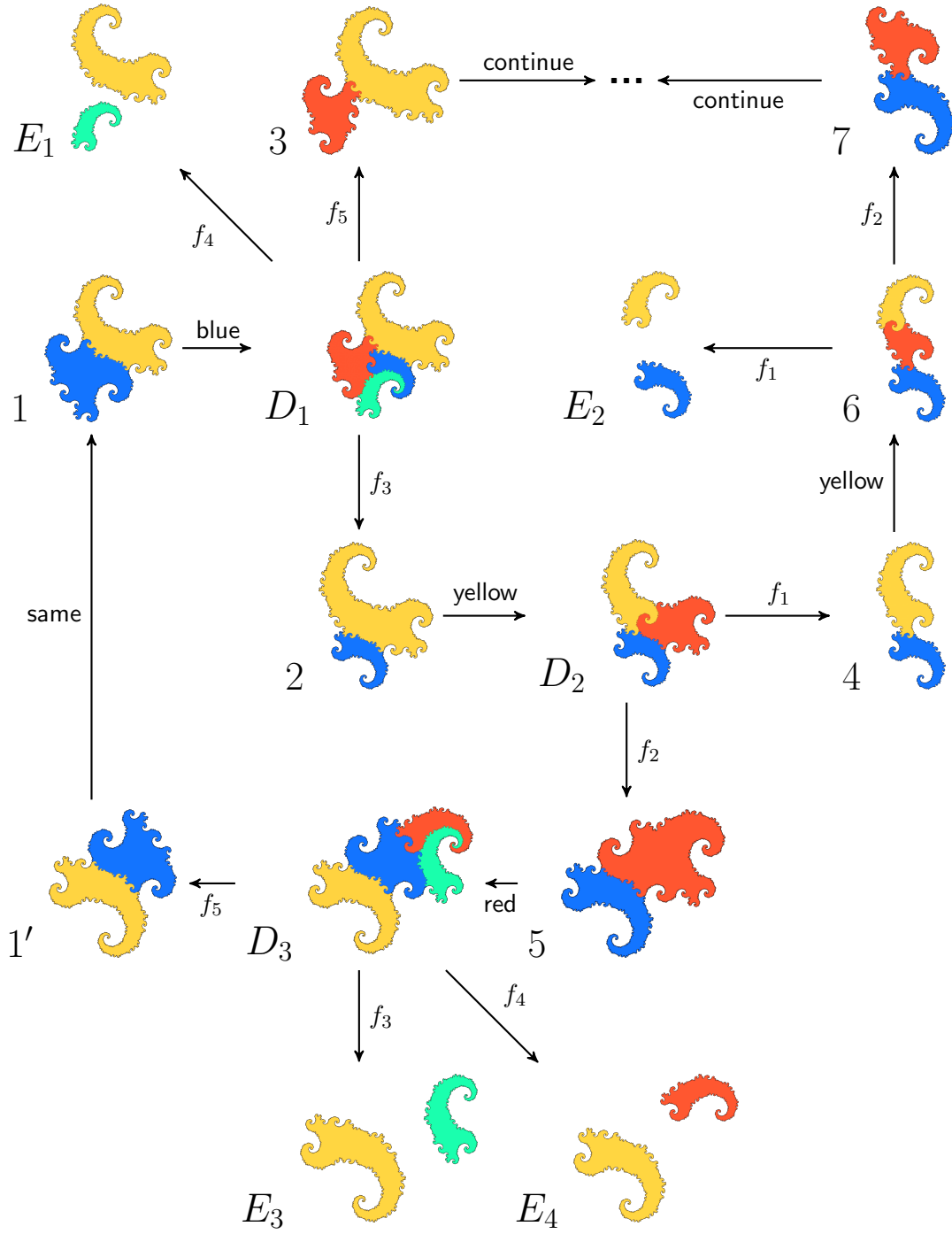


FIGURE 18. Part of the neighbors subdivision diagram.

$ \det \leq 1$	map	$vertex$	$edges$
+	$h_1 = f_3^{-1}f_4$	$v_1 = (1, 1, h_1)$	(v_1, v_9, f_1)
+	$h_2 = f_3^{-1}f_5$	$v_2 = (1, 2, h_2)$	$(v_2, v_{10}, f_1), (v_2, v_{11}, f_2)$
+	$h_3 = f_4^{-1}f_3$	$v_3 = (1, 1, h_3)$	$(v_3, v_{12}, f_1), (v_3, v_{13}, f_2)$
+	$h_4 = f_4^{-1}f_5$	$v_4 = (1, 2, h_4)$	(v_4, v_{14}, f_2)
+	$h_5 = f_5^{-1}f_3$	$v_5 = (2, 1, h_5)$	(v_5, v_{15}, f_5)
+	$h_6 = f_5^{-1}f_4$	$v_6 = (2, 1, h_6)$	$(v_6, v_{16}, f_3), (v_6, v_8, f_5)$
+	$h_7 = f_1^{-1}f_2$	$v_7 = (1, 2, h_7)$	(v_7, v_{17}, f_2)
-	$h_8 = f_2^{-1}f_1$	$v_8 = (2, 1, h_8)$	(v_8, v_{18}, f_5)
-	$h_9 = f_1^{-1}h_1$	$v_9 = (1, 1, h_9)$	$(v_9, v_1, f_4), (v_9, v_{19}, f_5)$
-	$h_{10} = f_1^{-1}h_2$	$v_{10} = (1, 2, h_{10})$	(v_{10}, v_{20}, f_3)
-	$h_{11} = f_2^{-1}h_2$	$v_{11} = (2, 2, h_{11})$	(v_{11}, v_{21}, f_3)
-	$h_{12} = f_1^{-1}h_3$	$v_{12} = (1, 1, h_{12})$	(v_{12}, v_3, f_4)
-	$h_{13} = f_2^{-1}h_3$	$v_{13} = (2, 1, h_{13})$	(v_{13}, v_{15}, f_4)
-	$h_{14} = f_2^{-1}h_4$	$v_{14} = (2, 2, h_{14})$	$(v_{14}, v_{22}, f_1), (v_{14}, v_{17}, f_3)$
-	$h_{15} = f_5^{-1}h_5$	$v_{15} = (2, 1, h_{15})$	$(v_{15}, v_{23}, f_4), (v_{15}, v_{24}, f_5)$
-	$h_{16} = f_3^{-1}h_6$	$v_{16} = (1, 1, h_{16})$	(v_{16}, v_{25}, f_5)
-	$h_{17} = f_2^{-1}h_7$	$v_{17} = (2, 2, h_{17})$	(v_{17}, v_{26}, f_3)
+	$h_{18} = h_8f_2$	$v_{18} = (2, 2, h_{18})$	(v_{18}, v_{26}, f_5)
+	$h_{19} = h_9f_2$	$v_{19} = (1, 2, h_{19})$	$(v_{19}, v_{20}, f_1), (v_{19}, v_{21}, f_2)$
+	$h_{20} = h_{10}f_5$	$v_{20} = (1, 2, h_{20})$	(v_{20}, v_{27}, f_2)
-	$h_{21} = h_{11}f_5$	$v_{21} = (2, 2, h_{21})$	(v_{21}, v_5, f_2)
-	$h_{22} = h_{14}f_3$	$v_{22} = (2, 1, h_{22})$	(v_{22}, v_{28}, f_5)
+	$h_{23} = h_{15}f_1$	$v_{23} = (2, 1, h_{23})$	$(v_{23}, v_{16}, f_4), (v_{23}, v_{22}, f_5)$
+	$h_{24} = h_{15}f_2$	$v_{24} = (2, 2, h_{24})$	(v_{24}, v_2, f_4)
+	$h_{25} = h_{16}f_2$	$v_{25} = (1, 2, h_{25})$	(v_{25}, v_{29}, f_2)
+	$h_{26} = h_{17}f_5$	$v_{26} = (2, 2, h_{26})$	$(v_{26}, v_{30}, f_3), (v_{26}, v_{31}, f_4)$
-	$h_{27} = f_2^{-1}h_{20}$	$v_{27} = (2, 2, h_{27})$	$(v_{27}, v_{22}, f_2), (v_{27}, v_{29}, f_3)$
+	$h_{28} = h_{22}f_2$	$v_{28} = (2, 2, h_{28})$	(v_{28}, v_4, f_3)
-	$h_{29} = f_2^{-1}h_{25}$	$v_{29} = (2, 2, h_{29})$	(v_{29}, v_6, f_1)
-	$h_{30} = f_3^{-1}h_{26}$	$v_{30} = (1, 2, h_{30})$	$(v_{30}, v_{32}, f_1), (v_{30}, v_3, f_2)$
-	$h_{31} = f_4^{-1}h_{26}$	$v_{31} = (1, 2, h_{31})$	$(v_{31}, v_1, f_1), (v_{31}, v_{32}, f_2)$
+	$h_{32} = h_{30}f_3$	$v_{32} = (1, 1, h_{32})$	(v_{32}, v_{33}, f_1)
-	$h_{33} = f_1^{-1}h_{32}$	$v_{33} = (1, 1, h_{33})$	(v_{33}, v_{32}, f_4)

TABLE 1. Complete neighbor graph of the dragon GIFS

6.4. Formal definition of the neighbor graph. Let G be a contractive GIFS in \mathbb{R}^d with the attractor (C_1, \dots, C_n) and adjacency lists Q_1, \dots, Q_n . We additionally assume that all $f \in \phi(G)$ are invertible. The procedure below defines a neighbor graph $N(G)$.

We denote the set of potential neighbor maps as

$$F^\times = \{f^{-1}g \mid f, g \in \phi^*(G), \quad 1/M \leq |\det(f^{-1}g)| \leq M\}.$$

where

$$(22) \quad M = \frac{\max_{g \in \phi^*(G)} |\det(g)|}{\min_{f \in \phi(G)} |\det(f)|}$$

We can see from Definition 5 that $1 \leq M < \infty$.

The name ‘neighbor map’ will be reserved for those maps $f^{-1}g \in F^\times$ for which there are pieces $f(C_i)$ and $g(C_j)$ inside C_k for some i, j, k which do intersect:

$$C_k \supset f(C_i) \cap g(C_j) \neq \emptyset.$$

The maps f and g with $f^{-1}g \in F^\times$ have approximately the same determinant (up to constant M), so we are only interested in those neighbors that have an approximately equal size.

We define an increasing sequence of directed graphs (V_m, E_m) , $m = 1, 2, \dots$, so $V_m \subset V_{m+1}$ and $E_m \subset E_{m+1}$. Vertices in every V_m are distinct triples (i, j, h) for some $i, j \in \{1, \dots, n\}$ and $h \in F^\times$. They correspond to intersections $C_i \cap h(C_j)$. Edges in E_m are labeled by maps $f \in \phi(G)$ as in the original GIFS. We represent E_m as a set of triples $(v_1, v_2, f) = v_1 \xrightarrow{f} v_2$ where $v_1, v_2 \in V_m$ and $f \in \phi(G)$.

The first graph (V_1, E_1) does not have edges, so $E_1 = \emptyset$. Vertices V_1 correspond to the first level intersections within any of the attractors C_k :

$$V_1 = \bigcup_{k=1}^n \{(i, j, f^{-1}g) \mid (i, f), (j, g) \in Q_k, (i, f) \neq (j, g), f(C_i) \cap g(C_j) \neq \emptyset\}$$

Let $U_m \subset V_m$ denote the set of vertices without outgoing edges that was added in step m . So $U_1 = V_1$ and for $m > 1$

$$U_m = \{u \in V_m \setminus V_{m-1} \mid (u, v, h) \notin E_m \text{ for any } v \in V_m \text{ and } h \in F^\times\}$$

Suppose that (V_m, E_m) is already constructed. If $U_m = \emptyset$ then we stop, and call the graph $N(G) = (V_m, E_m)$ the **neighbor graph**. Otherwise we construct the next graph (V_{m+1}, E_{m+1}) by adding outgoing edges with corresponding new or old vertices to every $v = (i, j, h) \in V_m \cap U_m = U_m$ in the following way.

- (1) If $|\det(h)| \leq 1$ then for every $(f, k) \in Q_i$ with $C_k \cap f^{-1}h(C_j) \neq \emptyset$ we add the vertex $v' = (k, j, f^{-1}h)$ (if it does not exist yet), and the edge (v, v', f) .
- (2) If $|\det(h)| > 1$ then for every $(f, k) \in Q_j$ with $C_i \cap hf(C_k) \neq \emptyset$ we add the vertex $v' = (i, k, hf)$ (if it does not exist yet), and the edge (v, v', f) .

In both cases if h belongs F^\times , then a new map $(f^{-1}h$ or $hf)$ will belong to F^\times too (22).

DEFINITION 11. [BM09] A GIFS has **finite type** if it has a finite neighbor graph.

DEFINITION 12. A GIFS has an **exact overlap** if the above procedure generates a vertex of the form (i, i, I_d) for some $i = 1, \dots, n$.

DEFINITION 13. A map $h \in F^\times$ from any vertex (i, j, h) of the neighbor graph is called a **neighbor map**.

Remarks.

- (1) There are non-finite type GIFS, so a finite neighbor graph does not always exist. Since (V_m, E_m) is an increasing sequence we can define an **infinite** neighbor graph as $(\bigcup_m V_m, \bigcup_m E_m)$. Even in this case it is possible to find each exact overlap in a finite number of steps.
- (2) A neighbor graph can be very large: for the Levy curve in Figure 9 it has about 100 vertices. It is easy to produce examples with arbitrary large neighbor graphs even in \mathbb{R}^1 .
- (3) If the neighbor graph is empty then there are no first level intersections, so every set of the attractor is a subset of Cantor set.
- (4) A finite type strongly connected GIFS without exact overlaps fulfills the open set condition [BG92, BM09, ME05].

6.5. Properties.

PROPOSITION 14. Let N be a neighbor graph. If a vertex (i, j, h) belongs to $V(N)$ and $\det(h) = 1$ then a vertex (j, i, h^{-1}) is also a vertex of $V(N)$.

PROPOSITION 15. For any neighbor graph there is an integer constant $M > 0$ such that any directed path of length M contains vertices (i_1, j_1, h_1) and (i_2, j_2, h_2) with $|\det(h_1)| \leq 1$ and $|\det(h_2)| > 1$.

PROOF. During the construction, if some map $h \in F^\times$ has $|\det(h)| \leq 1$ then we sequentially multiply it from the left by some $f_i^{-1} \in \phi(G)$. Since the attractor exists, at some step the product $h' = f_{i_m}^{-1}, \dots, f_{i_1}^{-1}h$ will have $|\det(h')| > 1$. The length m of the sequence cannot be arbitrary large since that would contradict Proposition 6. \square

PROPOSITION 16 (Neighbor graphs of isomorphic GIFS). Let G and G' be isomorphic GIFS: $TG = G'T$. Then $N(G')$ can be obtained from $N(G)$ by replacing labels f on all edges by TfT^{-1} and replacing neighbor maps h in all vertices by ThT^{-1} .

PROOF. The maps f and TfT^{-1} have the same determinant, so all steps in the neighbor graph procedures for G and G' are the same (up to affine isomorphism). \square

6.6. Extended neighbor graph. In practice it is useful to extend the procedure in 6.4 by replacing attractors C_1, \dots, C_n by larger sets $B_1, \dots, B_n \subset \mathbb{R}^d$.

DEFINITION 17. The graph produced by the procedure in Section 6.4 for sets $B_1, \dots, B_n \subset \mathbb{R}^d$ is called **extended neighbor graph** and denoted $N(G, B_1, \dots, B_n)$.

PROPOSITION 18. Let G be a GIFS with attractor (C_1, \dots, C_n) , and $C_i \subset B_i$ for some compact sets $B_1, \dots, B_n \subset \mathbb{R}^d$. Then the neighbor graph $N(G)$ exists iff

$N(G, B_1, \dots, B_n)$ exists. $N(G)$ is a subgraph of $N(G, B_1, \dots, B_n)$ and can be obtained from it by removing all vertices that do not lead to any cycle.

PROOF. Denote $N = N(G)$ and $N_B = N(G, B_1, \dots, B_n)$. The only difference between the procedures that generate N_B and N are conditions like $B_k \cap h(B_j) = \emptyset$ for $h \in F^\times$. Since $C_i \subset B_i$ for all i , we have $C_k \cap h(C_j) \subset B_k \cap h(B_j)$. So if the procedure creates a new edge for N then a corresponding edge will be created for N_B . This proves that N is a subgraph of N_B .

Consider any vertex $v = (i, j, h) \in V(N)$ of N_B without outgoing edges and let $|\det(h)| \leq 1$. By the definition it means that $B_k \cap f^{-1}h(B_j) = \emptyset$ for every $(f, k) \in Q_i$, so $B_i^2 \cap h(B_j^2) = \emptyset$ where

$$(23) \quad B_i^2 = \bigcup_{(f,k) \in Q_i} f(B_k) \quad i = 1 \dots n$$

We have $C_i \subset B_i^2 \subset B_i$, and the extended neighbor graph for B_i^2 is strictly smaller than N_B . If we continue this way, at some stage we will get an extended neighbor graph where every vertex has outgoing edges. This will be N . \square

6.7. Computation. Proposition 18 gives us a practical method to compute neighbor graphs. We can create the extended neighbor graph for bounding balls B_1, \dots, B_n of the attractors to compute $N(G, B_1, \dots, B_n)$ and then remove appropriate vertices. We have to prescribe a constant that limits the number of vertices in the extended neighbor graph to ensure that the procedure in Section 6.4 will stop after a finite number of steps.

6.8. GIFS of intersections. [AL11, DKV00, Gil86]

A neighbor graph $N = N(G)$ can be used to create another GIFS G' that has attractors equal to all possible **standardized** intersections of the comparable pieces in the attractors of G . The procedure is as follows:

- (1) The graph G' has the same vertices and edges as N .
- (2) The labels on edges are the same for N and G' , except for the case when $v = (i, j, h) \in V(N)$ and $|\det(h)| > 1$. In this case we replace the labels for all outgoing edges of v with the identity map: $(v, v', f) \Rightarrow (v, v', I_d)$.
- (3) As a simplification, we can exclude all vertices with $|\det(h)| > 1$ by substituting their definitions to other sets. This will remove edges labeled by identity maps.

Below we can see the result of the procedure applied to Table 1 for our dragon. Each D_i corresponds to v_i in the table. It is easy to see that the graph G' is not strongly connected, and the intersection $D_{32} = C_1 \cap h_{33}(C_1)$ is just a point.

$$\begin{aligned}
D_1 &= f_1(D_1) \cup f_1(D_{19}) \\
D_2 &= f_1(D_{20}) \cup f_2(D_5) \\
D_3 &= f_1(D_3) \cup f_2(D_{23}) \cup f_2(D_{24}) \\
D_4 &= f_2(D_{28}) \cup f_2(D_{26}) \\
D_5 &= f_5(D_{23}) \cup f_5(D_{24}) \\
D_6 &= f_3(D_{25}) \cup f_5(D_{18}) \\
D_7 &= f_2(D_{26}) \\
D_{18} &= f_5(D_{26}) \\
D_{19} &= f_1(D_{20}) \cup f_2(D_5) \\
D_{20} &= f_2(D_{28}) \cup f_2(D_6) \\
D_{23} &= f_4(D_{25}) \cup f_5(D_{28}) \\
D_{24} &= f_4(D_2) \\
D_{25} &= f_2(D_6) \\
D_{26} &= f_3(D_{32}) \cup f_3(D_3) \cup f_4(D_1) \cup f_4(D_{32}) \\
D_{28} &= f_3(D_4) \\
D_{32} &= f_1(D_{32})
\end{aligned}$$

6.9. Dynamical boundary. [Mor99] Elements of the vertex set $V(N)$ of a neighbor graph N from Section 6.4 are triples (i, j, h) that correspond to intersections $C_i \cap h(C_j)$. Define a **dynamical boundary** of the set C_i as

$$(24) \quad \partial C_i = \bigcup_{(i,j,h) \in V(N)} C_i \cap h(C_j) \quad i = 1, \dots, n$$

In the tiling case, when the GIFS fulfills the OSC and all C_i have non-empty interior, the dynamical boundary of any C_i coincides with its topological boundary. In the fractal case, the boundaries are different. For example, the dynamical boundary of the Sierpinski triangle 9.1 is just three points. Note that Equation (24) can be used even with an infinite neighbor graph if we consider the closure of the union. Let G' be the GIFS of intersections for G . Since every element of the union in (24) is some component of the attractor of G' , we can express ∂C_i as a union of such components (Figure 19).

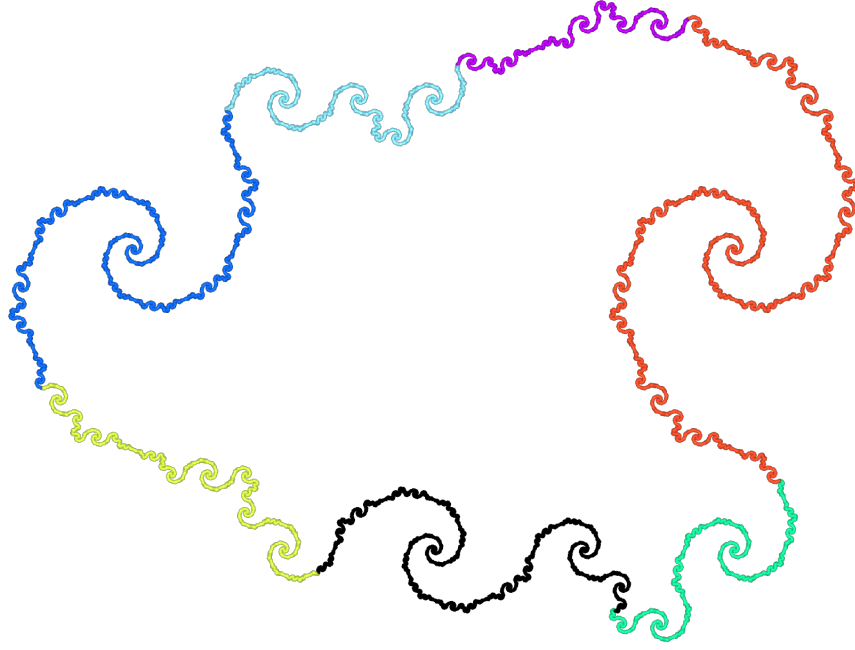


FIGURE 19. C_2 boundary $D_5 \cup D_6 \cup D_{18} \cup D_{23} \cup D_{24} \cup D_{26} \cup D_{28}$



FIGURE 20. C_2 neighborhood $h_5C_1 \cup h_6C_1 \cup h_{18}C_2 \cup h_{23}C_1 \cup h_{24}C_2 \cup h_{26}C_2 \cup h_{28}C_2$

C Algebraic iterated function systems

7. Lifting algebraic IFS to rational ones

7.1. Rational and algebraic iterated function systems. Iterated function systems are considered in \mathbb{R}^d or \mathbb{C}^d . We needed the topological completeness of the underlying field to define attractors as compact sets. In this section, however, we shall consider functions with coefficients in \mathbb{Q} or in an algebraic field. They play a crucial role for the IFStile package. Calculations with real data involve numerical errors, but calculations with rational or algebraic numbers can be done without any error.

A number $\beta \in \mathbb{C}$ is called *algebraic* if there is a non-zero polynomial

$$(25) \quad p(z) = a_0 + a_1z + \dots a_{n-1}z^{n-1} + a_nz^n$$

with integer coefficients a_k and $p(\beta) = 0$. The minimal degree of such a polynomial is called the degree of β . The *algebraic closure* of \mathbb{Q} is $\mathbb{A} = \{z \in \mathbb{C} \mid z \text{ is algebraic}\}$. It is well-known that \mathbb{A} is a subfield of \mathbb{C} . By definition, an algebraic field is a subfield of \mathbb{A} .

DEFINITION 19 (Rational and algebraic IFS). *Let $F = \{f_1, \dots, f_m\}$ be an affine iterated function system in \mathbb{R}^d or \mathbb{C}^d with $f_k(x) = a_kx + b_k$. If all coefficients $a_k(i, j)$ and $b_k(j)$ are rational numbers, we call F a rational IFS or IFS in \mathbb{Q}^d . (In the complex case, real and imaginary parts must be in \mathbb{Q} .) If the $a_k(i, j)$ and $b_k(j)$ are all contained in an algebraic field \mathbb{H} over \mathbb{Q} , we call the IFS algebraic.*

Note that this definition applies to any GIFS G by considering $\phi(G)$ as an IFS. Moreover, we can confine ourselves to finite extensions of the rational numbers since an IFS contains only finitely many coefficients.

Essentially all examples of self-affine tiles and fractals in the literature are defined with rational or algebraic numbers. So it is not a serious restriction to assume that all numbers in the definition of an IFS are algebraic. Below we show that we can replace an algebraic IFS in any dimension by a rational IFS in higher dimension. The use of rational numbers is essential for computer work. Integer arithmetic makes it possible to perform accurate calculations. Although IFStile can do numeric approximations, its essential feature is the exact determination of the neighbor graph of an IFS. Beside that, integer calculations are also much faster than calculations with real numbers. Actually, rational representation of tiles was considered by many authors, sometimes implicitly: [Ban91, Ban97, BG97, Gel97, Gel94, LW96, LLR, Lor12, Rau82]. We modify the known results in such a way that they fit our setting.

7.2. The lifting lemma for IFS. Our goal is to replace an algebraic IFS in low-dimensional space by a rational IFS in higher dimension.

DEFINITION 20 (Rational representation of an IFS). *Let $F = \{f_1, \dots, f_m\}$ be an IFS on \mathbb{C}^d . A **rational representation** of F is a pair (Q, U) where*

- (i) $Q = \{q_1, \dots, q_m\}$ is a rational IFS on \mathbb{Q}^D ,
- (ii) $U : \mathbb{Q}^D \rightarrow \mathbb{C}^d$ is a linear map given by a $d \times D$ -matrix,
- (iii) $Uq_k = f_k U$ for $k = 1, \dots, m$.

*Minimal possible dimension D is called **algebraic dimension** of F .*

It is well-known that accurate calculations with algebraic numbers over \mathbb{Q} can be performed as matrix calculations in some vector space \mathbb{Q}^D . All computer algebra packages work in this way. So the following proposition is not surprising. We provide a proof to indicate how algebraic IFS can be used in IFStile, and how the dimension will increase when different algebraic numbers are involved. The procedure is closely related with the Minkowski embedding, see [BG13, 3.4].

PROPOSITION 21. *Every algebraic IFS on \mathbb{C}^d has a rational representation.*

Proof. Let $F = \{f_k(x) = a_k x + b_k \mid k = 1, \dots, m\}$ be an algebraic IFS on \mathbb{C}^d , and let H be the finite set of all coefficients $a_k(i, j)$ and $b_k(j)$ of the mappings $f_k, k = 1, \dots, m$. Let \mathbb{H} be the field which is generated by H over \mathbb{Q} . Since H contains only algebraic numbers, \mathbb{H} is a finite algebraic field extension of \mathbb{Q} . Thus \mathbb{H} , considered as a vector space over \mathbb{Q} , must have finite dimension N .

Let S be a basis of this rational vector space. Typically, S contains 1, the irrational numbers of H , their powers and products of these powers. If β is an algebraic number of degree n , only powers $\beta, \beta^2, \dots, \beta^{n-1}$ need be considered. Since $p(\beta) = 0$, for the minimal polynomial of β , of the form (25), the number β^n can be expressed as

$$(26) \quad \beta^n = -\frac{1}{a_n} \cdot (a_0 + a_1\beta + \dots a_{n-1}\beta^{n-1})$$

Each coefficient $b_k(j)$ or $a_k(i, j)$ of the original IFS is now represented as a vector $\hat{b}_k(j)$ or $\hat{a}_k(i, j)$ in the N -dimensional rational vector space \mathbb{H} , as a linear combination of basis vectors.

We now consider d -dimensional vectors $v = (v_1, \dots, v_d)$ with entries $v_j \in \mathbb{H}$. They are generated by basis vectors $(s, 0, \dots, 0), (0, s, 0, \dots, 0), \dots, (0, \dots, 0, s)$ with $s \in S$. This new basis \hat{S} has Nd vectors and generate the $N \times d$ -dimensional rational vector space $\mathbb{H}^d = \mathbb{Q}^D$ with $D = Nd$. The IFS Q will now be constructed on this space. We set

$$q_k(v) = \hat{a}_k v + \hat{b}_k \text{ for } k = 1, \dots, m.$$

Entries of \mathbb{Q}^D , like v , will be column vectors. The translation vector is simply defined as $\hat{b}_k = (\hat{b}_k(1), \dots, \hat{b}_k(d))'$. The columns of the matrix \hat{a}_k have the form $\sum_{i=1}^d \hat{a}_k(i, j) \cdot \hat{s}(i)$, where \hat{s} is a basis vector in \hat{S} , thus one component $\hat{s}(i)$ is a vector $s \in S$ and all other components are zero. Since product and sum is calculated in the algebraic field \mathbb{H} , however, we must take care of the relation (26), and similar relations for products of the h . This will be demonstrated in the examples.

The map U is defined for basis vectors $\hat{s} \in \hat{S}$ and extended linearly to \mathbb{Q}^D . The vector $(0, s, 0..0) \in \mathbb{H}^d$ is mapped to $(0, s, 0..0) \in \mathbb{C}^d$, and similar for the other basis vectors. In fact, each $s \in S$ belongs to \mathbb{C} . This construction guarantees that $Uq_k(\hat{s}) = f_k U(\hat{s})$ holds for basis vectors \hat{s} , and hence for all vectors in \mathbb{Q}^D . \square

Remark. The statement also holds for IFS on \mathbb{R}^d where all algebraic numbers involved in F must be real. Our examples will be mostly in the complex plane, however, and will involve complex algebraic numbers. Note that the real dimension of the vector space \mathbb{C}^d is $2d$. We also assume that F has full rank in the sense that there is no real hyperplane invariant under all maps f_k . In that case D cannot be smaller than $2d$ by property (iii), and the proof indicates that D is usually much larger.

7.3. The viper tile. Three examples will demonstrate how lifting works in detail. They are taken from the tiling encyclopedia [Fre18] where they are presented with geometric substitutions. Their algebraic description requires some calculation, however. I thank C. Bandt for discussions and for providing details. Our first example shows that $D = 2d$ is possible.

Each triangle can be divided into $9 = 3 \times 3$ congruent subtriangles in a checkerboard pattern. We take an isosceles triangle with side lengths $a = b$ and $c = a/2$. Then four of the small triangles form a rhomb. Reflection of this rhomb at one of its diagonals yields a new subdivision of the triangle, shown in Figure 21. Due to the symmetry of the triangle, we will find a generating IFS which contains no reflections. The rotation angles are irrational since the angle $\alpha = \beta$ in the big triangle fulfills $\cos \alpha = \frac{1}{4}$. Tilings of the whole plane generated by this IFS have the property that the sides of small triangles show a dense set of directions in $[0, 2\pi]$ (statistical circular symmetry, see [Fre08, Rad94]).

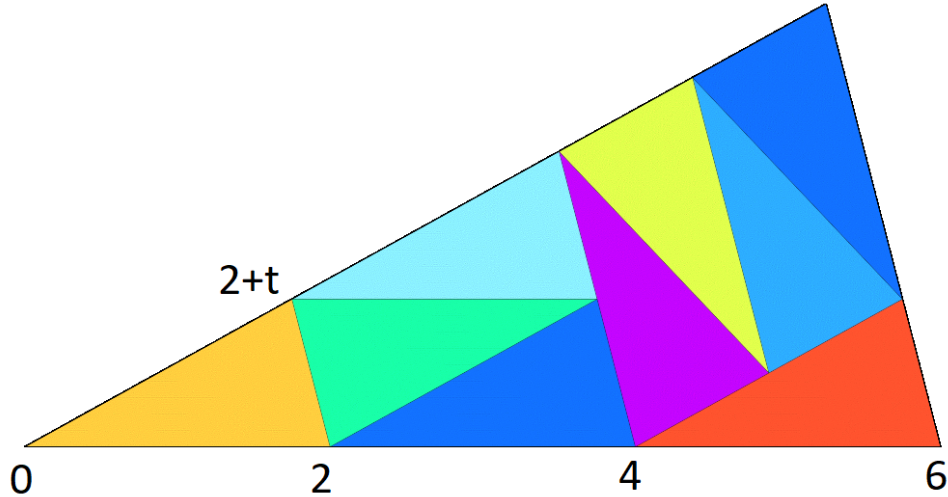


FIGURE 21. A simple algebraic tile with rational representation of the same dimension.

To analyse this construction, we introduce coordinates such that the triangle is in the upper half-plane, its tip is at zero, and one side is the segment $[0, 6]$ on the real axis, as shown in Figure 21. The small triangle with vertex zero has as other vertices the number 2 and the complex number $2 + t$ where $t = -\cos \alpha + \mathbf{i} \sin \alpha = (-1 + \mathbf{i} \cdot \sqrt{15})/4$. Obviously, t is a algebraic number: it is a root of $t^2 + \frac{1}{2}t + 1$. The IFS is now defined by the maps f_k which send the big triangle into the small ones: We write

$$f_k(z) = g^{-1}h_k(z) \quad \text{where } g(z) = 3z$$

and the h_k are translations or rotations. The h_k map the small triangle with vertex 0 to the other small triangles,

$$h_1 = id, \quad h_2(z) = z + 2, \quad h_3(z) = z + 4, \quad h_4(z) = z + 2 + t, \quad h_5(z) = -z + 4 + t.$$

The rotations by angles $\pi - \alpha$ and $-\alpha$ around the origin are $r(z) = tz$ and $-r(z)$, respectively. Thus we can complete our algebraic IFS:

$$h_6(z) = -tz + 4 + 2t, \quad h_7(z) = tz + 5 + \frac{1}{2}t, \quad h_8(z) = -tz + 5 + \frac{5}{2}t, \quad h_9(z) = tz + 6 + t.$$

Now we construct a rational representation. We have $\mathbb{H} = \mathbb{Q}(t)$, and since t is quadratic, our vector space basis is $S = \{1, t\}$. The complex map $g(z) = 3z$ corresponds to the linear map $\hat{g}(x) = \begin{pmatrix} 3 & 0 \\ 0 & 3 \end{pmatrix}x$ on \mathbb{Q}^2 . The rotation $r(z) = tz$ is expressed by the matrix $R = \begin{pmatrix} 0 & -1 \\ 1 & -1/2 \end{pmatrix}$ with respect to the basis S . The first column containing the image of 1 is $t = 0 \cdot 1 + 1 \cdot t$, the second column comes from $r(t) = t^2 = -1 - \frac{1}{2} \cdot t$. The translation vectors are expressed with respect to the basis S . They are columns, like $x = \begin{pmatrix} x_1 \\ x_2 \end{pmatrix}$, written as rows with square brackets.

$$\begin{aligned} \hat{h}_1 &= id, \quad \hat{h}_2(x) = x + [2, 0], \quad \hat{h}_3(x) = x + [4, 0], \quad \hat{h}_4(x) = x + [2, 1], \quad \hat{h}_5(x) = -x + [4, 1], \\ \hat{h}_6(x) &= -Rx + [4, 2], \quad \hat{h}_7(x) = Rx + [5, \frac{1}{2}], \quad \hat{h}_8(x) = -Rx + [5, \frac{5}{2}], \quad \hat{h}_9(x) = Rx + [6, 1]. \end{aligned}$$

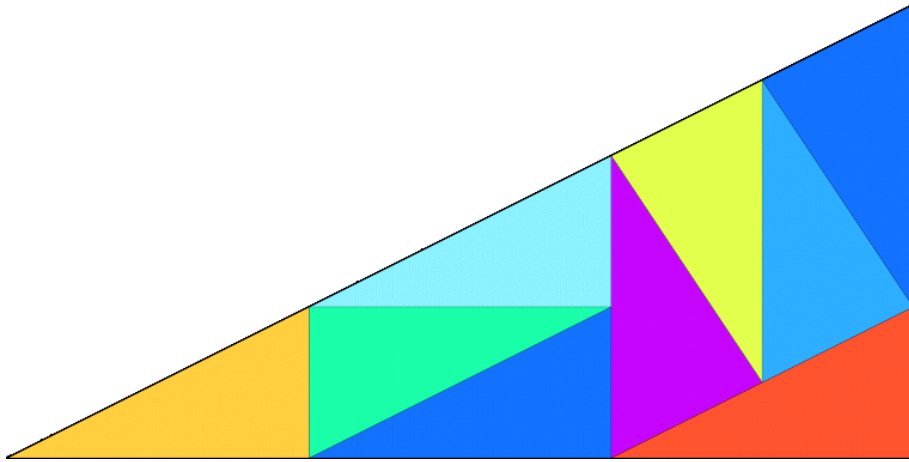


FIGURE 22. The rational representation generates a self-affine tile only.

The rational IFS now is $G = \{\hat{g}^{-1}\hat{h}_k = \frac{1}{3} \cdot \hat{h}_k \mid k = 1, \dots, m\}$. The mapping $U : \mathbb{Q}^2 \rightarrow \mathbb{C}$ is defined by $U(x) = (1, t) \cdot x = x_1 + tx_2$. Property (iii) follows from $UR = (t, -1 - t/2) = tU$ where the equation for t is used.

Note that R is not an orthogonal matrix. So the rational IFS, considered on \mathbb{R}^2 , will not generate a self-similar set. In Figure 22, the turned small triangles have no right angle. For instance, $((5, \frac{1}{2}) - (4, 2)) \cdot ([6, 1] - [4, 0]) = -\frac{1}{2} \neq 0$. This can be corrected by adapting the angle between the basic vectors so that the 'elliptic rotation' R becomes a Euclidean rotation.

7.4. The Ammann hexagon. This example is one of the best-known self-similar tiles [GS87, Fre18]. As Figure 23 shows, it consists of two pieces. If the similarity ratio for the larger part is t , the ratio for the smaller part is t^2 . Since area scales with the square of the similarity ratio, and the two parts do not overlap, we have $t^2 + t^4 = 1$. Moreover, the expansive map g transforming the larger part to the whole must be a rotation around 90° composed with a homothety with factor $\rho = 1/t$. Obviously, ρ is the root of the golden number, or Fibonacci number $(1 + \sqrt{5})/2$. If we take the fixed point of g as origin of the complex plane, we have $g(z) = i\rho z$.

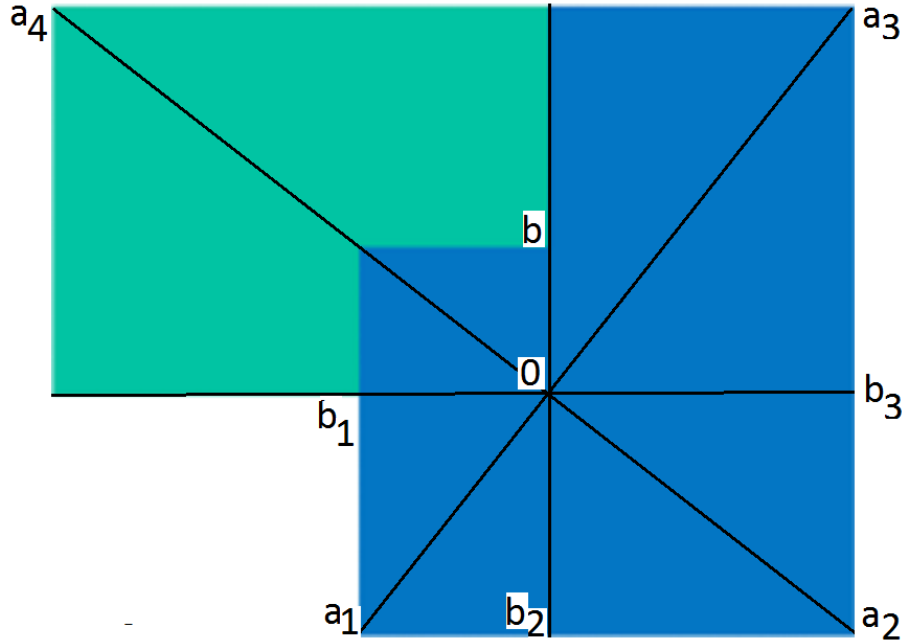


FIGURE 23. The Ammann hexagon is a well-known self-similar tile. From the landmark points one can easily determine the contraction maps.

Geometric arguments show that this fixed point is the intersection of two diagonals of the hexagon, and lies on the extensions of two sides of the small hexagon, as indicated in Figure 23. We have $g(a_k) = a_{k+1}$ and $g(b_k) = b_{k+1}$ for $k = 1, 2, 3$, and

$g(b) = b_1$. If we fix the origin and put $b = i$, then $b_1 = -\rho$ and $b_3 = \rho^3$ are on the real axis.

Now we determine the contraction maps for the equation $A = f_1(A) \cup f_2(A)$. We have $f_1(z) = g^{-1}(z)$. The map g^{-2} transforms A into a small hexagon which has vertices a_1, a_2 , and b_3 . This hexagon has to be reflected at the real axis and shifted by the vector $-\rho^3 + i$ in order to coincide with the hexagon $f_2(A)$. Thus

$$f_2(z) = r \cdot g^{-2}(z) - \rho^3 + i$$

where the reflection $r(z) = \bar{z}$ is the complex conjugation.

The minimal polynomial for $\beta = i\rho$ is $p(x) = x^4 + x^2 - 1$. So the dimension for the rational representation of this IFS is $D = 4$, and $\{1, \beta, \beta^2, \beta^3\}$ is taken as basis of the vector space \mathbb{Q}^4 which represents our algebraic field $\mathbb{Q}(\beta)$. Our expansion map $g(z) = \beta z$ is given by the linear map C on \mathbb{Q}^4 with $C(\beta^k) = \beta^{k+1}$ for $k = 0, 1, 2$ and $C(\beta^3) = \beta^4 = 1 - \beta^2$. The matrix of this map is the companion matrix of p which will be introduced in the next section.

It is important that the reflection map r contained in f_2 can also be lifted to a rational linear map on \mathbb{Q}^4 . For the basis vectors we have $r(1) = 1, r(\beta^2) = \beta^2$, since β^2 is real, and $r(\beta) = -\beta, r(\beta^3) = -\beta^3$ since these numbers are imaginary. The matrix R of this map is a diagonal matrix with entries 1, -1, 1, -1.

The translation vector $-\rho^3 + i$ is not in $\mathbb{Q}(\beta)$ and thus cannot be lifted to a vector in \mathbb{Q}^4 . However, this is not a problem since many other translation vectors yield isomorphic Ammann hexagons. We also prefer the form $f_2(z) = g^{-2}(r(z) + v)$ with a translation vector $v \in \mathbb{Q}^4$. No calculation is needed - the IFStile finder will automatically determine appropriate vectors v from the matrices C and R . As we show in the next section, the package will also find many other tiles which are related to the Ammann hexagon. Self-similar triangles from this same family were considered in detail in [DvO00].

7.5. The self-similar chord quadrangle. A slightly more complicated example with three pieces is shown in Figure 24. The contraction factors are t, t^2, t^3 for some t . Thus the areas of the pieces are $u = t^2, u^2 = t^4$ and $u^3 = t^6$ times the area of the whole quadrangle, which yields the equation $u^3 + u^2 + u = 1$, with solution $u \approx 0.5437$ and $t \approx 0.7374$. The number $1/u \approx 1.8393$ is sometimes called tribonacci constant.

This quadrangle is one instance of a continuous family of self-similar sets. It is distinguished by the finite type condition and special geometric properties [Fre18]. There are two opposite right angles, and two of the sides of the quadrangle have equal length. We check how this coincides with the similarity relations. If b denotes the vertical side of the whole quadrangle A , the corresponding sides of the pieces are tb, t^2b , and t^3b which is the the shortest side of A . Thus the short sides of the pieces are t^4b, t^5b and t^6b , respectively, and their opposite sides are t^{-3} larger, as in A . The characteristic equation for $u = t^2$ says that the baseline side has length $b = t^2b + t^4b + t^6b$.

Now we determine an algebraic IFS for A , which is considered as part of an angle α with vertex 0 in the complex plane. Let $q(z)$ denote a reflection which interchanges

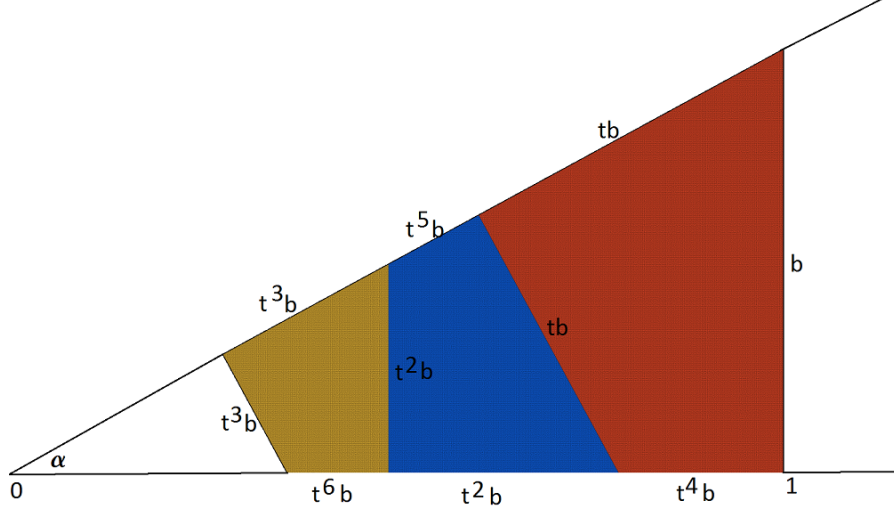


FIGURE 24. The self-similar chord quadrangle with three pieces.

the legs of this angle, composed with a homothety with factor t and center 0. Then q maps the large piece of A into the middle piece, and the middle piece into the small piece. Moreover, if we rotate A clockwise by a right angle around its lower right vertex, the image $r(A)$ fits into the angle and will be mapped by q onto the large piece of A . Thus we have the equation

$$A = q \cdot r(A) \cup q^2 \cdot r(A) \cup q^3 \cdot r(A) .$$

Assuming that the rotation center is point 1 in our coordinate system, we note the formula for r . In terms of the angle α , the formula of q is also standard:

$$(27) \quad r(z) = -iz + 1 + i \quad \text{and} \quad q(z) = t \cdot (\cos \alpha + i \sin \alpha) \bar{z} .$$

It remains to express $\cos \alpha$ by algebraic numbers. To this end, imagine that in Figure 24 a sequence of smaller and smaller quadrangles is extended to the left up to 0. Their sides on $[0, 1]$ form two geometric sequences with factor t^2 and initial terms t^4b and t^2b . Thus

$$\tan \alpha = \frac{b}{t^2b + t^4b + \dots + t^4b + t^6b + \dots} = \frac{1 - t^2}{t^2 + t^4} .$$

On the other leg of the angle we also have two geometric sequences of intervals, with initial terms tb and t^5b . We divide the length of the two sums in order to obtain $\cos \alpha$. Again, b cancels. We get

$$\cos \alpha = \frac{(t^2 + t^4)/(1 - t^2)}{(t + t^5)/(1 - t^2)} = \frac{t + t^3}{1 + t^4} \quad \text{and} \quad \sin \alpha = \cos \alpha \tan \alpha = \frac{1 - t^2}{t + t^5} .$$

We insert this in (27) and replace t^2 by u .

$$(28) \quad q(z) = \left(\frac{u + u^2}{1 + u^2} + i \cdot \frac{1 - u}{1 + u^2} \right) \bar{z} = \left(\frac{u^2}{1 - u} + i \cdot \frac{u}{1 + u} \right) \bar{z} .$$

The second form comes from the identity $\frac{1}{1+u^2} = \frac{u}{1-u^2}$ which is a consequence of the tribonacci equation.

Now we start with the lifting. We need two algebraic numbers, i and u . The complex number i is needed for the rotation r only, but this is essential as we shall see in the next section. Thus we have to take the algebraic field $\mathbb{Q}(i, u)$ with degree 6 over \mathbb{Q} . Thus $D = 6$ is the dimension of the vector space \mathbb{H} in Proposition 21. The standard basis is $S = \{1, u, u^2, i, iu, iu^2\}$. The rotation r in (27) can directly be lifted to an affine map on \mathbb{H} with integer coefficients:

$$R(x) = \begin{pmatrix} \mathbf{0}_3 & \mathbf{I}_3 \\ -\mathbf{I}_3 & \mathbf{0}_3 \end{pmatrix} \cdot x + (1, 0, 0, 1, 0, 0)' , \text{ with } x = (x_1, \dots, x_6)' ,$$

where $\mathbf{0}_3$ denotes the 3×3 zero matrix. The conjugation map $k(z) = \bar{z}$ is lifted to the reflection matrix K which has entries $(1, 1, 1, -1, -1, -1)$ on the diagonal and zeros outside. It remains to lift the multiplication by $v = \frac{u^2}{1-u} + i \cdot \frac{u}{1+u}$ in (28) to a matrix acting on \mathbb{H} .

Note that \mathbb{H} is a ring with multiplication inherited from $\mathbb{Q}(i, u)$. Since u is an algebraic unit (the constant term of its minimal polynomial is 1), $\mathbb{Q}(i, u)$ and hence \mathbb{H} is even a field. For the lifting of v , we must first express $\frac{1}{1-u}$ and $\frac{1}{1+u}$ as multiplication with a polynomial of u . We put $\frac{1}{1+u} = a + bu + cu^2$ and determine the values of a, b, c by comparing coefficients in the equation $1 = (1+u)(a + bu + cu^2)$. The result is

$$\frac{1}{1+u} = \frac{1}{2} \cdot (1 + u^2) \quad \text{and} \quad \frac{1}{1-u} = \frac{1}{2} \cdot (3 + 2u + u^2) .$$

With these formulas and the characteristic equation $u^3 = 1 - u - u^2$ we determine the image vector of each base vector in S under multiplication with v . These vectors form the columns of the following matrix V which is the lifting of multiplication with v to \mathbb{H} .

$$(29) \quad V = \frac{1}{2} \cdot \begin{pmatrix} 1 & 1 & 1 & 1 & 1 & -1 \\ 2 & 0 & 0 & 0 & 0 & 2 \\ 1 & 1 & -1 & 1 & -1 & 1 \\ -1 & -1 & 1 & 1 & 1 & 1 \\ 0 & 0 & -2 & 2 & 0 & 0 \\ -1 & 1 & -1 & 1 & 1 & -1 \end{pmatrix}$$

The lifting of q corresponds to the matrix VK . The lifting of the maps $q^j r, j = 1, 2, 3$ in the IFS of A is now immediate.

8. Projection of IFS

In this section we take another look on algebraic IFS from a higher dimensional point of view. Our goal is to define an algebraic IFS using rational data only, which are needed for processing by computer algebra techniques. Moreover, rational data are usually small, which is important for maintaining IFS databases.

The IFStile package performs the neighbor graph calculation and the search for new examples in a high-dimensional rational space where we have an integer lattice to perform a random walk. The search procedure produces rational IFS directly.

As we can see from Section 7, it is always possible to create a rational representation (Q, U) of an algebraic IFS, but such representation relies on the non-rational matrix U . Moreover, it is not sufficient to have Q and U since many different algebraic IFS correspond to them. Below we show how we can get an algebraic IFS from a rational one and additional integer data. A similar technique is used in computer algebra systems, where an algebraic number is defined by the minimal polynomial and some additional information that separates the number from its conjugates [Str97].

8.1. Basic definitions. Let $A \in \mathcal{M}_d$ be some matrix, we consider it as linear operator in \mathbb{R}^d . Denote the kernel (null space) and range (image) of A as

$$\ker(A) = \{x \in \mathbb{R}^d \mid A(x) = 0\}, \quad \text{ran}(A) = A(\mathbb{R}^d)$$

Let $X \subset \mathbb{R}^d$ be some linear subspace. We will denote by $A|_X : X \rightarrow A(X)$ the restriction of A to X . Obviously, the restriction is a linear operator.

A linear subspace X is called an **invariant subspace** for A , or, A -invariant, if $AX \subset X$. In this case $A|_X$ transform X to X and $sp(A|_X) \subset sp(A)$.

The following properties [GLR06, 1.1] will be important for us:

- (1) $\ker(A)$ and $\text{ran}(A)$ are invariant subspaces for A .
- (2) $\ker(A) \otimes \text{ran}(A) = \mathbb{R}^d$.

A matrix $P \in \mathcal{M}_d$ is called a **projector** if $P^2 = P$. It is easy to see that the matrix $1 - P$ is a projector too, and

$$(30) \quad \ker(P) = \text{ran}(1 - P), \quad \text{ran}(P) = \ker(1 - P).$$

For any two complementary subspaces $X_1, X_2 \subset \mathbb{R}^d$, $X_1 \otimes X_2 = \mathbb{R}^d$ there is a unique projector $P \in \mathcal{M}_d$ that fulfills [GLR06, Theorem 1.5.1]

$$\text{ran}(P) = X_1, \quad \ker(P) = X_2.$$

THEOREM 22 (Projector decomposition).

Let P be a projector in \mathbb{R}^D , and R be a $D \times d$ matrix with columns that form a basis in $\text{ran}(P)$. Then there is a unique $d \times D$ matrix L that fulfills:

$$P = RL, \quad LR = 1$$

Conversely, if R is a $D \times d$ matrix and L is a $d \times D$ matrix, $LR = 1$, then $P = RL$ is a projector.

PROOF. Let Q be a $d \times D$ matrix with rows that form a basis in the orthogonal complement of $\ker(P)$. According to [BR14, 7.16]

$$P = RL, \text{ where } L = (QR)^{-1}Q$$

Obviously $LR = (QR)^{-1}QR = 1$. If L' is any $d \times D$ matrix, with $P = RL'$ and $L'R = 1$, then

$$P = RL' = RL \Rightarrow LRL' = LRL \Rightarrow L' = L.$$

If R and L are any matrices with appropriate sizes and $LR = 1$, then $(RL)^2 = R(LR)L = RL$, so $P = RL$ is a projector. \square

PROPOSITION 23. *Let $A, P \in \mathcal{M}_D$, and P is a projector. Then*

- (1) $\text{ran}(P) = \ker(1 - P)$ is invariant for A iff $(1 - P)AP = 0$
- (2) $\ker(P) = \text{ran}(1 - P)$ is invariant for A iff $PA(1 - P) = 0$

PROOF. The first statement is [GLR06, 1.5.5]. The second statement is the first one applied to the projector $P' = 1 - P$. \square

DEFINITION 24. *Let $U \subset \mathcal{M}_D$ be a set of matrices. A projector $P \in \mathcal{M}_D$ is called a **common projector** for U , if $\ker(P)$ is a common invariant subspace for all matrices from U , or, according to Proposition 23, $PA(1 - P) = 0$ for any $A \in U$. A projector is common for a GIFS G if it is common for the linear parts of the maps from $\phi(G)$.*

8.2. Projected GIFS. Let $Q = \{q_1, \dots, q_n\}$ be an IFS in \mathbb{R}^D where $q_i(x) = A_i(x) + t_i$. Let P be a common projector for $\{A_1, \dots, A_n\}$ and $P = RL$ be the decomposition from Theorem 22 for some basis in $\text{ran}(P)$.

Define new IFS $F = \{f_1, \dots, f_n\}$ in \mathbb{R}^d where $d = \dim(\text{ran}(P))$.

$$(31) \quad f_i(x) = LA_iR(x) + Lt_i$$

For the new IFS we have the following important property (3):

$$(32) \quad Lq_i = f_iL \text{ for } i = 1, \dots, n$$

Indeed, since $PA_i(1 - P) = 0$ we have: $0 = RLA_i(1 - RL) = LA_i(1 - RL)$ or $LA_i = LA_iRL$. So $Lq_i = LA_i(x) + Lt_i = LA_iRL(x) + Lt_i = f_iL$.

If we take another projector decomposition $P = R'L'$, then $R' = RT$ and $L' = T^{-1}L$. In this case we get another IFS F'

$$(33) \quad f'_i(x) = T^{-1}LA_iRT(x) + T^{-1}Lt_i$$

It is easy to see, that $Tf'_i = f_iT$, so F and F' are isomorphic.

DEFINITION 25 (Projected GIFS). *Let G be a GIFS and $P = RL$ a decomposition of a common projector for G . Then $G' = LGR$ is called a **projected GIFS**.*

COROLLARY 26. *To define (up to isomorphism) a projected GIFS we only need a common projector for the linear parts of the maps.*

DEFINITION 27 (Family of algebraic GIFS). *The following data define a family of algebraic GIFS:*

- (1) A GIFS G with edges labeled by square rational matrices: $M = \phi(G) = \{M_1, \dots, M_n\}$.
- (2) A symmetry group S of rational matrices for M : $M_i S = S M_i$
- (3) A common projector P for M and S .

The family consists of all GIFS that can be obtained from G by replacing every map $M_i \in \phi(G)$ by $f_i(x) = L s_i M_i R(x) + L t_i$ where $s_i \in S$, $t_i \in \mathbb{Q}^D$ and $P = RL$ is a projector decomposition. Since (33), the projector defines the family up to isomorphism.

8.3. Defining a projector from rational data. Now consider the situation when we have a **rational** IFS. According to Corollary 26 we only need a common projector to describe a projected IFS. In the general case, the projector can be represented by its matrix, but in practice the matrix cannot be used directly for a mathematically correct description because it has non-rational entries. One way to define a projector by rational data is a subspace matrix.

DEFINITION 28. Let $P \in \mathcal{M}_D$ be a projector, $P^2 = P$. A matrix $A \in \mathcal{M}_D$ is called a **subspace matrix** for P if

- (1) $AP = PA$.
- (2) $sp(A|_{\ker P}) \cap sp(A|_{\text{ran} P}) = \emptyset$.

According to Proposition 23, the equation $AP = PA$ means that $\ker(P)$ and $\text{ran}(P)$ are A -invariant, so $sp(A|_{\ker P}) \cup sp(A|_{\text{ran} P}) \subset sp(A)$. Since $\ker(P) \otimes \text{ran}(P) = \mathbb{R}^D$, we have the stronger equality:

$$(34) \quad sp(A|_{\ker P}) \cup sp(A|_{\text{ran} P}) = sp(A)$$

So, the projector P divides $sp(A)$ into two disjoint sets.

Let

$$sp^+(A) = \{\lambda \in sp(A) \mid \text{Im } \lambda \geq 0\}.$$

Since the matrix A is real, Definition 28 and (34) are equivalent to

$$(35) \quad sp^+(A|_{\ker P}) \cap sp^+(A|_{\text{ran} P}) = \emptyset \quad sp^+(A|_{\ker P}) \cup sp^+(A|_{\text{ran} P}) = sp^+(A)$$

According to [GLR06, Theorem 12.2.1], for every $\lambda \in sp^+(A)$ there is the A -invariant root subspace X_λ and for every A -invariant subspace M :

$$(36) \quad M = \bigotimes \{M \cap X_\lambda \mid \lambda \in sp^+(A)\}$$

Using (36) and Definition 28, we get

$$\ker(P) = \bigotimes \{X_\lambda \mid \lambda \in sp^+(A|_{\ker P})\},$$

$$\text{ran}(P) = \bigotimes \{X_\lambda \mid \lambda \in sp^+(A|_{\text{ran} P})\},$$

Since $\ker(P)$ and $\text{ran}(P)$ completely define the projector, we have the following statement:

COROLLARY 29. A projector P can be completely defined by a subspace matrix A and the subset of its eigenvalues $sp^+(A|_{\text{ran} P}) \subset sp^+(A)$.

If a subspace matrix A is rational, we only need a way to specify any subset of $sp^+(A)$ using integer data. Usually, the eigenvalues of A are not rational, so we cannot use them directly. Instead, we can sort eigenvalues by some order, and then use their integer indices to create a **list of indices**. Thus, we define the ordered sequence of eigenvalues:

$$(37) \quad \xi_1, \dots, \xi_m \in sp^+(A), \quad \text{Im } \xi_j \geq 0$$

For definiteness we use the order by decreasing modulus, and by decreasing real parts if the moduli are equal. So for any successive ξ_j, ξ_{j+1} :

$$(38) \quad |\xi_{j+1}| < |\xi_j| \text{ or } |\xi_{j+1}| = |\xi_j| \text{ and } \text{Re } \xi_{j+1} \leq \text{Re } \xi_j$$

PROPOSITION 30. *A projector P is completely defined by a subspace matrix A and the list of integer indices:*

$$(39) \quad \Lambda(A, P) = \{l \in \mathbb{Z} \mid \xi_l \in sp^+(A|_{\text{ran } P})\}.$$

In the following rational subspace matrices play a key role, and we shall discuss ways to define them. First we see how we can modify one subspace matrix to get other ones.

PROPOSITION 31 (Properties of subspace matrices). *Let $A \in \mathcal{M}_D$ be a subspace matrix for projector P , then*

- (1) *For any invertible $T \in \mathcal{M}_D$, the matrix $A' = TAT^{-1}$ is a subspace matrix for the projector $P' = TPT^{-1}$ and $\Lambda(A, P) = \Lambda(A', P')$.*
- (2) *The matrix A is a subspace matrix for the projector $1 - P$ and*

$$\Lambda(A, 1 - P) = \{1, \dots, \#sp^+(A)\} \setminus \Lambda(A, P)$$

PROOF. The first statement follows from the fact that the eigenvalues of A and A' are the same and $A'P' = P'A'$. The second one follows from the equation $A(1 - P) = (1 - P)A$, (30) and (35). \square

The first property shows that we can always use an integer subspace matrix instead of a rational one. The second property shows that if there is an isomorphism T between two rational IFS: $Q'T = TQ$, then we can use a subspace matrix A of Q to create the subspace matrix TAT^{-1} for Q' .

The following is a key concept for the IFStile package. It specifies those GIFS which are defined only by rationals.

DEFINITION 32 (Rational form of an algebraic GIFS). *Up to isomorphism, the following data completely define an algebraic GIFS.*

- (1) *A rational GIFS G in \mathbb{Q}^D .*
- (2) *A rational subspace matrix $A \in \mathcal{M}_D$ for a common projector P of $\phi(G)$.*
- (3) *A list of integer indices $\Lambda(A, P)$.*

*We call it a **rational form** of PG .*

8.4. The real Jordan decomposition. Although any subspace matrix defines the projector, we need the decomposition in Theorem 22 to create an instance of the projected IFS (31). The most natural way to create such decomposition is to use the real Jordan form of the subspace matrix. In other words, we use the eigenvectors of the subspace matrix as the basis of the range of the projector.

According to [GLR06, Theorem 12.2.2], every real matrix $A \in \mathcal{M}_D$ can be transformed into the block-diagonal real Jordan form:

$$(40) \quad J = TAT^{-1} = \begin{pmatrix} J_1 & 0 & \dots & 0 \\ 0 & J_2 & \dots & 0 \\ \dots & \dots & \dots & \dots \\ 0 & 0 & \dots & J_w \end{pmatrix}$$

$$J_s = \begin{pmatrix} C_s & 0 & \dots & 0 & 0 \\ I & C_s & \dots & 0 & 0 \\ \dots & \dots & \dots & \dots & \dots \\ 0 & 0 & \dots & C_s & 0 \\ 0 & 0 & \dots & I & C_s \end{pmatrix}$$

Every cell J_s corresponds to some eigenvalue $\lambda \in sp^+(A)$, and

$$C_s = \lambda \text{ for real } \lambda$$

$$C_s = \begin{pmatrix} \operatorname{Re} \lambda & -\operatorname{Im} \lambda \\ \operatorname{Im} \lambda & \operatorname{Re} \lambda \end{pmatrix} \text{ for complex } \lambda$$

We can suppose that the order of the blocks J_1, \dots, J_w in (40) agrees with (38). So J_1 corresponds to an eigenvalue with maximal module. If A is rational, then J is always algebraic, and we can choose an algebraic T .

Let A be a subspace matrix for the projector P . The columns of T^{-1} that correspond to the blocks J_s for the eigenvalues $sp^+(\operatorname{ran}(P))$ form a basis in $\operatorname{ran}(P)$. We can use this basis to uniquely define the projector decomposition $P = RL$. It is easy to see that the matrix L is formed from the corresponding rows of T .

8.5. Companion matrix. Rational companion matrices provide a useful tool to describe algebraic IFS. The following will be discussed below:

- (1) A companion matrix is defined by a small amount of data.
- (2) There is a unique way to transform a companion matrix to the real Jordan form.
- (3) Any rational matrix is similar to some rational block-companion matrix.
- (4) There are special matrices that have common invariant subspaces with companion matrices.

DEFINITION 33 (Monic polynomial). *A polynomial $p(x) = a_0 + a_1x + \dots + a_{d-1}x^{d-1} + a_nx^d$ is called **monic** if $a_n = 1$.*

DEFINITION 34 (Companion matrix). *The companion matrix of the monic polynomial $p(x) = a_0 + a_1x + \dots + a_{d-1}x^{d-1} + x^d$ is a square matrix defined as:*

$$C(p) = \begin{pmatrix} 0 & 0 & \dots & 0 & -a_0 \\ 1 & 0 & \dots & 0 & -a_1 \\ \dots & \dots & \dots & \dots & \dots \\ 0 & 0 & \dots & 1 & -a_{d-1} \end{pmatrix}$$

The eigenvalues of the matrix C are exactly the roots of the polynomial p .

Many algebraic IFS examples use some companion matrix as a subspace matrix. We consider the uniquely defined real Jordan form of the companion matrix in order to get an explicit algebraic IFS from a rational one.

Let $\lambda_i, \dots, \lambda_m$ be all eigenvalues of the companion matrix $C \in \mathcal{M}_d$ with algebraic multiplicities d_1, \dots, d_m , so $\sum_{i=1}^m d_i = d$. If all eigenvalues are distinct ($d_i = 1$) then C can be diagonalized using the **Vandermonde** matrix:

$$J = VCV^{-1}$$

where

$$V = \begin{pmatrix} 1 & \lambda_1 & \lambda_1^2 & \dots & \lambda_1^{d-1} \\ 1 & \lambda_2 & \lambda_2^2 & \dots & \lambda_2^{d-1} \\ 1 & \lambda_3 & \lambda_3^2 & \dots & \lambda_3^{d-1} \\ \dots & \dots & \dots & \ddots & \dots \\ 1 & \lambda_d & \lambda_d^2 & \dots & \lambda_d^{d-1} \end{pmatrix}$$

When C has eigenvalue λ_i with $d_i > 1$, we can use the **confluent** Vandermonde matrix [BG06] to transform C to get (8.5). For such eigenvalues, V has d_i corresponding rows:

$$(41) \quad V = \begin{pmatrix} \dots & \dots & \dots & \dots & \dots & \dots \\ 1 & \lambda_i & \lambda_i^2 & \lambda_i^3 & \dots & \lambda_i^{d-1} \\ 0 & 1 & 2\lambda_i & 3\lambda_i^2 & \dots & (d-1)\lambda_i^{d-2} \\ \dots & \dots & \dots & \dots & \dots & \dots \end{pmatrix}$$

where each row is a derivative of the previous one.

To transform a companion matrix to the **real** Jordan form, we need the real confluent Vandermonde matrix V_R . Every complex pair λ_i and $\overline{\lambda_i}$ with $\text{Im } \lambda_i > 0$ has $2d_i$ corresponding rows:

$$V_R = \begin{pmatrix} \dots & \dots & \dots & \dots & \dots & \dots \\ 1 & \text{Re } \lambda_i & \text{Re } \lambda_i^2 & \text{Re } \lambda_i^3 & \dots & \text{Re } \lambda_i^{d-1} \\ 0 & \text{Im } \lambda_i & \text{Im } \lambda_i^2 & \text{Im } \lambda_i^3 & \dots & \text{Im } \lambda_i^{d-1} \\ 0 & 1 & \text{Re } 2\lambda_i & \text{Re } 3\lambda_i^2 & \dots & \text{Re } (n-1)\lambda_i^{d-2} \\ 0 & 0 & \text{Im } 2\lambda_i & \text{Im } 3\lambda_i^2 & \dots & \text{Im } (n-1)\lambda_i^{d-2} \\ \dots & \dots & \dots & \dots & \dots & \dots \end{pmatrix}$$

The following theorem shows that, up to IFS isomorphism, we can always use a rational block-companion matrix as a subspace matrix:

THEOREM 35 (Frobenius normal form). [Gan60, p. 149]

Let $A \in \mathcal{M}_d$ be a rational matrix. Then there are rational matrices $B \in \mathcal{M}_d$ and $T \in \mathcal{M}_d$, that

$$B = TAT^{-1} = \begin{pmatrix} C_1 & 0 & \dots & 0 \\ 0 & C_2 & \dots & 0 \\ \dots & \dots & \dots & \dots \\ 0 & 0 & \dots & C_m \end{pmatrix}$$

where C_1, \dots, C_m are rational companion matrices.

Let $Q = \{q_1, \dots, q_n\}$ be a rational IFS with a rational subspace matrix A . Let $B = TAT^{-1}$ be a block-companion Frobenius normal form of A with a rational T . According to Proposition 31, the matrix B is a subspace matrix for the rational IFS $F = TQT^{-1}$ that is isomorphic to Q .

DEFINITION 36 (Rational normal form of an algebraic IFS).

A rational form as in Definition 32 is **normal** if the subspace matrix is a block-companion matrix, and the rational space has minimal possible dimension.

8.6. Matrices with common invariant subspace. To produce new algebraic IFS examples, we describe families of rational matrices that have a common invariant subspace. The following proposition gives some methods:

PROPOSITION 37. [GLR06, Proposition 1.4.1] Let the matrix $A \in \mathcal{M}_d$ have an invariant subspace $X \subset \mathbb{R}^d$, so $A(X) \subset X$. Then

- (1) If A is invertible then $A^{-1}(X) \subset X$.
- (2) If $B(X) \subset X$ then $(A + B)(X) \subset X$ and $(AB)(X) \subset X$.
- (3) If $p(x)$ is a polynomial and $A' = p(A)$ then $A'(X) \subset X$.

□

Companion matrices give us less trivial explicit examples.

DEFINITION 38. A polynomial $p(x) = a_0 + \dots + a_n x^n$ is called **palindromic** if $a_i = a_{n-i}$ for $i = 0, \dots, n$ or, equivalently, $p(x) = x^n p(1/x)$

THEOREM 39. [Con16, Theorem 1.1] Let $z \in \mathbb{A}$ be an algebraic rotation of the complex plane: $|z| = 1$. Then the minimal polynomial for z is palindromic and has even degree.

In the case of rational rotations when $|z^n| = 1$ for some integer $n > 0$, the minimal palindromic polynomial $p(z) = 0$ is called **cyclotomic**.

DEFINITION 40. The following matrix $\chi_d \in \mathcal{M}_d$ is called the **exchange matrix**:

$$\chi_d = \begin{pmatrix} 0 & 0 & \dots & 0 & 1 \\ \dots & \dots & \dots & \dots & \dots \\ 0 & 1 & \dots & 0 & 0 \\ 1 & 0 & \dots & 0 & 0 \end{pmatrix}$$

It is easy to see that $\chi_d^2 = I_d$.

The exchange matrix is closely related with some companion matrices.

PROPOSITION 41. *Let $C \in \mathcal{M}_d$ be a companion matrix for some monic palindromic polynomial. Then*

$$(C\chi_d)^2 = (\chi_d C)^2 = I_d$$

PROOF.

$$C\chi_d C = \begin{pmatrix} 0 & \dots & 0 & 0 & a_0^2 \\ 0 & \dots & 0 & 1 & a_0 a_1 - a_{d-1} \\ 0 & \dots & 1 & 0 & a_0 a_2 - a_{d-2} \\ \dots & \dots & \dots & \dots & \dots \\ 1 & \dots & 0 & 0 & a_0 a_{d-1} - a_1 \end{pmatrix}$$

If $a_0 = 1$ and $a_{d-k} = a_k$ for any k , then $C\chi_d C = \chi_d$. \square

When we use a palindromic companion matrix as a subspace matrix for projecting to \mathbb{R}^2 , we can use the exchange matrix to represent reflections of the plane. Another way to represent reflections is to use the following block-diagonal matrix:

$$\tau_d = \begin{pmatrix} 1 & 0 & \dots & 0 & 0 \\ 0 & -1 & \dots & 0 & 0 \\ \dots & \dots & \dots & \dots & \dots \\ 0 & 0 & \dots & 1 & 0 \\ 0 & 0 & \dots & 0 & -1 \end{pmatrix}$$

PROPOSITION 42. *Let $C \in \mathcal{M}_d$ be a companion matrix for polynomial $p(x) = a_0 + a_2 x^2 + \dots + x^n$ of even degree with $a_k = 0$ for all odd k . Then*

$$C\tau_d = -\tau_d C$$

8.7. An algebraic IFS constructed explicitly from a rational one. We consider the Ammann hexagon constructed in Section 7.4 as example for the lifting procedure. We start from the rational normal form in \mathbb{Q}^4 and then create an algebraic projected IFS.

$$A = \begin{pmatrix} 0 & 0 & 0 & 1 \\ 1 & 0 & 0 & 0 \\ 0 & 1 & 0 & -1 \\ 0 & 0 & 1 & 0 \end{pmatrix} \quad U = \begin{pmatrix} 1 & 0 & 0 & 0 \\ 0 & -1 & 0 & 0 \\ 0 & 0 & 1 & 0 \\ 0 & 0 & 0 & -1 \end{pmatrix}$$

Matrix A is used as a subspace matrix, and $\{1, 2\}$ are indices of eigenvalues A that define common projector for A and U (Definition 32).

Let $Q = \{q_1, q_2\}$ be a the following rational IFS:

$$q_1(x) = -A^{-2}U(x) \quad q_2(x) = A^{-1}(-x + t)$$

$$t = (0, -1, -1, -1)$$

Matrix A is a companion matrix for the polynomial $-1 + x^2 + x^4$ that has 4 roots:

$$\lambda_{1,2} = \pm i\rho$$

and

$$\lambda_{3,4} = \pm 1/\rho$$

where

$$\rho = \sqrt{\frac{1}{2}(\sqrt{5} + 1)} \approx 1.272$$

The Vandermonde matrix is

$$\begin{pmatrix} 1 & i\rho & -\rho^2 & -i\rho^3 \\ 1 & -i\rho & -\rho^2 & i\rho^3 \\ 1 & \rho^{-1} & \rho^{-2} & \rho^{-3} \\ 1 & -\rho^{-1} & \rho^{-2} & -\rho^{-3} \end{pmatrix}$$

The real Vandermonde matrix T is

$$T = \begin{pmatrix} 1 & 0 & -\rho^2 & 0 \\ 0 & \rho & 0 & -\rho^3 \\ 1 & \rho^{-1} & \rho^{-2} & \rho^{-3} \\ 1 & -\rho^{-1} & \rho^{-2} & -\rho^{-3} \end{pmatrix} \quad T^{-1} = \frac{1}{1 + \rho^4} \begin{pmatrix} 1 & 0 & \rho^4/2 & \rho^4/2 \\ 0 & 1/\rho & \rho^5/2 & -\rho^5/2 \\ -\rho^2 & 0 & \rho^2/2 & \rho^2/2 \\ 0 & -\rho & \rho^3/2 & -\rho^3/2 \end{pmatrix}$$

The real Jordan form is

$$J = \begin{pmatrix} 0 & -\rho & 0 & 0 \\ \rho & 0 & 0 & 0 \\ 0 & 0 & 1/\rho & 0 \\ 0 & 0 & 0 & -1/\rho \end{pmatrix}$$

Now we can define RL decomposition of the projector. We use $\lambda_{1,2}$ roots, so the matrix L should be constructed from the first two rows of T and the matrix R should be constructed from the first two columns of T^{-1} :

$$L = \begin{pmatrix} 1 & 0 & -\rho^2 & 0 \\ 0 & \rho & 0 & -\rho^3 \end{pmatrix}$$

$$R = \frac{1}{1 + \rho^4} \begin{pmatrix} 1 & 0 \\ 0 & 1/\rho \\ -\rho^2 & 0 \\ 0 & -\rho \end{pmatrix}$$

Finally we have the following equations for the attractor:

$$C = f_1(C) \cup f_2(C)$$

Where

$$f_1(x) = -\hat{A}^{-2}\hat{U}(x)$$

$$f_2(x) = \hat{A}^{-1}(-x + \hat{t})$$

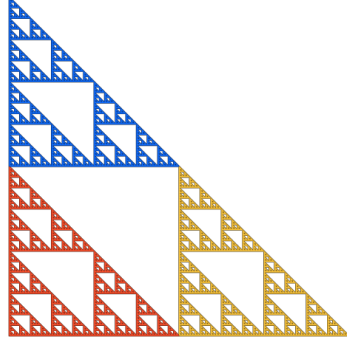
$$\hat{A} = LAR = \begin{pmatrix} 0 & -\rho \\ \rho & 0 \end{pmatrix} \quad \hat{U} = LUR = \begin{pmatrix} 1 & 0 \\ 0 & -1 \end{pmatrix}$$

$$\hat{t} = Lt = (\rho^2, -\rho + \rho^3)$$

9. Examples of rational forms

In this section we show additional examples of the rational representation of some algebraic IFS. Rational forms of the viper tile, Ammann hexagon and Chord quadrangle were constructed in Section 7. An algebraic representation of the following examples can be obtained by a procedure similar to Section 8.7. The first two examples are fractals, the others are tiles.

9.1. The Sierpinski triangle. This is a well-known rational IFS (algebraic dimension is 2).



$$g(A) = h_1(A) \cup h_2(A) \cup h_3(A)$$

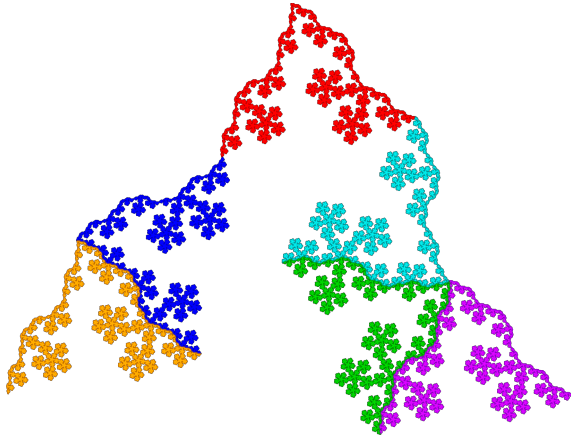
$$h_1(x) = x + [0, 0]$$

$$h_2(x) = x + [1, 0]$$

$$h_3(x) = x + [0, 1]$$

$$g = 2I = \begin{pmatrix} 2 & 0 \\ 0 & 2 \end{pmatrix}$$

9.2. McWorter's pentadendrite. [Edg90, p.197], [Rid18] This is a self-similar curve with pentagonal symmetry group and connected exterior. It was discovered by McWorter as an L-system fractal.



$$gA = \bigcup_{i=1}^6 h_i(A)$$

$$s = C(1 - x + x^2 - x^3 + x^4)$$

$$g = 3 - s + s^2 - s^3$$

$$h_1(x) = x + [0, 0, 0, 0]$$

$$h_2(x) = s^2(x + [0, 0, 0, -1])$$

$$h_3(x) = x + [1, 0, 1, 0]$$

$$h_4(x) = s^6(x + [-2, 1, -2, 2])$$

$$h_5(x) = s^8(x + [-1, 1, 1, 0])$$

$$h_6(x) = x + [2, -1, 1, -1]$$

The matrix s with index 1 can be used to identify the projector (Definition 32). There is another overlapping attractor in the complementary plane (with index 2).

Since s is a companion matrix for the cyclotomic polynomial $\Phi_{10}(x) = x^4 - x^3 + x^2 - x + 1 = 0$, after projecting it becomes a rotation by $\frac{\pi}{5}$.

The Hausdorff dimension of the set is equal to $2 \log(6) / \log(6 + \sqrt{5}) = 1.69953985\dots$. The intersections of pieces are either singletons or Jordan curves similar to the curve $gB = h_2(B) \cup h_3(B) \cup h_5(B)$ with $\dim(B) = 2 \log(3) / \log(6 + \sqrt{5}) = 1.042068\dots$

9.3. Golden 2334 triangle. This is a self-similar isosceles triangle with an infinite symmetry group. It could be new, some related examples based on the golden mean can be found in [Fre18].



$$g^4 A = g^2 h_1(A) \cup g h_2(A) \cup g h_3(A) \cup h_4(A)$$

$$s = C(x^4 - 3x^3 + 3x^2 - 3x + 1)$$

$$g = -1 + s$$

$$h_1 = -s(x + [0, 0, 0, 0])$$

$$h_2 = -s(x + [1, -1, 0, 0])$$

$$h_3 = s(x + [-1, 1, -1, 0])$$

$$h_4 = s^2(x + [1, -1, 2, -1])$$

The matrix s with index 1 can be used to identify the projector (Definition 32). After projecting, the matrix s represents an algebraic number that corresponds to an irrational rotation ($\approx 79^\circ$). The rotation cannot be rational because the polynomial $x^4 - 3x^3 + 3x^2 - 3x + 1$ is palindromic but not cyclotomic, see Definition 38. The matrix $-g^2 s^{-1}$ is a scaling by $\tau = \frac{\sqrt{5}+1}{2}$.

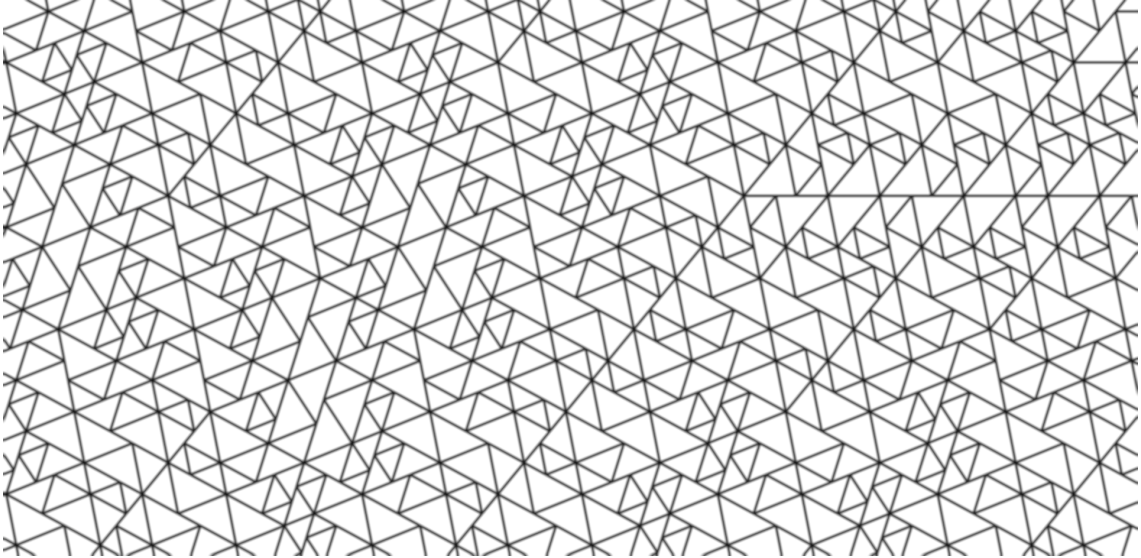
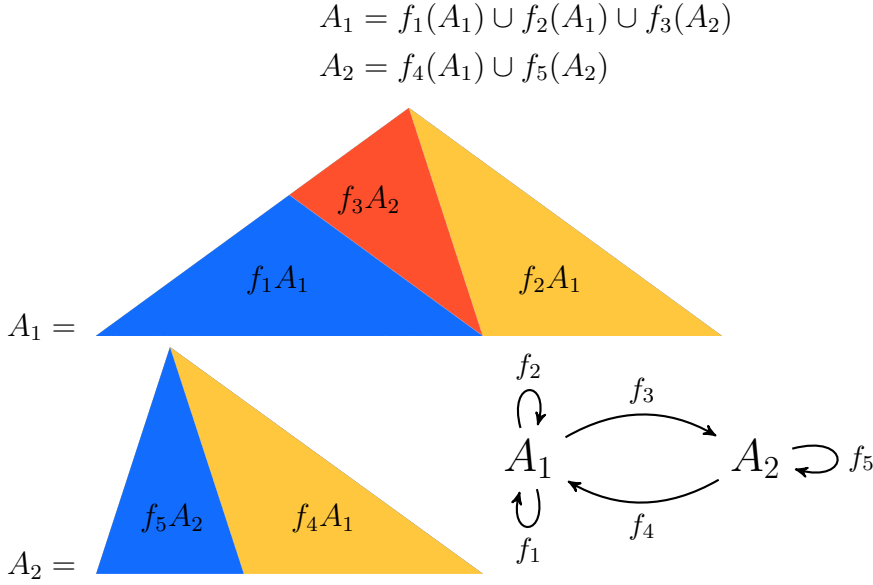


FIGURE 25. Tiling produced by Golden 2334 triangle.

9.4. Robinson triangles. [GS87, Fig.10.3.14] This is a well-known example that produces an aperiodic plane tiling. It consists of two isosceles triangles A_1 (with angles 36 and 108) and A_2 (with angles 36 and 72).



The yellow triangles $f_2(A_1)$ and $f_4(A_1)$ are obtained by orientation-reversing maps f_2 and f_4 . All the maps f_1, \dots, f_5 are similitudes with the same factor $\tau = \frac{\sqrt{5}-1}{2}$. The rational representation is

$$gA_1 = h_1(A_1) \cup h_2(A_1) \cup h_3(A_2)$$

$$gA_2 = h_4(A_1) \cup h_5(A_2)$$

$$s = C(x^4 - x^3 + x^2 - x + 1)$$

$$r = \chi_4$$

$$g = s - s^4$$

$$h_1 = s^4(x + [-1, 0, -1, 0])$$

$$h_2 = s^2r(x + [-1, 0, 0, 0])$$

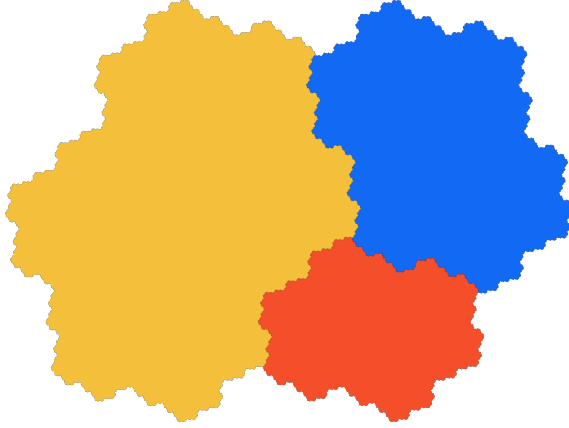
$$h_3 = s^9(x + [0, 0, 0, 0])$$

$$h_4 = s^6r(x + [0, -1, 0, -1])$$

$$h_5 = s^3(x + [1, -1, 0, -1])$$

The matrix s with index 1 can be used to identify the projector (Definition 32). The symmetry group is the same as for the Pentadendrite (9.2). After projecting, the matrix r is a reflection generated by the exchange matrix (Definition 40) and g is a scaling by $\tau = \frac{\sqrt{5}+1}{2}$.

9.5. Rauzy fractal. [Rau82] This is a well-known tile associated with the tribonacci constant. It has a fractal boundary. The scaling factors of the maps are the same as for the chord quadrangle from Section 7.5.



$$g^3 A = g^2 h_1(A) \cup g h_2(A) \cup h_3(A)$$

$$g = C(-1 + x + x^2 + x^3)$$

$$h_1(x) = x + [0, 0, 0]$$

$$h_2(x) = x + [0, 1, 0]$$

$$h_3(x) = x + [0, 1, 1]$$

The matrix g with index 1 can be used to identify the projector (Definition 32).

9.6. Danzer's ABCK tetrahedra. ([BG13, 6.7.1],[Fre14]) This example shows a rational representation in \mathbb{Q}^6 for the aperiodic ABCK tiles in \mathbb{R}^3 with icosahedral symmetry group. This is a natural extension of the Robinson triangles to the third dimension. Moreover, it has the same inflation factor τ . Instead of two triangles, we have 4 tetrahedra with names A,B,C,K.

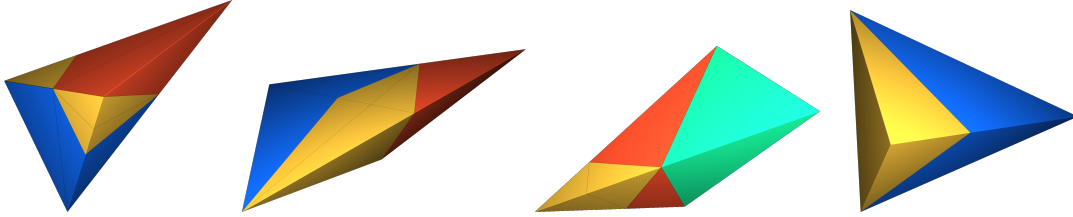


FIGURE 26. Danzer's ABCK tiles.

The table of the rational maps below was obtained by reversing numeric data from [Pao18]. The numeric data were obtained from the geometric description from [Fre14]. Then the tiling property was checked by the IFStile package which found 1909 different neighbor types.

We use 3 generators of the icosahedral group (with 120 elements): a, b, c , where $a^2 = b^3 = 1$ and $c = -1$ (see [BG13, Appendix A]).

$$a = \begin{pmatrix} -1 & 0 & 0 & 0 & 0 & 0 \\ 0 & -1 & 0 & 0 & 0 & 0 \\ 0 & 0 & 0 & 1 & 0 & 0 \\ 0 & 0 & 1 & 0 & 0 & 0 \\ 0 & 0 & 0 & 0 & 0 & -1 \\ 0 & 0 & 0 & 0 & -1 & 0 \end{pmatrix} \quad b = \begin{pmatrix} 0 & -1 & 0 & 0 & 0 & 0 \\ 0 & 0 & 0 & 0 & 0 & 1 \\ 0 & 0 & 0 & 0 & 1 & 0 \\ 0 & 0 & 1 & 0 & 0 & 0 \\ 0 & 0 & 0 & 1 & 0 & 0 \\ -1 & 0 & 0 & 0 & 0 & 0 \end{pmatrix}$$

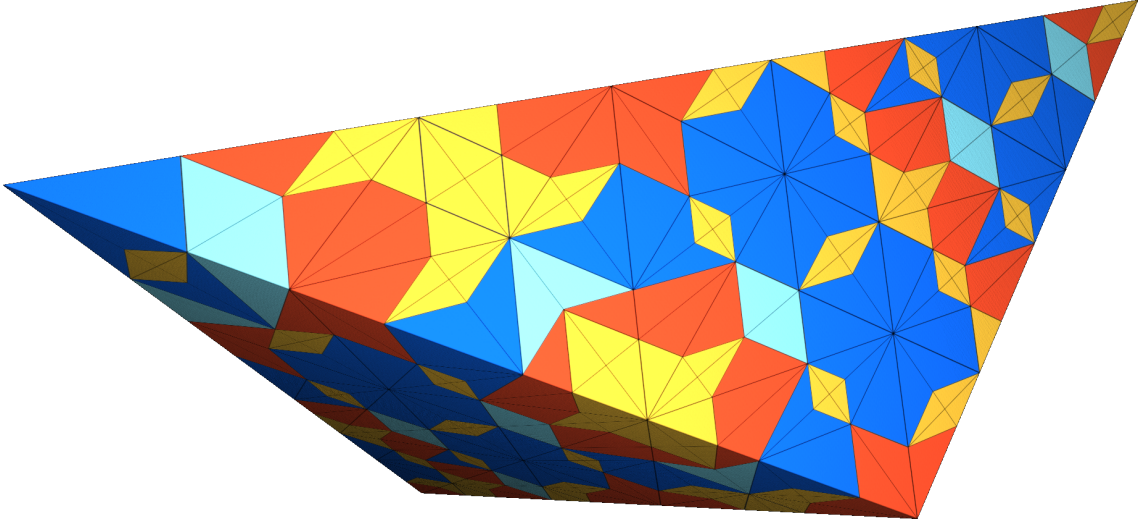


FIGURE 27. 'A' tetrahedron subdivision.

There are two mutually orthogonal 3-dimensional subspaces $X, X' \subset \mathbb{Q}^6 = X \otimes X'$, both invariant under a, b, c . There is an integer matrix q with $q(x) = \sqrt{5}x$ for any $x \in X$ and $q(x) = -\sqrt{5}x$ for any $x \in X'$.

$$q = \begin{pmatrix} 0 & 1 & 1 & -1 & 1 & 1 \\ 1 & 0 & 1 & -1 & -1 & -1 \\ 1 & 1 & 0 & 1 & 1 & -1 \\ -1 & -1 & 1 & 0 & 1 & -1 \\ 1 & -1 & 1 & 1 & 0 & 1 \\ 1 & -1 & -1 & -1 & 1 & 0 \end{pmatrix}$$

The projected IFS corresponds to X . It is easy to see that the matrix $g = \frac{1}{2}(q+1)$ is an expansion on X with the factor $\tau = \frac{\sqrt{5}+1}{2}$.

The GIFS with 4 vertices and 25 edges has the following representation.

$$\begin{aligned} gA &= h_0(B) \cup h_1(B) \cup h_2(B) \cup h_3(C) \cup h_4(C) \cup \\ &\quad h_5(K) \cup h_6(K) \cup h_7(K) \cup h_8(K) \cup h_9(K) \cup h_{10}(K) \\ gB &= h_{11}(B) \cup h_{12}(B) \cup h_{13}(C) \cup h_{14}(K) \cup h_{15}(K) \cup h_{16}(K) \cup h_{17}(K) \\ gC &= h_{18}(A) \cup h_{19}(C) \cup h_{20}(C) \cup h_{21}(K) \cup h_{22}(K) \\ gK &= h_{23}(B) \cup h_{24}(K) \end{aligned}$$

Where $h_i(x) = s_i(x + t_i)$ and

$s_0 = b^2abac$	$t_0 = [-1, -1, -2, -1, -1, 1]$
$s_1 = a$	$t_1 = [-2, -1, -1, 1, -1, -1]$
$s_2 = bacb^2abab^2a$	$t_2 = [-2, -1, -1, 1, -1, -1]$
$s_3 = c$	$t_3 = [-1, 0, -1, 0, -1, 0]$
$s_4 = bab^2abab^2$	$t_4 = [-1, 0, -1, 0, -1, 0]$
$s_5 = babab^2ab^2c$	$t_5 = [1, 0, 1, 0, 1, 0]$
$s_6 = ab$	$t_6 = [1, 1, 1, -1, 0, -1]$
$s_7 = abab^2aba$	$t_7 = [-1, -1, -1, 0, 0, 0]$
$s_8 = b^2acbab$	$t_8 = [-1, 0, -1, -1, -1, -1]$
$s_9 = baba$	$t_9 = [-1, 0, -1, -1, -1, -1]$
$s_{10} = acbab^2ab$	$t_{10} = [-1, -1, -1, 0, 0, 0]$
$s_{11} = b^2abac$	$t_{11} = [-1, -1, -2, -1, -1, 1]$
$s_{12} = a$	$t_{12} = [-2, -1, -1, 1, -1, -1]$
$s_{13} = c$	$t_{13} = [-1, 0, -1, 0, -1, 0]$
$s_{14} = babab^2ab^2c$	$t_{14} = [1, 0, 1, 0, 1, 0]$
$s_{15} = ab$	$t_{15} = [1, 1, 1, -1, 0, -1]$
$s_{16} = abab^2aba$	$t_{16} = [-1, -1, -1, 0, 0, 0]$
$s_{17} = b^2acbab$	$t_{17} = [-1, 0, -1, -1, -1, -1]$
$s_{18} = babc$	$t_{18} = [-1, 0, -1, 0, -1, 0]$
$s_{19} = acb$	$t_{19} = [-1, 0, -1, 0, -1, 0]$
$s_{20} = babab^2ab^2$	$t_{20} = [-1, 0, -1, 0, -1, 0]$
$s_{21} = 1$	$t_{21} = [1, 0, 1, 0, 1, 0]$
$s_{22} = b^2ab^2cabab$	$t_{22} = [-1, -1, -1, 0, 0, 0]$
$s_{23} = c$	$t_{23} = [-1, 0, -1, 0, -1, 0]$
$s_{24} = ab^2abab$	$t_{24} = [0, 0, 0, -1, 0, 0]$

Now we define a subspace matrix. Let

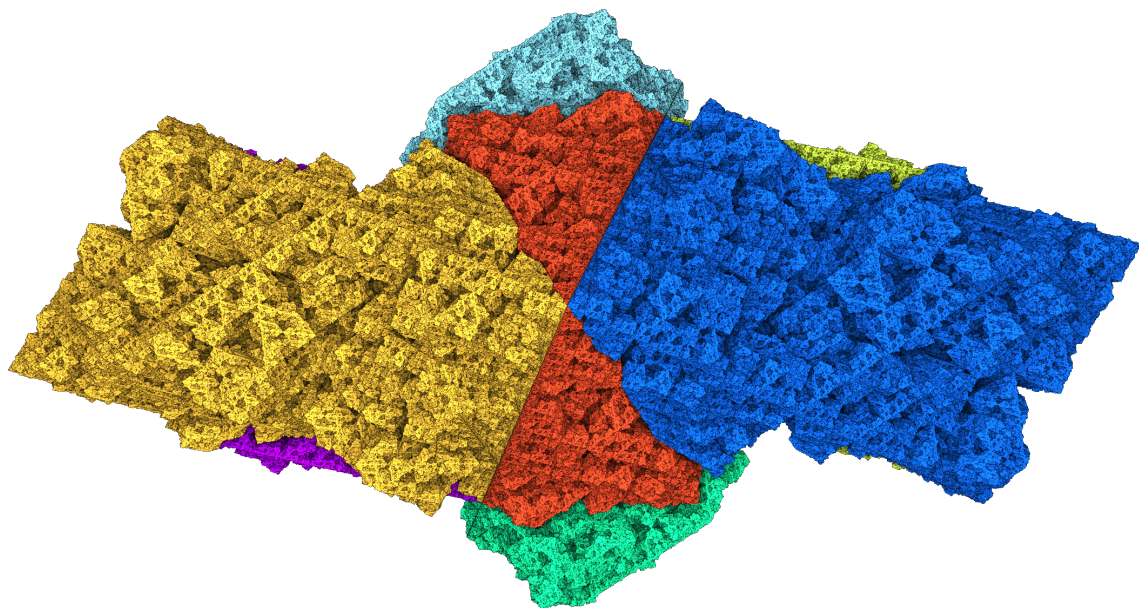
$$d_x = I_6 + abab^2abab^2ab, \quad d_y = I_6 + a, \quad d_z = I_6 + b^2abab^2abab^2.$$

These matrices d_x, d_y, d_z have three eigenvalues $(2, 0, 0)$ with eigenvectors from X and three other eigenvalues $(2, 0, 0)$ with eigenvectors from X' . Let v_x, v_y, v_z be some integers. Define matrices $m_x = v_x q d_x$, $m_y = v_y q d_y$ and $m_z = v_z q d_z$. The sum $m_x + m_y + m_z$ has eigenvalues $(2v_x\sqrt{5}, 2v_y\sqrt{5}, 2v_z\sqrt{5})$ on X and $(-2v_x\sqrt{5}, -2v_y\sqrt{5}, -2v_z\sqrt{5})$ on X' . For our example we can use $v_x = 3, v_y = 2, v_z = 1$, and the integer subspace matrix d

$$d = m_x + m_y + m_z = q(3d_x + 2d_y + d_z)$$

The matrix d has six distinct eigenvalues $(6\sqrt{5}, -6\sqrt{5}, 4\sqrt{5}, -4\sqrt{5}, 2\sqrt{5}, -2\sqrt{5})$, positive for X , and negative for X' . So X can be identified by the indices 1, 3, 5.

There are many other tiles with icosahedral symmetry group. In Figure 28 we can see <ABCK> tile [KPSZ94, Fre14] with a fractal boundary of dimension ≈ 2.4543526 (see Section 10.5).

FIGURE 28. $\langle \text{ABCK} \rangle$ tile.

9.7. Quaquaversal tiling. [CR98] This rep-8 tile is an analog of the Pinwheel tile [Rad94] in three dimensions. It produces a non-periodic tiling of \mathbb{R}^3 . The orientations of small pieces of the tile, considered as unit vectors, form a dense set on the three-dimensional sphere. In the original paper [CR98, Sec.4], there is a statement that the number of different neighbors for the tiling is finite. The IFStile package found that there are exactly 1291 neighbors.

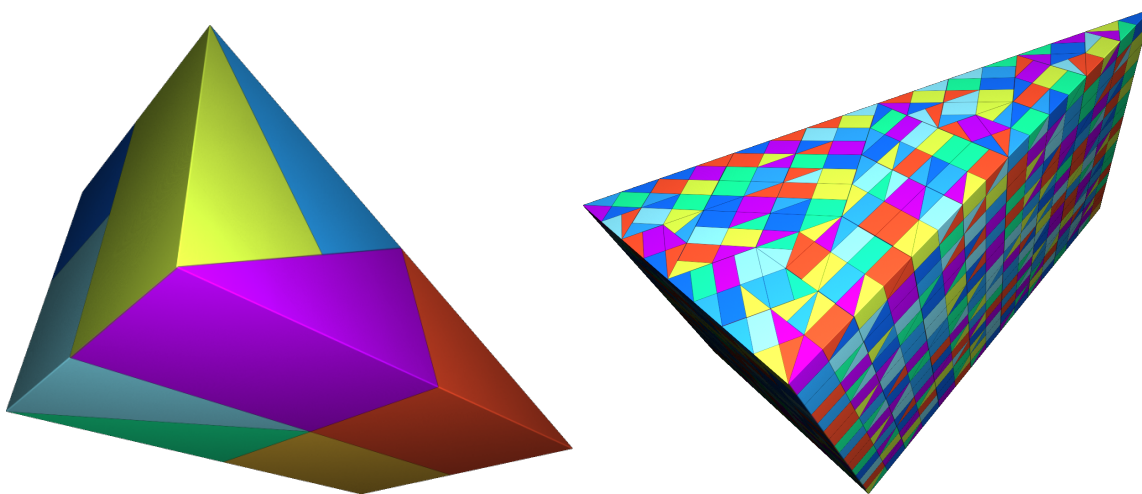


FIGURE 29. Quaquaversal tiling.

The symmetry group is dense in $\text{SO}(3)$. It can be generated by the following rotations (by 90 and 60 degrees).

$$a' = \begin{pmatrix} 0 & -1 & 0 \\ 1 & 0 & 0 \\ 0 & 0 & 1 \end{pmatrix} b' = \begin{pmatrix} 1 & 0 & 0 \\ 0 & \cos(\pi/3) & -\sin(\pi/3) \\ 0 & \sin(\pi/3) & \cos(\pi/3) \end{pmatrix}$$

The rational representation of the generators can be obtained by applying the scheme from Proposition 21:

$$a = \begin{pmatrix} 0 & -1 & 0 & 0 & 0 & 0 \\ 1 & 0 & 0 & 0 & 0 & 0 \\ 0 & 0 & 1 & 0 & 0 & 0 \\ 0 & 0 & 0 & 0 & -1 & 0 \\ 0 & 0 & 0 & 1 & 0 & 0 \\ 0 & 0 & 0 & 0 & 0 & 1 \end{pmatrix} b = \begin{pmatrix} 1 & 0 & 0 & 0 & 0 & 0 \\ 0 & 1/2 & 0 & 0 & 0 & -3/2 \\ 0 & 0 & 1/2 & 0 & 3/2 & 0 \\ 0 & 0 & 0 & 1 & 0 & 0 \\ 0 & 0 & -1/2 & 0 & 1/2 & 0 \\ 0 & 1/2 & 0 & 0 & 0 & 1/2 \end{pmatrix}$$

It is easy to see, that $a^4 = b^6 = 1$. The tile has a rational representation in \mathbb{Q}^6 and can be expressed as:

$$2A = \bigcup_{i=1}^8 h_i(A)$$

$$h_1 = x + [1, 0, 0, 0, 0, 1]$$

$$h_2 = x + [1, 1, 0, 0, 0, 0]$$

$$h_3 = x + [0, 0, 0, 0, 0, 1]$$

$$h_4 = a^3(x + [-1, 1, 0, 0, 0, 0])$$

$$h_5 = a^3b^3(x + [-1, -2, 0, 0, 0, -1])$$

$$h_6 = a^2b^3(x + [-1, 0, 0, 0, 0, -1])$$

$$h_7 = b^4(x + [0, -1, 0, 0, 0, 0])$$

$$h_8 = b^4a^2(x + [-1, 1, 0, 0, 0, 0])$$

There are two 3-dimensional subspaces $X, X' \subset \mathbb{Q}^6 = X \otimes X'$. Both X and X' are invariant under a and b . The projected IFS corresponds to X . As a subspace matrix we can use the following matrix:

$$q = \begin{pmatrix} 0 & 0 & 0 & 9 & 0 & 0 \\ 0 & 0 & 0 & 0 & 6 & 0 \\ 0 & 0 & 0 & 0 & 0 & 3 \\ 3 & 0 & 0 & 0 & 0 & 0 \\ 0 & 2 & 0 & 0 & 0 & 0 \\ 0 & 0 & 1 & 0 & 0 & 0 \end{pmatrix}$$

The indices 1, 3, 5 identify the common projector, see Definition 40.

D Invariants of GIFS attractors

The search for new fractals can provide thousands or even millions of new examples within a short time, depending on the GIFS family. For relatives of the Sierpinski gasket, considered in our paper [BM18], two seconds are sufficient to get thousand examples with open set condition. For tilings, the search is usually slower. For some families, as for instance Rauzy fractals (ex. 9.5), only few examples seem to exist.

It is necessary to let the computer screen large sets of examples, since visual inspection is too time-consuming. Various invariants have to be calculated for each dataset. This allows to improve the database in different ways:

- (1) The whole database can be ordered with respect to appropriate invariants.
- (2) Bad examples, characterized by extreme values of certain invariants, can be excluded.
- (3) Good examples, characterized by values of the invariants in certain prescribed intervals, can be selected.

The term ‘invariant’ is used with respect to isomorphism of GIFS by affine maps or by similarity maps, introduced in Definition 3. We discussed some aspects of the isomorphism in the last section of the paper on Sierpinski relatives in the appendix. There we defined conjugacy, and a focus was set on keeping only one element of every conjugacy class in the database. Here we just consider invariants as properties or numerical descriptors of the GIFS. Of course we should define them in such a way that isomorphic GIFS are assigned the same number.

In the IFStile program, quite a few descriptors are implemented:

- (1) Hausdorff dimension and measure of the attractor,
- (2) Hausdorff dimension and measure of the boundary of the attractor,
- (3) the structure of the neighbor graph,
- (4) moments of Hausdorff measure on the attractor,
- (5) diameters of the attractor,
- (6) number of orientations of pieces.

While the structure of the neighbor graph was considered above, Hausdorff measure and dimension of sets and boundary sets will be considered in Section 10. Moments will be considered in Section 11. We have no time to discuss the last two properties. One can also think about calculating the number and structure of the extreme points of the attractor, which is also an affine invariant of the GIFS.

10. Hausdorff measure and dimension

10.1. Definition. For any $\alpha \geq 0$ and any Borel $S \subset \mathbb{R}^d$ the α -dimensional Hausdorff measure of S is [Fed69, 2.10.2]

$$H^\alpha(S) = \liminf_{\delta \rightarrow 0} \left\{ \sum_i (\text{diam } U_i)^\alpha \mid S \subset \bigcup_i U_i, \text{diam } U_i < \delta \right\}$$

The Hausdorff dimension of set S is:

$$\dim(S) = \inf_{\beta > 0} \{H^\beta(S) = 0\}$$

It is easy to see, that for any similitude T in \mathbb{R}^d with the similarity factor $r = r(T)$

$$(42) \quad H^\alpha(TS) = r^\alpha H^\alpha(S)$$

10.2. Ordinary IFS case. Consider an ordinary IFS in \mathbb{R}^d with the attractor $C \subset \mathbb{R}^d$

$$(43) \quad C = f_1(C) \cup f_2(C) \cup \dots \cup f_m(C) .$$

where f_1, \dots, f_m are similitudes with factors r_1, \dots, r_m . Suppose that for some $\alpha \geq 0$

$$(44) \quad 0 < H^\alpha(C) < \infty$$

and for any $1 \leq i, j \leq m, i \neq j$

$$(45) \quad H^\alpha(f_i(C) \cap f_j(C)) = 0$$

Then from (42), (43), (44) and (45) we have:

$$(46) \quad \begin{aligned} H^\alpha(C) &= r_1^\alpha H^\alpha(C) + \dots + r_m^\alpha H^\alpha(C) \\ 1 &= r_1^\alpha + \dots + r_m^\alpha \end{aligned}$$

An unique solution α of (46) is called the **similarity dimension** of IFS.

If an IFS fulfills the open set condition, then equations (44), (45) hold [Hut81] for the Hausdorff dimension of the attractor. It means that the Hausdorff dimension is equal to the similarity dimension. Although we can easily calculate α , the exact value of $H^\alpha(A)$ is not known for such simple examples as the Sierpinski gasket. Even if an IFS does not satisfy the open set condition, it is still possible to find Hausdorff dimension in the finite type case [NW01, Zer96, HLR03].

10.3. Strongly connected GIFS case. Let G be a GIFS in \mathbb{R}^d with attractors C_1, \dots, C_n and adjacency lists Q_1, \dots, Q_n :

$$(47) \quad C_i = \bigcup_{(f,j) \in Q_i} f(C_j) \quad i = 1 \dots n$$

Like before, we assume that all $f \in \phi(G)$ are similitudes and suppose that for some $\alpha \geq 0$

$$(48) \quad 0 < \sum_i H^\alpha(C_i) < \infty$$

and for any $i = 1, \dots, n$ and any different $(f_1, j_1), (f_2, j_2) \in Q_i$

$$(49) \quad H^\alpha(f_1(C_{j_1}) \cap f_2(C_{j_2})) = 0, \text{ and } 0 < H^\alpha(C_i) < \infty$$

Then from (42), (47), (48) and (49) we have:

$$(50) \quad H^\alpha(C_i) = \sum_{(f,j) \in Q_i} r^\alpha(f) H^\alpha(C_j) \quad i = 1 \dots n$$

For strongly connected graph G , we can show (using Perron-Frobenius theory) that there is an unique $\alpha \geq 0$ and a positive eigenvector (μ_1, \dots, μ_n) corresponding to the eigenvalue 1, that

$$(51) \quad \mu_i = \sum_{(f,j) \in Q_i} r^\alpha(f) \mu_j, \quad \mu_i > 0 \quad i = 1 \dots n$$

Additionally supposing that

$$(52) \quad \sum_i \mu_i = 1$$

we can uniquely define the vector (μ_1, \dots, μ_n) . We call μ_i a **relative measure** of C_i and we call α a **similarity dimension** of G .

Now we suppose that a GIFS fulfills the open set condition. In this case the similarity dimension is equal to the Hausdorff dimension of the attractors and (48) holds [MW88]. According to (50) and (51) there is a constant $w > 0$ that

$$(53) \quad \mu_i = w H^\alpha(C_i) \quad i = 1 \dots n$$

In practice it is very difficult to calculate the constant w .

10.4. General GIFS case. The case of general GIFS is more interesting. Even in the OSC case, sets from different strongly connected components can have different Hausdorff dimensions, and some sets with dimension α can have infinite α -Hausdorff measure.

Let G be a GIFS in \mathbb{R}^d with attractors C_1, \dots, C_n and adjacency lists Q_1, \dots, Q_n and assume that all $f \in \phi(G)$ are invertible. As in 4.4 we suppose that for every $v_i \in V(G)$ the vertex component index $1 \leq \psi_i \leq M$ defined, where M is the number of strongly connected components.

For every component k of the graph we formally define three values that we call internal dimension γ_k , external dimension $\bar{\gamma}_k$ and dimension α_k . For every vertex v_i of the graph we define two values that we call internal measure ρ_i and measure μ_i . Internal measures and dimension for a component are calculated by removing all the edges that lead to other components, and conversely, external dimension is calculated by removing all edges that lead from outside the component. Dimension α_k and measures μ_i are calculated by combining internal and external values.

For self-similar GIFS that fulfill OSC, the value α_k is equal to the Hausdorff dimension of the attractors of the component k and the values μ_i of the component k are proportional to the α_k -dimensional Hausdorff measure of the set i .

Consider some strongly connected component m of the graph G , $1 \leq m \leq M$. We define the **internal dimension** γ_m of the component and the **internal measure** $\rho_i \geq 0$ for every vertex v_i in the component. If a component does not have directed cycles (that means it has exactly one vertex v_i), we define $\gamma_m = -1$ and $\rho_i = 0$. If

a component has directed cycles then γ_m and ρ_i for all vertexes of the component ($\psi_i = m$) can be obtained from the following system of (non-linear) equations:

$$(54) \quad \sum_{\psi_i=m} \rho_i = 1$$

$$(55) \quad \rho_i = \sum_{(f,j) \in Q_i} \{\rho_j r^{\gamma_m}(f) \mid \psi_j = m\} \quad \text{for all } i \text{ with } \psi_i = m$$

If the attractors exist, the solution always exists and is unique (see Section 10.3).

In (54) we sum over all vertices of the component. In (55) we sum over all edges that lead from a vertex of the component to the component.

Now we can define a **measure** μ_i for every vertex v_i , the **dimension** α_m and the **external dimension** $\bar{\gamma}_m$ for every component of the graph G . We start from the component $m = 1$. According to 4.4 this component does not have edges that lead to another component. So we simply define $\alpha_1 = \bar{\gamma}_1 = \gamma_1$ and $\mu_i = \rho_i$ for all sets of the component (that have $\psi_i = 1$). If we already have defined α_k and $\bar{\gamma}_k$ for all $k < m$, we can define α_m and $\bar{\gamma}_m$.

$$\bar{\gamma}_m = \max_{\psi_i=m} \max_{(f,j) \in Q_i} \{\gamma_k \mid k = \psi_j, \psi_j < m\}$$

$$\alpha_m = \max\{\gamma_m, \bar{\gamma}_m\}$$

Now we define the measure for all sets of the component m :

(1) If $\gamma_m > \bar{\gamma}_m$ then

$$\mu_i = \rho_i = \sum_{(f,j) \in Q_i} \{\rho_j r^{\gamma_m}(f) \mid \psi_j = m\}$$

(2) If $\gamma_m < \bar{\gamma}_m$ then

$$\mu_i = \sum_{(f,j) \in Q_i} \{\mu_j r^{\alpha_m}(f) \mid \alpha_{\psi_j} = \alpha_m\}$$

(3) If $\gamma_m = \bar{\gamma}_m$ then

$$\mu_i = \infty$$

Finally, combining the cases of the definition of μ_i , we can get the following equation:

$$(56) \quad \mu_i = \sum_{(f,j) \in Q_i} \{\mu_j r^{\alpha_{\psi_i}}(f) \mid \alpha_{\psi_j} = \alpha_{\psi_i}\}$$

Moreover, the equation (56) holds for any uniform subdivision $Q_i(\epsilon)$ (4.3).

Now we can define the self-affine measure on every attractor C_i with $\mu_i < \infty$. We denote it by the same symbol μ_i :

$$(57) \quad \mu_i(B) = \sum_{(f,j) \in Q_i} \{r^{\alpha_{\psi_i}}(f) \mu_j(f^{-1}(B)) \mid \alpha_{\psi_j} = \alpha_{\psi_i}\}, \text{ for any } B \subset C_i$$

If the GIFS fulfills the open set condition and all $f \in \phi(G)$ are similitudes, then for every component m the dimension α_m is the Hausdorff dimension and there is a

constant $w_m > 0$ that for all sets of the component their measure are proportional to Hausdorff measure:

$$(58) \quad \mu_i(B) = w_m H^\alpha(B \cap C_i)$$

PROPOSITION 43. *Corresponding attractors of isomorphic GIFS G and G' have the same measures. Corresponding strongly connected components have the same dimension.*

PROOF. This directly follows from the fact that our definition uses determinants that coincide for similar GIFS. \square

It is easy to see, that all GIFS from the same family (see Definition 27) have the same corresponding dimensions and relative measures.

10.5. Examples. Consider the GIFS dragon from Figure 11.

$$\begin{aligned} C_1 &= f_1(C_1) \cup f_2(C_2) \\ C_2 &= f_3(C_1) \cup f_4(C_1) \cup f_5(C_2) \end{aligned}$$

Let $r_i = r(f_i)$, so $r_1 = r_3 = r_4 = r_5 = 1/\sqrt{2}$, $r_2 = 1/2$

Applying (54) and (55), we obtain the following equations

$$\begin{aligned} \mu_1 &= r_1^\alpha \mu_1 + r_2^\alpha \mu_2 \\ \mu_2 &= r_3^\alpha \mu_1 + r_4^\alpha \mu_1 + r_5^\alpha \mu_2 \\ \mu_1 + \mu_2 &= 1 \end{aligned}$$

with a unique solution $\alpha = 2$ and $\mu_1 = 1/3$, $\mu_2 = 2/3$.

A similar calculation for the dimension of the boundary in Figure 19 gives $\alpha = 2 \frac{\log(x)}{\log(2)} \approx 1.267$ where $x^7 - 2x^6 + x^5 - x^4 + 2x^3 - x^2 - 2 = 0$.

Calculations can be performed using the IFStile package. They can be done numerically or analytically by computing rational polynomial coefficients.

A strongly connected part of the boundary GIFS for the three-dimensional $\langle \text{ABCK} \rangle$ tile in Figure 28 have 72 vertices. The calculation gives

$$\dim(\partial \langle \text{ABCK} \rangle) = \frac{\log(x)}{\log(\tau)} \approx 2.4543526$$

where $\tau = \frac{\sqrt{5}+1}{2}$ and $x^5 - 4x^4 + 3x^3 - x^2 - 2x - 3 = 0$.

11. Moments

Moments are widely used to distinguish shapes of two- and three-dimensional objects [Hu62, SF11]. The main idea is to use moments to construct expressions that are invariant under similitudes (or even more general maps like affine or projective). Applications include image (2D) and mesh (3D) processing [DP06]. Self-affine sets have a very specific equation (57) for the measure distribution, that allow the **exact** computation of moments of any order. For our purpose, the most useful are second order moments, since they have relatively low computational cost.

DEFINITION 44. For any measure μ in \mathbb{R}^d and integers $p_1, p_2, \dots, p_d \geq 0$ the number

$$(59) \quad M(p_1, p_2, \dots, p_d) = \int x_1^{p_1} x_2^{p_2} \dots x_d^{p_d} d\mu$$

is called a moment of order $p_1 + \dots + p_d$.

The mass of the measure the moment of order zero:

$$(60) \quad \mu(\mathbb{R}^d) = M(0, 0, \dots, 0) = \int d\mu$$

11.1. Moments of first order. We can use the zero and first order moments to compute the center of mass $c(\mu) \in \mathbb{R}^d$ of a measure μ :

$$(61) \quad c(\mu) = \frac{1}{\mu(\mathbb{R}^d)} \int x d\mu$$

As an example, consider the simplest case of an ordinary IFS:

$$(62) \quad C = f_1(C) \cup \dots \cup f_n(C)$$

In this case, equations (58) and (61) give

$$(63) \quad c = r^\alpha(f_1)f_1(c) + \dots + r^\alpha(f_n)f_n(c)$$

where α is the similarity dimension (46).

11.2. Moments of second order. The Euler tensor of a measure μ in \mathbb{R}^d can be represented by the matrix $E(\mu) \in \mathcal{M}_d$:

$$(64) \quad E(\mu) = \int x \cdot x^T d\mu$$

As we can see, the entries of the matrix $E(\mu)$ are exactly the moments of order 2.

11.3. Calculation. The recursive nature of Equation (57) gives us a method to calculate moments without integrating. Moreover, it is possible to calculate the first and the second order moments at once using an **extended matrix**.

For any affine map $f = Ax + b$ in \mathbb{R}^d define the extended matrix $L(f) \in \mathcal{M}_{d+1}$ as a block matrix:

$$L(f) = \begin{pmatrix} A & b \\ 0^T & 1 \end{pmatrix}$$

It is easy to see, that $L(f^{-1}) = L^{-1}(f)$ and $L(f_1 f_2) = L(f_1)L(f_2)$ for any affine f_1 and f_2 .

Applying [DP06, Theorem 3.3] for (57) and (64) we can define the **extended Euler tensor** $E_i \in \mathcal{M}_{d+1}$ for all attractors C_i with $\mu_i < \infty$

$$E_i = \sum_{(f,j) \in Q_i} \{\mu_j L(f) E_j L^T(f) \mid \alpha_{\psi_j} = \alpha_{\psi_i}\}$$

$$E_i(d+1, d+1) = 1$$

This system of equations has a unique solution. All matrices E_i are symmetric and can be expressed in block form:

$$E_i = \begin{pmatrix} P_i & X_i \\ X_i^T & 1 \end{pmatrix}$$

where $P_i \in \mathcal{M}_d$ and $X_i \in \mathbb{R}^d$ is the **center of mass** of the attractor C_i .

Now we can define the **central Euler tensors** $M_i \in \mathcal{M}_d$ by moving the center of mass to the origin:

$$M_i = P_i - X_i X_i^T$$

It is easy to see that for probability measure, the matrix M_i is the covariance matrix:

$$(65) \quad M_i = \int (x - c(\mu))(x - c(\mu))^T d\mu_i$$

All matrices M_i are self-adjoint and can be expressed in the eigenvalue decomposition form:

$$M_i = V_i \text{diag}(I_i) V_i^{-1}$$

where $I_i \in \mathbb{R}^d$ is a vector with non-negative non-decreasing entries: $0 \leq I_i(k) \leq I_i(k+1)$ for all $k = 1, \dots, d$. For a probability measure, I_i denotes the variance along principal axes.

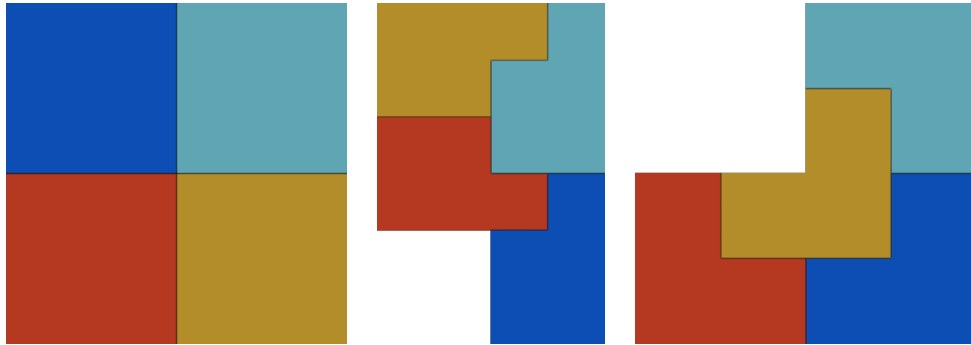
PROPOSITION 45. *Let C, C' be a finite measure attractors of two self-similar GIFS that fulfill the open set condition. If $C' = T(C)$ for some similitude T then*

$$I'_i / I'_d = I_i / I_d$$

PROOF. Because of the open set condition, the measures μ_i and μ'_i are proportional to the positive and finite $H^{\dim(C)}$. Substituting $C' = T(C)$ into (65) we directly get our statement. \square

We can use Proposition 45 to distinguish two attractors by comparing normed vectors I for both of them. In \mathbb{R}^d this gives us $d - 1$ invariant real numbers for each attractor.

11.4. Examples. Consider the following well-known rep-4 tiles.



The value I_1/I_2 is equal to 1 for the square, $\frac{17}{41}$ for the middle figure and $\frac{7}{15}$ for the chair on the right. For the 3D Notched cube of Figure 2, calculation gives $I = (\frac{145}{217}, 1, 1)$

E Notes on the IFStile program

The thesis focussed on mathematical foundations for the main procedures of the IFStile package. In this last chapter I shall give some comments on the implementation of the algorithms, and on other features of the package which were developed for the comfort of the mathematical user. We start with the language that has specifically developed for the program.

12. The language of IFStile

12.1. Robinson triangle. We start with the IFStile definition of the Robinson triangle. The file contains the matrices g , s and r , the maps h_1, \dots, h_5 and the equations for the triangles A_1 and A_2 as described in the example 9.4. Green lines are comments and are not part of the definition.

```
@@version 3
#this is a block identifier for Robinson triangle
@G
#user-define name of the block
$n=Robinson triangle
#dimension of the rational space
$dim=4
#s - subspace matrix, 0 - index of the eigenplane
$subspace=s 0
#companion 4*4-matrix - rotation by pi/5
s=$companion([1,-1,1,-1])
#exchange 4*4-matrix - reflection
r=$exchange()
#expansion matrix (golden ratio)
g=s-s^4
#five isometries in the eigenplane
h1=s^4*([-1,0,-1,0])
h2=s^2*r*([-1,0,0,0])
h3=s^9*([0,0,0,0])
h4=s^6*r*([0,-1,0,-1])
h5=s^3*([1,-1,0,-1])
#equations for the A1 and A2 triangles
A1=g^-1*(h1*A1|h2*A1|h3*A2)
A2=g^-1*(h4*A1|h5*A2)
```

12.2. The family concept. As explained in Definition 27, IFStile usually considers fractals and tiles as instances of families. The family fixes the rational space dimension, projection to the algebraic space, graph structure of the self-similar equations, expansion, and symmetry group. Each instance is obtained by a choice of symmetries and translations. Given the family, the search function of IFStile will find random examples which fulfill the OSC criteria. The Robinson triangle was found in this way. Below you see the family description and in the last block the specification of the maps h_i .

```
@@version 3

#block G with the family definition:
@G
$dim=4
$subspace=s 0
s=$companion([1,-1,1,-1])
r=$exchange()
g=s-s^4
#semigroup generated by s and r
&T=$semigroup([s,r])
#acceptable isometries of the family
#rotations, reflections, integer translations
&Q=T*$vector(0)
h1=Q
h2=Q
h3=Q
h4=Q
h5=Q
A0=g^-1*(h1*A0|h2*A0|h3*A1)
A1=g^-1*(h4*A0|h5*A1)

#Robinson triangle block that
#inherits definitions from 'G' block:
@:G
$n=Robinson triangles
h1=s^4*([-1,0,-1,0])
h2=s^2*r*([-1,0,0,0])
h3=s^9*([0,0,0,0])
h4=s^6*r*([0,-1,0,-1])
h5=s^3*([1,-1,0,-1])
```

As in the previous file we define maps h_1, \dots, h_5 , but instead of concrete affine maps we use the macro Q that describes some abstract maps. Any such map is equal to a composition of some element of the semigroup T generated by the rotation matrix s and the reflection matrix r and integer 4D-translation (**\$vector**

keyword). The second block describes the concrete instance - the Robinson triangle. It inherits all definitions from the previous block (except for h_1, \dots, h_5 maps). We can use this family description together with the "Finder" module to find other tiles from the family.

12.3. Files.

AIFS is a text format for representation of the iterated function systems.

Any .aifs file consists of an arbitrary number of blocks (even millions).

Usually each block corresponds to a family or a particular IFS.

Every file starts with **@@version 3** string.

One file can include another one using the command **@@import file_to_include.ext** with a relative path.

Every block starts with **@ID:ParentID**, where ID and ParentID are the unique identifiers of the block and its parent block.

ID can be empty if we do not refer to the block from elsewhere.

ParentID can be empty if the block has no parent.

A block can use all definitions from its parent, and can override some of them.

It is possible to call one block from another one as a function by ID. In that case the first variables in the called block are replaced by arguments, and the last variable is used as return value.

12.4. Blocks.

To perform calculation with numbers and affine maps it is possible to use ordinary operations like $+$, $-$, $*$, $/$, $^$ and brackets.

For numbers 'sin', 'cos', 'tan', 'asin', 'acos', 'atan', 'exp', 'log', 'floor', 'ceil', 'arg' are defined.

Also 'if' function defined: $if(cond, val1, val2)$ is equivalent to $(cond > 0)?val1 : val2$ in C-like languages.

A variable with name beginning with '\$' is considered as built-in variable and has a special meaning.

A variable with name beginning with '&' is considered as substitution, it is recalculated in every place where it is used.

12.5. Identifiers.

An identifier is a case-sensitive string that denotes a variable, an operator or a block.

An identifier can consist of symbols $[a-z]$, $[A-Z]$, $[0-9]$ and $_-$, but cannot start with a digit.

Identifiers beginning with \$ and & symbols have a special meaning.

12.6. Vectors.

Like in many other languages, $[a_1, a_2, \dots, a_n]$ defines the vector of elements (a_1, a_2, \dots, a_n) . We can access to the elements of a vector using square brackets, so if $v = [a_1, a_2, \dots, a_n]$, then a_1 can be accessed as $v[0]$, and $a_n = v[n - 1]$.

A vector of appropriate length can be automatically converted to a matrix or to a translation.

12.7. Affine maps. When $\$dim=n$, the following definitions of maps in \mathbb{R}^n are available:

$$[t_1, t_2, \dots, t_n] \text{ - translation: } \begin{pmatrix} x'_1 \\ x'_2 \\ \dots \\ x'_n \end{pmatrix} = \begin{pmatrix} x_1 + t_1 \\ x_2 + t_2 \\ \dots \\ x_n + t_n \end{pmatrix}$$

$$[a_{11}, a_{12}, \dots, a_{1n}, \dots, a_{n1}, a_{n2}, \dots, a_{nn}] \text{ - square matrix:}$$

$$\begin{pmatrix} x'_1 \\ x'_2 \\ \dots \\ x'_n \end{pmatrix} = \begin{pmatrix} a_{11} & a_{12} & \dots & a_{1n} \\ a_{21} & a_{22} & \dots & a_{2n} \\ \dots & \dots & \dots & \dots \\ a_{n1} & a_{n2} & \dots & a_{nn} \end{pmatrix} \begin{pmatrix} x_1 \\ x_2 \\ \dots \\ x_n \end{pmatrix}$$

$\$companion([a_0, a_1, a_2, \dots, a_{n-1}])$ - the companion matrix (Definition 34) for the polynomial $a_0 + a_1x + \dots + a_{n-1}x^{n-1} + x^n$.

$\$exchange()$ - the exchange matrix $n \times n$ (Definition 40).

12.8. Templates.

Templates allow to describe entire sets of affine maps together with a random distribution that can be used in the search procedure and in the editor window. Templates can be used in the same places where affine maps appear: within compositions, unions, etc.

$\$semigroup([g_1, g_2, \dots, g_m], T)$ - element of the semigroup (possibly infinite) generated by the affine maps g_1, g_2, \dots, g_m . T - [optional, for infinite semigroups] $\$integer$ that represents normal distribution for the length of compositions of the generators.

$\$vector(L, T)$ - vector of numbers, L - length of the vector, $L = 0$ means $L = \$dim$. T - [optional] type and a random distribution for the vector entries: $\$integer$ or $\$real$.

$\$number(T)$ - real or integer number. T - [optional] type and a random distribution of the number: $\$integer$ or $\$real$.

$\$real(a, b)$, $\$integer(a, b)$ - type and uniform distribution for real or integer numbers from a to b .

$\$real(v)$, $\$integer(v)$ - type and (half-)normal distribution for real or integer numbers.

$|v|$ - variance.

if $v < 0$ then distribution is normal.

if $v > 0$ then distribution is half-normal.

12.9. Operators.

$f_1 * f_2 * \dots * f_n$ - composition of the maps (or operators) $x \Rightarrow f_1(f_2(\dots(f_n(x))\dots))$. For example, $2 * [1, 0]$ corresponds to $2(x + [1, 0])$, and $[1, 0] * 2$ corresponds to $2x + [1, 0]$.

$S_1 | S_2 | \dots | S_m$ - union of the sets (or operators) $S_1 \cup S_2 \cup \dots \cup S_m$. For example, $(f_1 | f_2) * S$ means $f_1(A) \cup f_2(A)$.

f^n - composition f with itself n times $f(f(f(\dots)))$

f^{-1} - inverse map

\emptyset - empty set

i - identity map

12.10. Special variables.

$\$dim = d$ - dimension of the rational space. All affine maps must have dimension equal d .

$\$subspace = s \ i_1 \ i_2 \ i_3 \dots$ - defines the projection from the rational to the algebraic space (where the attractor lives). The first argument is an identifier of the **subspace matrix** (Definition 28). The other arguments are the indices (zero-based) of the eigenvalues of the subspace matrix that define the image of the projector (Definition 30).

13. Using the IFStile package

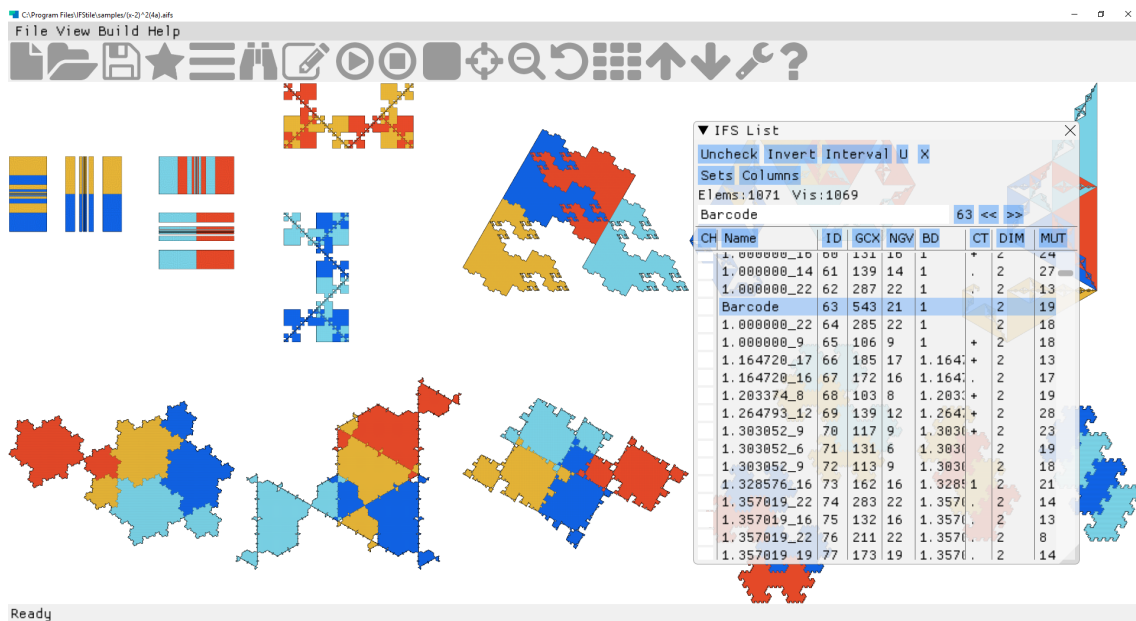


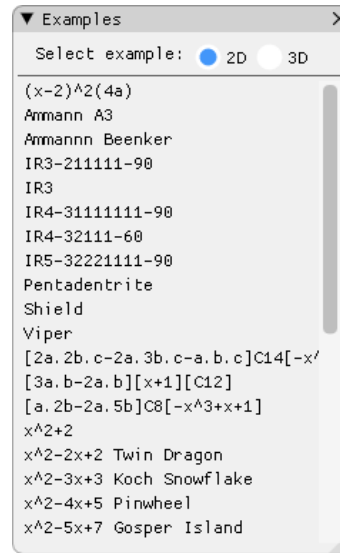
FIGURE 30. IFStile user interface.

On Figure 30 we can see the IFStile user interface, that consist of

- (1) the main menu

- (2) the toolbar with icons
- (3) the main window with rendered attractor(s)
- (4) the tool window that can contain different contents (IFS List, Finder, etc)
- (5) the status bar with context-sensitive information.

13.1. The built-in examples. The simplest way to start working with the package is to use the built-in examples, that can be opened by clicking the "Star" button in the toolbar or by using the menu item "File → Open example". Every entry in the list represents a family of GIFS and can contain many examples.

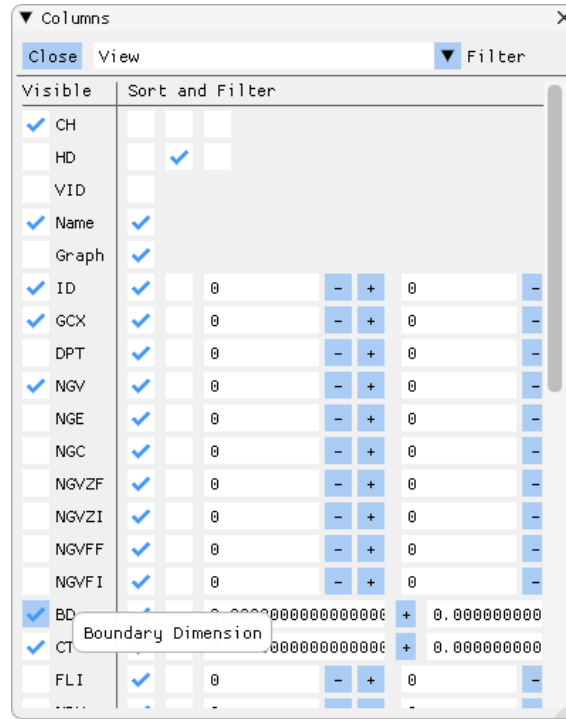


13.2. IFS List Editor/Viewer. This window will be displayed after the user opens a file (using File → Open menu item) or chooses some example. Also it can be opened from the menu (View → IFS List). The window displays the contents of the current file and every list entry corresponds to some GIFS.

CH	Name	ID	GCX	NGV	BD	CT	DIM
	Square	3	56	8	1	+	2
	Trapeze	4	161	18	1	+	2
	Trapeze 3	5	276	20	1	+	2
	Trapeze 2	6	120	15	1	+	2
	Triangle	7	98	12	1	+	2
	Triangle 3	8	239	33	1	+	2
	Triangle 2	9	113	14	1	+	2
	Flag	10	779	60	1	+	2
	Flag2	11	731	60	1	+	2
	Chair	12	217	19	1	+	2
	L	13	295	20	1	+	2
	Sphinx	14	690	54	1	+	2
	Rectangle 1	15	129	14	1	+	2
	Rectangle 2	16	280	28	1	+	2
	Rectangle 3	17	65	8	1	+	2
	f1	18	91	9	1	+	2
	f2	19	88	9	1	+	2

If the user selects an element, the package immediately begins to build the attractor (the progress will be shown in the status bar). It is possible to sort elements by clicking the head of any column. The user can check/uncheck any element by clicking the first column. It is possible to remove checked elements, invert check marks, and sort by checked state.

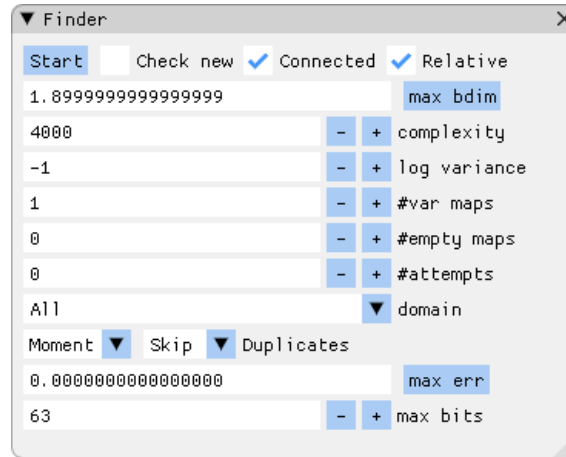
If the user clicks the "Columns" button, the following window will be opened:



The user can choose visible columns, sort order for the columns, and set up a filter to see only specific elements. It is possible to separately specify the filtering properties for searching and displaying.

13.3. The finder. This window can be opened using the menu item "View → Finder" or by clicking the "Binoculars" toolbar icon. The module allows to find GIFS that fulfill OSC using a family description. The algorithm performs random walk by mutating integer parameters of the GIFS maps. The scheme can be described in the following way:

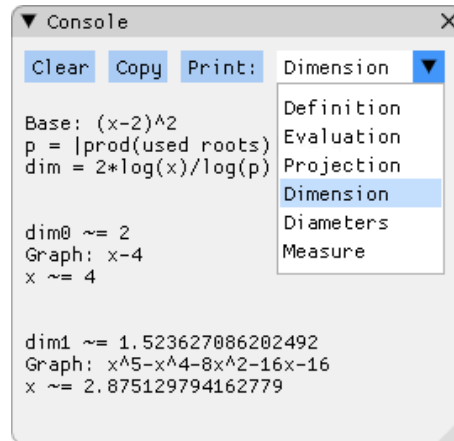
- (1) Select a random "seed" entry in the currently loaded list (or only from the checked elements).
- (2) Change several affine maps - those ones that was defined using **\$semi-group**, **\$vector** or **\$number** keywords.
- (3) Ignore GIFS if it is a duplicate or does not fulfill the OSC.
- (4) Compute many numeric characteristics of the attractor (like the boundary dimension) and ignore GIFS if some properties are out of range.
- (5) Add the new entry to the list and continue search.



There are many useful parameters that control the search, for instance.

- (1) max bdim - The maximum acceptable dimension of the boundary.
- (2) complexity - Describes how big can the neighbors graph be.
- (3) log variance - Logarithm of the variance for the normal distribution for **\$semigroup**, **\$vector** or **\$number** templates (if the last optional parameter is omitted).
- (4) var maps - Describes how many maps can be changed at once to get new GIFS from the seed.
- (5) domain - Describes which subset of the whole list can be used to select the seed.

13.4. Console and reports. It is possible to see a lot of information about the currently selected GIFS using the console window.

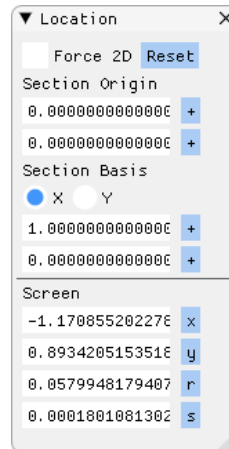


Among others, we can see

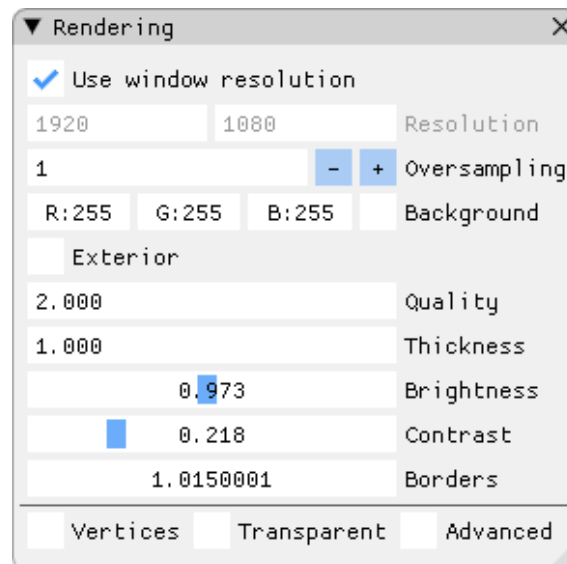
- (1) The Hausdorff dimension of the attractor.
- (2) The diameters.
- (3) The relative Hausdorff measure.
- (4) The moments.
- (5) The bounding balls.

13.5. Attractor rendering.

To choose a fragment of the attractor that we need we can use the "Location" window. Another way to change a fragment is to use mouse selection of the area of interest.



To control resolution, brightness and other rendering parameters, we can use the "Rendering" window:



To change colors of the attractor, we can use the "Palette" window:

set "b". The set "b" is equal "a.b", that means that it consists of one smaller copy of the set "a" and one smaller copy of itself (see 9.4).

We can see that the module was able to find several families of GIFS that have the same substitution matrix. The Robinson triangle belongs to the "C10" family that means it has a rotation symmetry group of order 10. The polynomial $p(x) = -x^3 + x^2 + 1$ means that expanding matrix on the plane corresponds to the complex number $p(e^{\pi i/5})$.

The user can control the maximal dimension of the rational space, the Hausdorff dimension of the target GIFS (2 for plane tilings), the search radius for polynomial coefficients and other parameters.

Bibliography

- [AL11] S. Akiyama and B. Loridant. Boundary parametrization of self-affine sets. *J. Math. Soc. Japan*, 63(2):525–579, 2011.
- [Ban91] C. Bandt. Self-similar sets 5. Integer matrices and fractal tilings of \mathbb{R}^n . *Proc. Amer. Math. Soc.*, 112:549–562, 1991.
- [Ban97] C. Bandt. Self-similar tilings and patterns described by mappings. In R.V. Moody, editor, *The Mathematics of Long-range Aperiodic Order*, volume C 489 of *NATO ASI Series*, pages 45–84. Kluwer Academic Publishers, 1997.
- [Ban10] C. Bandt. Combinatorial topology of three-dimensional self-affine tiles. *arXiv e-prints*, page arXiv:1002.0710, February 2010.
- [Bar93] M. F. Barnsley. *Fractals everywhere*. Academic Press, 2nd edition, 1993.
- [BG92] C. Bandt and S. Graf. Self-similar sets 7. A characterization of self-similar fractals with positive Hausdorff measure. *Proc. Amer. Math. Soc.*, 114:995–1001, 1992.
- [BG97] C. Bandt and P. Gummelt. Fractal Penrose tilings 1. Construction and matching rules. *Aequ. Math.*, 53:295–307, 1997.
- [BG06] F.S.V. Bazán and S. Gratton. An explicit Jordan decomposition of companion matrices. *Trends in Applied and Computational Mathematics*, 7(2):209–218, 2006.
- [BG13] M. Baake and U. Grimm. *Aperiodic Order, Vol. 1: A mathematical invitation*. Cambridge University Press, Cambridge, 2013.
- [BG17] M. Baake and U. Grimm. *Aperiodic Order, Vol. 2: Crystallography and almost periodicity*. Cambridge University Press, Cambridge, 2017.
- [BM09] C. Bandt and M. Mesing. Self-affine fractals of finite type. In *Convex and fractal geometry*, volume 84 of *Banach Center Publ.*, pages 131–148. Polish Acad. Sci. Inst. Math., Warsaw, 2009.
- [BM18] C. Bandt and D. Mekhontsev. Elementary fractal geometry. new relatives of the Sierpinski gasket. *Chaos: An Interdisciplinary Journal of Nonlinear Science*, 28(6):063104, 2018.
- [BMT18] C. Bandt, D. Mekhontsev, and A. Tetenov. A single fractal pinwheel tile. *Proc. Amer. Math. Soc.*, 146:1271–1285, 2018.
- [BR14] S. Banerjee and A. Roy. *Linear Algebra and Matrix Analysis for Statistics*. CRC Press, 01 2014.
- [CLRS09] T.H. Cormen, C.E. Leiserson, R.L. Rivest, and C. Stein. *Introduction to Algorithms*. The MIT Press, 3rd edition, 2009.
- [Con16] K. Conrad. Roots on a circle. expository notes at <http://www.math.uconn.edu/~kconrad/blurbs>, 2016.
- [CR98] J.H. Conway and C. Radin. Quaquaversal tilings and rotations. *Invent. Math.*, 132:179–188, 1998.
- [CT16] G. R. Conner and J. M. Thuswaldner. Self-affine manifolds. *Advances Math.*, 289:725–783, 2016.
- [DKV00] P. Duvall, J. Keesling, and A. Vince. The Hausdorff dimension of the boundary of a self-similar tile. *J. London Math. Soc.*, 61:748–760, 2000.
- [DP06] A. DiCarlo and A. Paoluzzi. Fast computation of inertia through affinely extended euler tensor. *Computer-Aided Design*, 38(11):1145–1153, 2006.

- [DvO00] L. Danzer and G. van Ophuyssen. A species of planar triangular tilings with inflation factor $\sqrt{-7}$. *Panjab Univ. Res. Bull.*, 50:137–175, 2000.
- [Edg90] G.A. Edgar. *Measure, Topology, and Fractal Geometry*. Springer, New York, 1990.
- [Fal14] K. J. Falconer. *Fractal geometry: mathematical foundations and applications*. J. Wiley & sons, 3 edition, 2014.
- [Fed69] H. Federer. *Geometric measure theory*. Springer, 1969.
- [Fre05] D. Frettlöh. Duality of model sets generated by substitutions. *Romanian Journal of Pure and Applied Math*, 50:619–639, 2005. arXiv:math/0601064v1.
- [Fre08] D. Frettlöh. Substitution tilings with statistical circular symmetry. *European J. Comb.*, 29:1881–1893, 2008.
- [Fre14] D. Frettlöh. Icosahedral tilings in \mathbb{R}^3 : The abck tilings. math.uni-bielefeld.de/baake/frettlloe/papers/ikosa.pdf, 2014.
- [Fre18] D. Frettlöh. Tilings Encyclopedia, 2018. tilings.math.uni-bielefeld.de.
- [FS10] D. Frettlöh and I. Suschko. 3-torus rep-tile. *Electronic Geometry Model No. 2010.02.001*, 2010.
- [Gan60] F.R. Gantmacher. *The Theory of Matrices, Vol. 1*. Chelsea Pub. Co., 1960.
- [Gar63] M. Gardner. On rep-tiles, polygons that can make larger and smaller copies of themselves. *Scientific Amer.*, 208:154–164, 1963.
- [Gel94] G. Gelbrich. Crystallographic reptiles. *Geometria Dedicata*, 51:235–256, 1994.
- [Gel97] G. Gelbrich. Fractal Penrose tilings 2. Tiles with fractal boundary as duals of penrose triangles. *Aequ. Math.*, 54:108–116, 1997.
- [Gil86] W.J. Gilbert. The fractal dimension of sets derived from complex bases. *Canad. Math. Bull.*, 29(4):495–500, 1986.
- [GLR06] I. Gohberg, P. Lancaster, and L. Rodman. *Invariant Subspaces of Matrices with Applications*. Society for Industrial and Applied Mathematics, 2006.
- [Gol64] S.W. Golomb. Replicating figures in the plane. *Math. Gaz.*, 48:403–412, 1964.
- [GS87] B. Grünbaum and G.C. Shephard. *Patterns and Tilings*. Freeman, New York, 1987.
- [Hil95] M.J.M. Hill. Determination of the volumes of certain species of tetrahedra without employment of the method of limits. *Proc. Lond. Math. Soc.*, 2:39–53, 1895.
- [HLR03] X.-G. He, K.-S. Lau, and H. Rao. Self affine sets and graph-directed systems. *Constr. Approx.*, 19:373–397, 2003.
- [HR00] R. Hochberg and M. Reid. Tiling with notched cubes. *Discrete Mathematics*, 214:255–261, 2000.
- [Hu62] M.-K. Hu. Visual pattern recognition by moment invariants. *IRE Transactions on Information Theory*, 8(2):179–187, 1962.
- [Hut81] J. E. Hutchinson. Fractals and self-similarity. *Indiana University Mathematics Journal*, 30:713–747, 1981.
- [IRI92] K.-H. Indlekofer, P. Racsó, and I. Káta. Number systems and fractal geometry. In *Probability Theory and Applications: Essays to the Memory of József Mogyoródi*, pages 319–334. Springer Netherlands, 1992.
- [Ken96] R. Kenyon. The construction of self-similar tilings. *Geom. Funct. Anal.*, 6:471–488, 1996.
- [KPSZ94] P. Kramer, Z. Papadopolos, M. Schlottmann, and D. Zeidler. Projection of the danzer tiling. *Journal of Physics A: Mathematical and General*, 27(13):4505–4517, 1994.
- [KS10] R. Kenyon and B. Solomyak. On the characterization of expansion maps for self-affine tilings. *Discrete Comput. Geom.*, 43:577–593, 2010.
- [Kwa16] J. Kwapisz. Inflations of self-affine tilings are integral algebraic perron. *Invent. math.*, 205:173–220, 2016.
- [LLR] C.K. Lai, K.-S. Lau, and H. Rao. Classification of tile digit sets as product-forms. arXiv 1305.0202.
- [Lor12] B. Loridant. Crystallographic number systems. *Monatsh. Math.*, 167:511–529, 2012.
- [LW96] J.C. Lagarias and Y. Wang. Integral self-affine tiles in \mathbb{C}^n . i. standard and non-standard digit sets. *J. London Math. Soc.*, 54:161–179, 1996.

- [ME05] D. Manav and G. Edgar. Separation properties for graph-directed self-similar fractals. *Topology and its Applications*, 152:138–156, 07 2005.
- [Mek18] D. Mekhontsev. IFStile package. <https://ifstile.com>, 2018.
- [Mor99] M. Morán. Dynamical boundary of a self-similar set. *Fundamenta Mathematicae*, 160(1):1–14, 1999.
- [MS11] J. Matoušek and S. Safernová. On the nonexistence of k -reptile tetrahedra. *Discrete Comput. Geom.*, 46:599–609, 2011.
- [MW88] R.D. Mauldin and S.C. Williams. Hausdorff dimension in graph-directed constructions. *Trans. Amer. Math. Soc.*, 309:811–829, 1988.
- [NW01] S.-M. Ngai and Y. Wang. Hausdorff dimension of self-similar sets with overlaps. *J. London Math. Soc.*, 63:655–672, 2001.
- [Pao18] M. Paolini. Danzer tiles with pov-ray, 2018. dmf.unicatt.it/~paolini/danzer/.
- [Rad94] C. Radin. The pinwheel tilings of the plane. *Annals Math.*, 139:661–702, 1994.
- [Rad99] C. Radin. *Miles of Tiles*, volume 1 of *Student Mathematical Library*. Amer. Math. Soc., Providence, 1999.
- [Rau82] G. Rauzy. Nombres algébriques et substitutions. *Bulletin de la Société Mathématique de France*, 110:147–178, 1982.
- [Rid18] L. Riddle. Pentadentrite, 2018. ecademy.agnesscott.edu/~lriddle/ifs/pentaden/penta.htm.
- [Sen95] M. Senechal. *Quasicrystals and geometry*. Cambridge University Press, Cambridge, 1995.
- [SF11] Tomáš Suk and Jan Flusser. Tensor method for constructing 3d moment invariants. In *Computer Analysis of Images and Patterns*, pages 212–219, Berlin, Heidelberg, 2011. Springer Berlin Heidelberg.
- [ST03] K. Scheicher and J.M. Thuswaldner. Neighbors of self-affine tiles in lattice tilings. In P. Grabner and W. Woess, editors, *Fractals in Graz 2001*, pages 241–262. Birkhäuser, 2003.
- [Str97] A. Strzeboński. Computing in the field of complex algebraic numbers. *Journal of Symbolic Computation*, 24(6):647 – 656, 1997.
- [SW99] R.S. Strichartz and Y. Wang. Geometry of self-affine tiles 1. *Indiana Univ. Math. J.*, 48:1–24, 1999.
- [Thu89] W.P. Thurston. Groups, tilings, and finite state automata. AMS Colloquium Lectures, Boulder, CO, 1989.
- [Ven12] J. Ventrella. *Brainfilling Curves - A Fractal Bestiary*. Lulu.com, Raleigh, North Carolina, 2012.
- [Zer96] M.P.W. Zerner. Weak separation properties for self-similar sets. *Proc. Amer. Math. Soc.*, 124:3529–3539, 1996.